Cruft Laboratory

Harvard University · Cambridge, Massachusetts
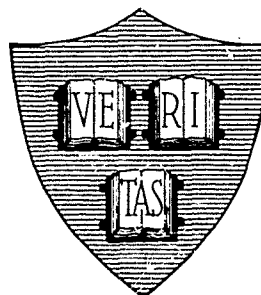
ANNUAL PROGRESS REPORT NO. 64

COVERING PERIOD

JULY 1, 1961 · JULY 2, 1962

August - 1962

Cruft Laboratory

Harvard University

Cambridge, Massachusetts

ANNUAL PROGRESS REPORT NO. 64

Covering Period

July 1, 1961----June 30, 1962

Office of Naval Research Contracts	Submitted by
Nonr-1866(07)	J. A. Pierce
Nonr-1866(16)	The Steering Committee
Nonr-1866(26)	R. W. P. King
Nonr-1866(28)	N. Bloembergen
Nonr-1866(32)	R. W. P. King

Air Force Contracts	
AF19 (604)-4118	R. W. P. King
AF19 (604)-5487	R. V. Jones
AF19 (604)-7262	R. W. P. King

August 1, 1962

<div align="center">TABLE OF CONTENTS</div>

<div align="center">-i-</div>

TABLE OF CONTENTS

TABLE OF CONTENTS Page

TABLE OF CONTENTS   <u>Page</u>

LIST OF FIGURES

July 1, 1961 - June 30, 1962

ADMINISTRATIVE STAFF

Contract Nonr-1866(16)

Steering Committee

Dean H. Brooks
Assoc. Dean F. K. Willenbrock
Prof. N. Bloembergen
Prof. A. E. Bryson, Jr.
Assoc. Prof. R. V. Jones
Assoc. Prof. R. E. Kronauer
Asst. Prof. K. S. Narendra
Asst. Prof. D. W. Tufts
Dr. R. G. Leahy
Dr. H. J. Riblet

Director

Contract Nonr-1866(07)	Mr. J. A. Pierce
Contract Nonr-1866(26)	Prof. R. W. P. King
Contract Nonr-1866(28)	Prof. N. Bloembergen
Contract Nonr-1866(32)	Prof. R. W. P. King
Contract AF19(604)-4118	Prof. R. W. P. King
Contract AF19(604)-5487	Assoc. Prof. R. V. Jones
Contract AF19(604)-7262	Prof. R. W. P. King

RESEARCH STAFF

Dr. J. A. Armstrong	Dr. P. S. Pershan
Dr. N. Bloembergen	Dr. G. Peterson
Dr. H. Brooks	Dr. W. F. Pickard
Dr. A. E. Bryson, Jr.	Mr. J. A. Pierce
Dr. A. Dymanus	Dr. S. Prasad
Dr. D. Gill	Dr. H. J. Riblet
Dr. F. A. Hinchey	Dr. S. S. Sandler
Dr. Y. C. Ho	Dr. G. Seidel
Dr. K. Iizuka	Dr. S. R. Seshadri
Dr. R. V. Jones	Dr. H. J. Schmitt
Dr. R. W. P. King	Dr. J. Shefer
Dr. R. E. Kronauer	Dr. T. Soejima
Dr. Y. Obata	Dr. D. W. Tufts
Dr. S. C. Nath	Dr. E. B. Treacy
Dr. A. A. Pandiscio	Dr. T. T. Wu

VERY LOW FREQUENCY PROPAGATION[*]

Personnel

J. A. Pierce   Dr. S. C. Nath

Introduction

The studies reported below are a part of a program intended to find ways to make the best use of the special characteristics of radio propagation at the very low frequencies. Transmissions in this domain are characterized by relatively small and slow variations in amplitude and by very great constancy of phase, except for diurnal effects. Thus, although atmospheric noise is high at these frequencies, transmission for narrow-band information has a reliability that is not approached at any other frequencies capable of long-distance transmission.

The useful radio service that requires the least bandwidth is standard-frequency transmission. Here there is no information rate at all, and the required bandwidth closely approaches zero. It follows that, with suitable instrumentation, very low transmitter power can provide a useful service. An example is the 20 kc signal from the Bureau of Standards at Boulder, Colorado. This signal is transmitted at a radiated power of only 14 watts, yet for measurement, with a properly designed receiver, over long periods (an hour a day, for example) this signal is just as useful as one of higher power would be.

Although it is not often mentioned in these reports, a useful part of our work lies in comparison of a number of standard frequencies. This is essentially a "free" service, as the frequency values are scaled from the records made for propagational studies. We usually observe most of the following stations:

- - - - - -

Rugby, England
Cutler, Maine
Ottawa, Ontario
Beltsville, Maryland
Summit, Panama Canal Zone
Boulder, Colorado
Oso, Washington
Lualualei, Hawaii

The frequency of each transmission is measured daily in terms of a cesium standard. These values are exchanged, usually on a monthly basis, with a number of standardization laboratories, particularly those at:

Washington, D. C.
Boulder, Colorado
Ottawa, Canada
Teddington, England
Neuchâtel, Switzerland
Paris, France
Brussels, Belgium
Stockholm, Sweden
Johannesburg, South Africa

At most of these places, similar measurements are made on at least one or two of the same signals (usually Rugby and Summit). Thus, a frequency can be rated with respect to a very widespread and presumably accurate average standard. In general, the daily frequencies are measured with a standard deviation of 2 to 4 parts in 10^{11} , a figure limited by propagational considerations.

Our measurement figures are also made available to a small number of other laboratories that do not participate in the same measurements program, but which seem to find our values useful.

The five aspects into which we usually try to divide our reports are discussed in the following paragraphs. As usual, this division is somewhat arbitrary.

1. Navigation

Our most useful contributions in this area in the past year have been in measurement of the phase velocity of propagation of VLF signals with data taken by the Omega system. Earlier reports have shown how the velocity is found to be of the order of 1.003 times the velocity of light, the high phase velocity being a waveguide effect.

A VLF signal is made up of components having different modes of propagation. Much of the detailed behavior of the signal as a function of distance is, therefore, a function of the phases in which these various modes arrive at a receiver. As this kind of interaction is most to be feared at short transmission ranges, it is wise to form our preliminary ideas from the behavior of long-distance signals. It has turned out that for distances greater than about 3000 kilometers we are unable to find any evidence of a variation of velocity with distance. We further find that velocities, as might be expected, are somewhat different for transmission over land and over sea water. It is probable that the velocity can eventually be related to the conductivity of the land, but so far we do not have enough observations to measure the effect. There is, however, a clear reduction in the phase velocity for transmission over the Greenland ice-cap, and further measurements will presumably yield the required relationship.

Having delineated the long-distance phase velocity, we have been able to examine the navigational observations made at positions where two of the three transmission paths were long and one was short. Any discrepancies between observation and the long-distance computation could then be attributed to the short path.

By thus working back from longer to shorter distances, we have been able to recognize and measure the deviations in phase as a function of distance. The gap near zero distance has not been closed yet, in the data available, but,

except for the case of overwater transmission at night, there do not seem to be any great surprises in store. Figures 1 and 2 show diagrams which have been deduced to date. Figure 1 shows the noon variation of the observed phase from the phase computed at the velocity of light, for sea water and for "average" land. The ordinate is negative, because the observed phase is earlier than the computed. At night, in Fig. 2, the long-distance velocity is slightly less than the velocity of light and the phase correction is added to the computed value. It appears that, at the long distances, the velocity is known to about a part in 10^4, and at the short distances the phase is determinate to the order of five microseconds, or $1/20$ period.

The navigational behavior of the system in the past year has been in accordance with these estimates. In one case an apparent discrepancy of about 10 microseconds, or one mile, was resolved by the discovery that the Naval charts of a region on the west coast of Mexico were in error by a mile. In many cases agreement between computations and observation has been good to a few hundred yards.

2. Noise

Although we have made certain plans for the future, there has been almost no activity in noise analysis during the past year.

3. Regulation of Oscillator Frequency

Our recent efforts in this area are in the combination of several standard frequency sources to yield a combined source of high accuracy and improved reliability. These sources might be cesium-controlled devices, or good crystals, or oscillators locked to distant radio signals, or a combination of these. The intent is to establish a standard that will maintain its integrity when one or more sources fail, and which will (to some extent) have a precision greater than that of a single source.

Breadboard operation indicates that this combination of sources will be very satisfactory, but we realize that questions of reliability can only be answered after the fact.
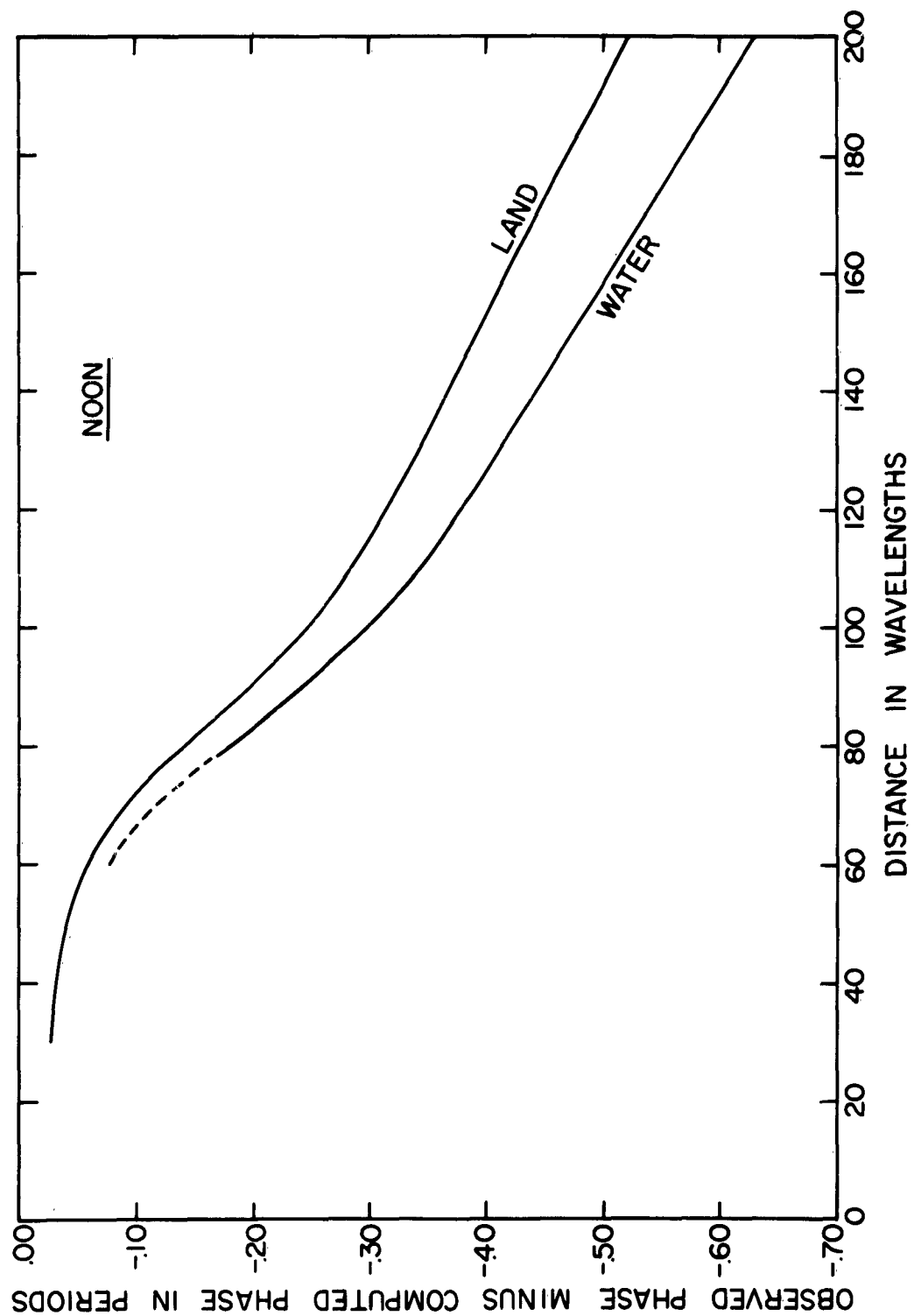
FIG. 1 THE "SHORT-DISTANCE" DEPARTURE OF THE OBSERVED PHASE
FROM THAT COMPUTED AT THE VELOCITY OF LIGHT. DAYTIME.
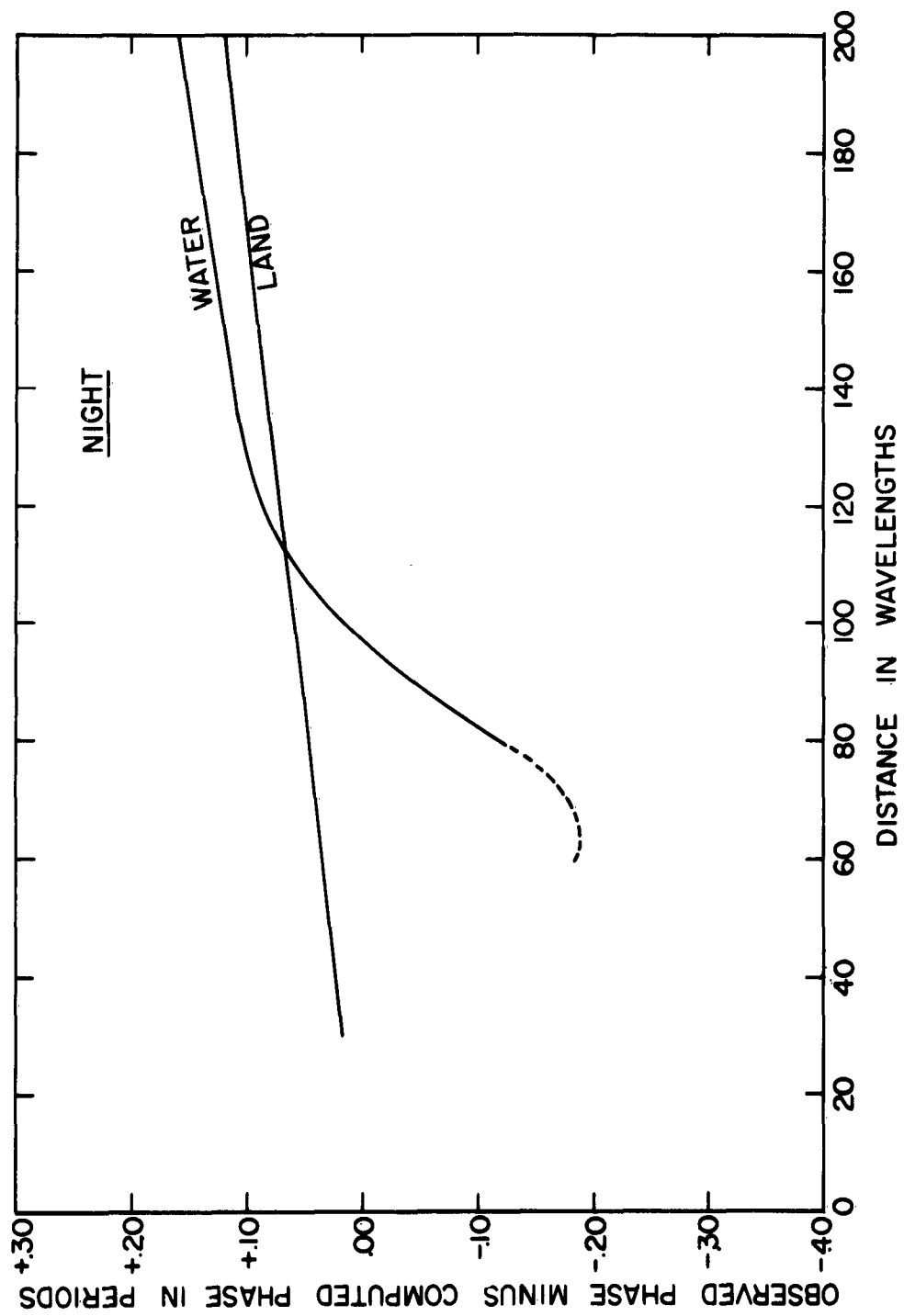
FIG. 2 THE FUNCTION OF FIG. 1 AT NIGHT. In both cases the relative phase velocity (or the slope of these curves) approaches a constant at a longer distance.

We have plans for the use of this kind of a time base in studies of the stability of time-signal transmission and for general laboratory purposes, but we also recognize the utility of such a device for the synchronization of navigation stations in which we are so much interested.

4. Transmission Time

Some parts of this problem at low frequencies can be kept distinct from the navigational data mentioned above. There are two long-term experiments, in particular, that are leading to more complete understanding of the problem.

The first, and perhaps the most interesting, is a long study of the phase of the Naval Station at Summit, Canal Zone, received at Cambridge. In November and again in February, the sunrise line coincides with the transmission path so that the speed of the change from nighttime to daytime conditions can be observed directly. The transition, incidentally, is completed in about 40 minutes. It occurs almost entirely _before_ sunrise, and thus coincides approximately with the twilight period.

Delineation of the way the path is affected by sunlight can be studied by observing the way the timing of the transition varies throughout the year. We find, for example, that the "control points" are, as might be considered reasonable, in the neighborhood of the points one-sixth and five-sixths of the way along the path. Between the ends of the path and these points the energy making up the signal at the receiver is presumably traveling between the earth and the reflecting layer and is unaffected by the state of the layer. The amount of sunlit path between the "control points" is then uniquely related to the transmission time.

Further delineation of these effects, and checking of them (as far as possible) on other paths, can presumably give us the computational methods we need for utilization of the low frequencies to greater precision than is now possible.

In a similar sense, data taken between Hawaii and Cambridge at a frequency of 19.8 kc are giving us ideas that the ultimate in timing precision has not yet been reached.

Figure 3 shows the variation in noontime phase of the Hawaiian signal over a period of 35 days. During this remarkably long time no corrections to the transmitter frequency were made. Consequently, the nearly parabolic shape of the curve reflects the small and relatively constant aging of the crystal oscillator at the transmitter. (Aging at the receiver is not a factor, because of the use of an Atomichron, as attested by a number of records made simultaneously.) By a process of fitting parabolas to the whole and to various parts of this curve, as described elsewhere, it is possible to estimate the degree to which variations from a true parabola are caused by propagational variations as distinguished from rate changes in the oscillator. In this case, as in previous shorter samples for this same transmission, it seems impossible to attribute an uncertainty of more than 0.3 or 0.4 μs to the propagation. This value is several times better than that customarily atrributed to VLF transmission. It is startling to realize that such a number corresponds to a fluctuation of the height of the reflecting layer of the order of 0.1 kilometer.

It may be that the combination of distance and frequency makes this transmission particularly immune to phase uncertainties. In some cases there are clearly "good" and "bad" distances or frequencies at which phase interference effects are very pernicious. It is unlikely, however, that the results on this path can exceed those attainable on others by any large factor. We are, therefore, led to the conclusion that most available data are still controlled to a considerable degree by instrumental error, and that new standards of excellence await more careful studies.

5. Communications

After our phase-shift keying experiment had operated successfully through the high noise period in the summer of 1961, the transmitting antenna in Hawaii was lost to us. It will be recalled that, with a power of 75 watts radiated and a speed of two-sevenths of a word a minute, errors were of the order of one percent. This condition was not appreciably altered by the changes in noise level between April and August.
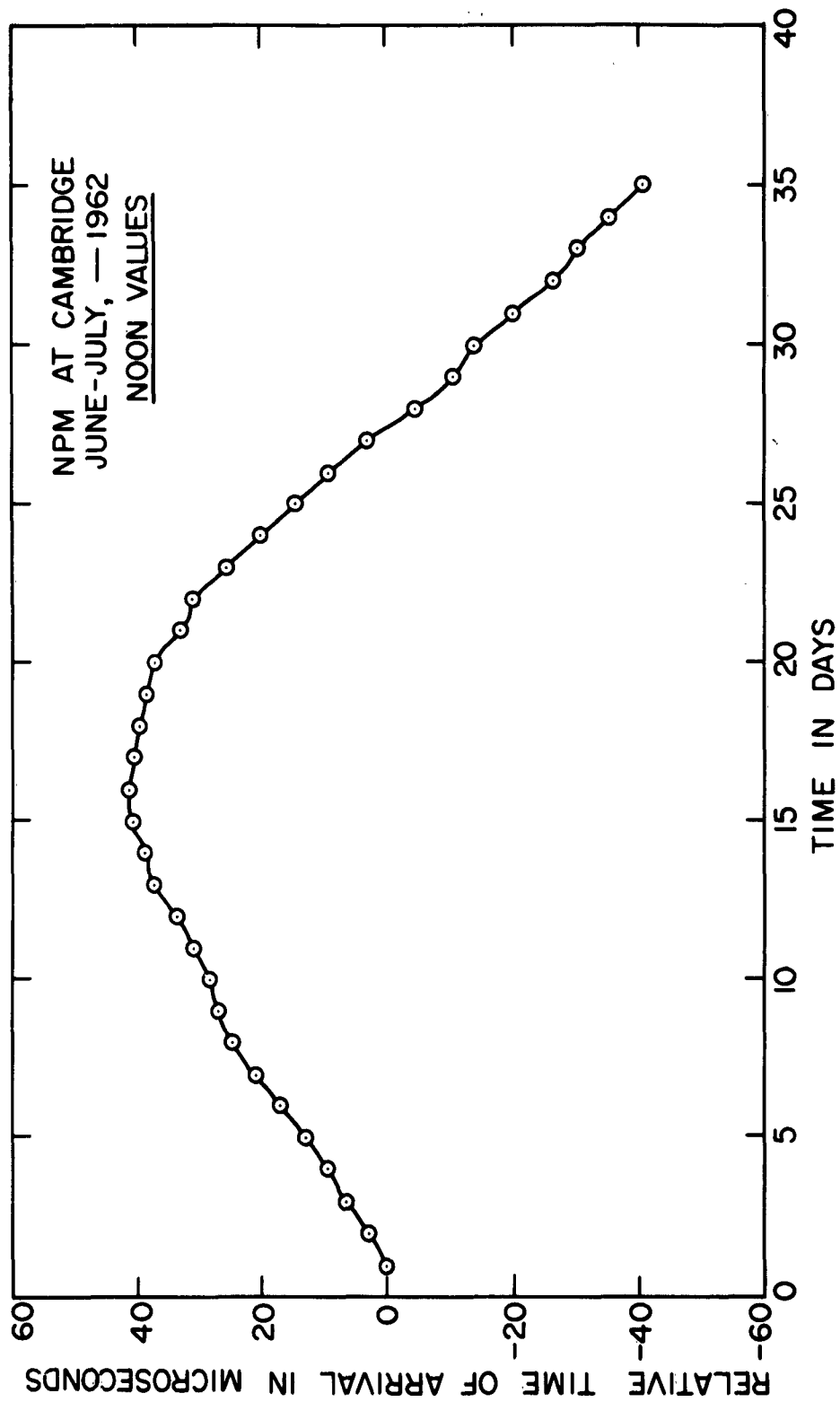
FIG. 3 THE DRIFT IN PHASE OF AN OSCILLATOR IN HAWAII, OBSERVED AT CAMBRIDGE. The variation is caused primarily by oscillator changes, and only slightly by propagational factors.

Since then, experiments with an artificial signal have continued, and the idiosyncrasies of the equipment have become familiar. It is now clear that a considerable fraction of the observed errors were locally produced in the teletypewriter, which was of ancient vintage, or in our translating equipment.

This discovery does not greatly change our conclusions about the experiment. It is still clearly operable with a signal some 38 decibels below the natural noise in a bandwidth of one kilocycle, and this value is at least ten decibels larger than the corresponding figure for interference by white noise.

This is perhaps the best result of the work so far: the delineation of the methods that permit operation near the white noise background between the large peaks in the natural VLF noise.

II. ELECTRON AND SOLID STATE PHYSICS[*]

Personnel

Dean H. Brooks	Mr. F. A. Collins
Assoc. Dean F. K. Willenbrock	Mr. R. F. Dixon
Prof. N. Bloembergen	Mr. S. Dmitrevski
Asst. Prof. P. S. Pershan	Mr. P. Heller
Dr. J. A. Armstrong	Mr. S. L. Hou
Dr. A. Bienenstock	Mr. C. U. Huang
Dr. S. Y. Feng	Mr. J. L. Merz
Dr. D. Gill	Mr. R. A. Myers
Dr. B. Harris	Mr. J. C. Owens
Dr. G. Peterson	Mr. E. Royce
Dr. G. Seidel	Mr. Y. R. Shen
Dr. E. B. Treacy	Mr. I. Svare
Mr. D. Adler	Mr. L. I. Van Zandt
Mr. M. G. Cohen	Mr. J. P. van der Ziel

1. Electrically Induced Quadrupole Splitting in GaAs , N. Bloembergen and D. Gill.

The nuclear spins Ga^{69} , Ga^{71} , and As^{75} have $I = \frac{3}{2}$. There is, however, no quadrupole splitting of the nuclear spin levels in GaAs , because of the cubic symmetry, $T_d = \bar{4} 3m$, at the nuclear spin sites. There is no center of inversion in this case of tetrahedral symmetry. The first and second derivatives of the electrostatic potential all vanish, but the third derivatives do not. A quadrupole interaction can be induced by an external electric field. There will be a shift in charge distribution of the tetrahedral bonds and a displacement of the atoms away from the center of each tetrahedron of surrounding atoms. The four originally degenerate spin levels will be split into two Kramers doublets by the electric field.

This effect can be observed, if one applies a large magnetic field as well. In the absence of an electric field the usual single resonance line at $h\nu_o = g\beta H_o$ is observed, corresponding to transitions between the four equally spaced Zeeman levels. The application of an electric field splits this line into a triplet.

- - - - - - -

Gallium arsenide represents a judicious choice from among the many III-V compounds, all of which should, in principle, show the same effect. Since one wishes to apply an electric field of $20\,kv/cm$ or more, the semiconducting material has to be available in a high resistivity form with almost perfect compensation of the carriers. Our sample has a resistivity higher than 10^8 ohm cm at $77°\,K$ and the voltage could be applied without heating the sample. Furthermore, the linewidths of the nuclear resonances should be as narrow as possible. For compounds with heavier elements the lines are severely broadened by indirect exchange interactions. Gallium arsenide is a good choice with fairly large quadrupole moments and relatively narrow lines.

The high symmetry reduces considerably the number of non-vanishing components in the tensors of Eq. 1 in reference 1. One has $R_{14} = R_{25} = R_{36}$ in Voigt's notation ($4 \equiv yz \equiv zy$ etc.), $S_{11} = S_{22} = S_{33}$, and $S_{12} = S_{21} = S_{13} = S_{31} = S_{23} = S_{32} = -\frac{1}{2}S_{11}$, $S_{44} = S_{55} = S_{66}$ for each isotope. The piezoelectric tensor for the crystal as a whole has the non-vanishing components $d_{14} = d_{25} = d_{36}$. Note that the crystal has the same point symmetry as each individual lattice site.

If the electric field is applied along the [111] direction, $E_x = E_y = E_z = 3^{-1/2} E$, one finds an axially symmetric gradient tensor with a value $e\,q_{z'z'}$ along [111] given by

$$<e\,\Delta q_E>_{111} = (2/3^{1/2})\,(R_{14} + S_{44}\,d_{14})\,E \quad .$$

The observed splitting of the Zeeman lines between the central component and the observed satellite on either side is

$$h\,\Delta\nu_E = \frac{3}{2}^{-1/2}\,(3\cos^2\theta_H - 1)\,e\,Q\,(R_{14} + S_{44}\,d_{14})\,E \qquad (1)$$

where θ_H is the angle between H_o and the [111] direction.

We have measured $\Delta\nu_E$ for the three isotopes when both E and H are parallel to [111], ($\theta_H = 0$) . The satellites are broadened because of an inhomogeneous distribution of electric field strength over the sample. (The sample consisted of several small slabs (approximately 5 x 5 x 1mm each). The high resistivity GaAs was kindly supplied by Dr. Hilsum of

Baldock, England and by Dr. Weisberg of RCA. Slight variations in thickness, edge effects of the electrodes, or inhomogeneity of the resistivity inside the sample are responsible for this. The piezoelectric constant is $d_{14} = (2.0 \pm 0.5) \times 10^{-8}$ cgs , and an upper limit was put on S_{44} by applying an external uniaxial stress on a GaAs crystal along [111] direction. We found $S_{44} < 2 \times 10^{15}$ cgs , and, therefore, $d_{14} S_{44} < 0.005 R_{14}$. The results for $\Delta \nu_E$ and R_{14} are listed at the end of this report. Note that R_{14} is the same, within the limits of error, for the two Ga isotopes. This was, of course, expected. The gradient is the same, and $\Delta \nu_E$ is proportional to the quadrupole moment. The gradient at the As site, and, therefore, R_{14} , is somewhat larger. The effect of the electric field on the covalent orbital near As can be different, and there exists a somewhat different shielding by the atom core from external charge displacements.

A comparison with theory is facilitated by the simple structure. First, the effect of the displacement of external charges will be considered. The effective charge can be estimated from the Szigeti relation,

$$e_{eff} = \frac{3\omega_o}{n^2 + 2} \left(\frac{M(\epsilon - n^2)}{4\pi N_o} \right)^{1/2} \quad . \tag{2}$$

With the dielectric constant $\epsilon = 12.5 \pm 0.2$, the index of refraction $n = 3.3$, the transverse fundamental optical mode frequency $\omega_o = 5.04 \times 10^{13}$ sec^{-1} , one finds $e_{eff} = 0.46e$. The displacement of the As lattice, relative to the Ga lattice, is

$$\Delta r = 3(\epsilon_{dc} - n^2) \, E / 4\pi N e_{eff} (n^2 + 2) \tag{3}$$

where N is the number of GaAs molecules per unit volume. The effective charge e_{eff} at each of the corners of the tetrahedron includes the effect of electronic polarization due to nuclear displacements. A displacement Δr from the center towards one of the corners leads to a gradient at the nucleus,

$$<e \, q_E^{ion}>_{111} = \frac{40}{3} (1 - \gamma_\infty) \frac{3(\epsilon_{dc} - n^2)}{4\pi N a^4 (n^2 + 2)} E$$

where $a = 2.44 \text{Å}$ is the Ga-As distance; $1 - \gamma_\infty$ the Sternheimer antishielding factor of the gradient by core electrons[see reference 1]. Substituting numerical values $1 - \gamma_\infty = 25$ for Ga, and 30 for As , one finds

$$R_{14}{}^{ion}(Ga) = +1.2 \times 10^9 \text{ cm}^{-1}. \quad R_{14}{}^{ion}(As) = 1.4 \times 10^9 \text{ cm}^{-1}.$$

This includes the effect of electron polarization insofar as it is produced by atomic displacement.

Next, the distortion of the covalent orbitals at fixed nuclear positions has to be considered. This may be labeled the "optical" contribution [2]. Since an _average_ property of the valence and conduction bands is to be computed, localized molecular orbitals should give a fair representation of the average structure of the valence and conduction bands. The "closed shell" structure of the covalent crystal bonding suggests that linear combinations of tetrahedral orbitals pointing from the Ga and As atoms along the [111] direction and three other body diagonals, are appropriate zero-order wave functions (the overlap integral is assumed small compared to $\lambda \simeq 1$) ,

$$\Psi_{val} = (\psi_{Ga}{}^{tet} + \lambda \psi_{As}{}^{tet})(1 + \lambda^2)^{-1}$$

$$\Psi_{cond} = (\lambda \psi_{Ga}{}^{tet} - \psi_{As}{}^{tet})(1 + \lambda^2)^{-1} \tag{4}$$

$$\psi^{tet} = \tfrac{1}{2}(\psi_{4s} + \psi_{4px} + \psi_{4py} + \psi_{4pz})$$

Higher excited states, 4d, 5s, etc., are ignored and the four tetrahedral orbitals are treated independently as mutually orthogonal wave functions.

The electric field along the bond direction will change the ionic character $(1 - \lambda^2)(1 + \lambda^2)^{-1}$ of the bond. It admixes some conduction band wave function to the valence band. If the perturbation equation is used with one term, $|n) = |\Psi_{cond})$ and an average value $(W_n - W_o)^{-1}$ is adopted, the change in the electric field gradient due to the tetrahedral orbital along [111] is

$$\lambda(1 + \lambda^2)^{-1} < (W_n - W_o)^{-1} > \frac{3}{4} q_{at} e E_{loc}^2 \int \Psi_{cond} r \Psi_{val} d\tau \quad .$$

The other three orbitals have each a component $-\frac{1}{3} E_{loc}$ along the bond direction. Components perpendicular to the bond have zero matrix elements. If the gradient tensors along these three other bonds are transformed to a coordinate system with the z-axis along $[111]$, it is found that the total change in field gradient from the covalent effect is:

$$< e q_E^{cov} >_{111} = 2\lambda(1 + \lambda^2)^{-1} < (W_o - W_n)^{-1} > e q_{at} E (cond|er| val) . \quad (5)$$

The acting local field has been taken equal to the macroscopic field E in this problem for the same reason as in the preceding section.

The dipole moment matrix element may be calculated numerically from the appropriate atomic wave functions. It may also be directly related to the observed optical polarizability. The same approximations about the local field should be used in this calculation. Instead of the Lorentz-Lorenz formula, one has

$$\frac{4}{3} N\alpha = \frac{8N}{3} \frac{|(cond|er|val)|^2}{W_n - W_o} = \frac{n^2 - 1}{4\pi} \quad . \quad (6)$$

Substitution of numerical values, $q_{at}(Ga) = -18.9 \times 10^{24} cm^{-3}$ $q_{at}(As) = -40.8 \times 10^{24} cm^{-3}$, $W_n - W_o = 4 eV$ (the forbidden gap is about $2 eV$), $\lambda = 0.5$ into Eqs. 5 and 6 yields:

$$R_{14}^{cov}(Ga) = 1.05 \times 10^{10} cm^{-1}. \quad R_{14}^{cov}(As) = -2.3 \times 10^{10} cm^{-1}.$$

The covalent effect is an order of magnitude larger than the ionic displacement effect. The theoretical value $R_{14}(Ga) \approx 12 \times 10^{10}$ is within twenty percent of the observed value. The theoretical value for $R_{14}(As)$ is almost sixty percent higher than the observed value. This may be indicative of the relatively larger importance of 4d and 5s admixtures on the As wave function. The agreement is satisfactory in view of the drastic theoretical approximations, which treat the covalent crystal and molecular crystal similarly. The effective local field value on the orbital still constitutes the largest single uncertainty.

GaAs DATA

	NMR Frequency at 10^4 Oe	$Q \times 10^{24}$ cm^2	$\Delta \nu_E$ $\dfrac{kc/sec}{10^{4v}/cm}$	R_{14}
Ga^{69}	10.23 Mc/sec	0.2318	3.5 $\pm$ 0.6	1.05 $\times$ 10^{10} cm^{-1}
Ga^{71}	12.99	0.1416	1.9 $\pm$ 0.2	0.9 $\times$ 10^{10} cm^{-1}
As^{75}	7.29	0.3	6.5 $\pm$ 1.5	1.55 $\times$ 10^{10} cm^{-1}

$$d_{1y} = (2.0 \pm 0.5) \times 10^{-8} \, cgs$$

$$S_{yy}(Ga) < S_{yy}(As^{75}) < 2 \times 10^{15} \, cgs$$

Measured electric field effects are in the third column from the left.

References

1. Armstrong, Bloembergen, and Gill, Phys. Rev. Letters, 7, 11 (1961).

2. N. Bloembergen, J. Chem. Phys., 35, 1131 (1961).

- - - - -

2. **L-Band Traveling Wave Maser for Radioastronomy, E. B. Treacy.**

An L-band traveling wave maser (TWM) has been developed for observation of hydrogen line emission in radioastronomy. The development and construction were carried out at Bell Telephone Laboratories, Murray Hill, New Jersey, in cooperation with M. L. Hensel of the B. T. L. staff. The maser is tunable over the approximate range 1330 Mc to 1430 Mc with an instantaneous bandwidth in excess of 10 Mc throughout the tuning range.

The active (maser) material used is ruby with the magnetic field applied at 90° to the c-axis of the crystal. The signal is amplified by the $m_s = -1/2 \rightarrow m_s = -3/2$ transition (in the high-field notation), while the pump power

is applied between the $m_s = -3/2$ and $m_s = 1/2$ levels. For this mode of operation in the frequency region of interest, one requires a magnetic field range of 1940-2000 gauss and a pump frequency in the range 11.13 to 11.29 kMc. In these respects the operation is identical to that used in the cavity maser built by Cooper and Jelley[4].

Physically, the maser consists of two six-inch sections placed side by side in the magnetic field and joined in series. Each section contains a comb-type slow wave structure of the type described by the B. T. L. workers [2]. The comb structure is loaded with ruby on both sides and trimmed with rutile and alumina to produce the desired transmission characteristics. Isolation is provided internally through the use of polycrystalline YIG wafers located in the regions of strong r f . magnetic field. The magnetic field is applied along the direction of the individual fingers, while the c-axis of the ruby lies in a plane at right-angles to this direction. The polarization effects described in reference 2 are not so pronounced in this frequency region, since the matrix elements of the $-3/2 \rightarrow -1/2$ transition are not circularly polarized any more. The two senses of circular polarization have associated with them transition probabilities in the ratio of about three to one.

Therefore, the filling factor can be raised significantly by adding the second slab of ruby, as contrasted with the higher frequency TWM's, which are loaded with ruby on one side only.

The device has been designed to operate at $4.2^{\circ}K$. Although the design problems are significantly simplified by operating at lower temperatures, one then faces the problems of pumping the helium through a long line and of temperature stability of the bath.

A dewar has been purchased from Hofman Laboratories. A tunable permanent magnet has been constructed. It is a cut-down version of the magnet used for the masers in Project Echo [3].

The maser has provided net gain of about 30dB in the frequency range of interest. In recent months the comb structure has suffered from the effects of thermal cycling between helium and ambient temperatures as a result of the clamping action of the ruby on the fingers of the comb. The resulting

irregularities cause reflection of the signal into the isolator. It is expected that this trouble will be corrected soon by a slight alteration in the structure.

The package for installation on the 60-foot disk is being designed by Mr. F. Robie, and construction is to begin shortly. After some laboratory tests, the maser will be incorporated into a Dicke-type switched radiometer and installed at the Agassiz Station of Harvard.

An article on the design of L-band TWM's has been submitted for publication in the Bell System Technical Journal with M. L. Hensel as co-author.

References

1. J. V. Jelley and B. F. C. Cooper, Rev. Sci. Instr. 32, 166 (1961).

2. R. W. DeGrasse, E. O. Schulz-DuBois, and H. E. D. Scovil, Bell System Technical Journal 38, 1 (1959) .

3. R. W. DeGrasse, J. J. Kostelnick, and H. E. D. Scovil, Bell System Technical Journal, "Project Echo, " 40, 1117 (1961).

- - - - -

3. Electrically Induced Shift of the F^{19} Hyperfine Interaction in MnF_2 , P. S. Pershan and N. Bloembergen.

The initial work on this problem was described in the Annual Progress Report No. 60 and in published papers[1, 2]. Crude estimates of the size of the effect that are made in APR60 must be modified as follows. If one takes proper account of the electronic polarization caused by the ionic displacements, Eq. 2 on page 44 becomes:

$$\Delta r_{II} = \Delta ua \sqrt{2} = \frac{\epsilon_{\perp} - n_{I\!I}^2}{4\pi Ne} \left(\frac{3}{n_{I\!I}^2 + 2} \right) \cdot E \qquad (1)$$

where $n_{I\!I}^2 = \epsilon_{\perp} (W)$ for W equal to an optical frequency. The correction is small and of little importance.

The proper electric field to use in estimating the covalency effects, Eq. 4 on page 45 (APR60), is not the local field $(\epsilon_{\perp} + 2) E/3 \approx 3E$, but the local field averaged over the molecular orbit. The average is just the macroscopic field E in the material. Equation 4 thus becomes:

$$\frac{1}{\lambda} \left(\frac{\partial \lambda}{\partial E} \right)_u = \frac{er}{W_{Mn} - W_F} \quad . \tag{2}$$

Due to an improper identification of the optical absorption spectrum, $W_{Mn} - W_F$ was taken to be 5 ev . A better value, obtained by Keffer, Oguchi, O'Sullivan, and Yamshita is 25 ev . Covalency effects are thus estimated to be at least a factor 15 smaller than originally given. One can attempt to calculate this effect from first principles following the method of Keffer et al. [3], but the integrals that enter such a calculation cannot be evaluated at the present time.

With a combination of electric and magnetic fields, it is possible to study the domains of antiferromagnetic $Mn F_2$. Consider the $Mn F_2$ unit cell shown in the upper portion of Fig. 1. Without any external fields, all F^{19} nuclei have the same resonant frequency, and the absorption versus frequency is as shown in the first curve: E, H = 0 . With an electric field applied in the [110] direction and without any magnetic field, the F^{19} nuclei at A sites will split and the B sites will be unaffected; this is shown in the second curve $E \neq 0$, H = 0 . The third curve shows the absorption when there is an applied H field in the [001] direction, but no E field. The A sites all have local fields pointed up, and thus add to the applied field; i. e. ,

$$| H_A^{total} | = | H + H_{HYPER} | \quad .$$

The B sites have opposite hyperfine fields:

$$| H_B^{total} | = | H - H_{HYPER} | \quad .$$

The magnetic splitting is $2\gamma_F H$.

If the electric and magnetic fields are applied simultaneously, the A spins split into a doublet while the B spins remain unaffected, as shown in the fourth curve. Had we chosen to illustrate these splittings with the opposite domain in which the Mn^{++} magnetic moments, that is, the arrows, were reversed, the local fields would also reverse sign, and we would have obtained the fifth curve. If a given single crystal were composed of equal fractions of the two opposite types of domains, the last curve would be obtained.
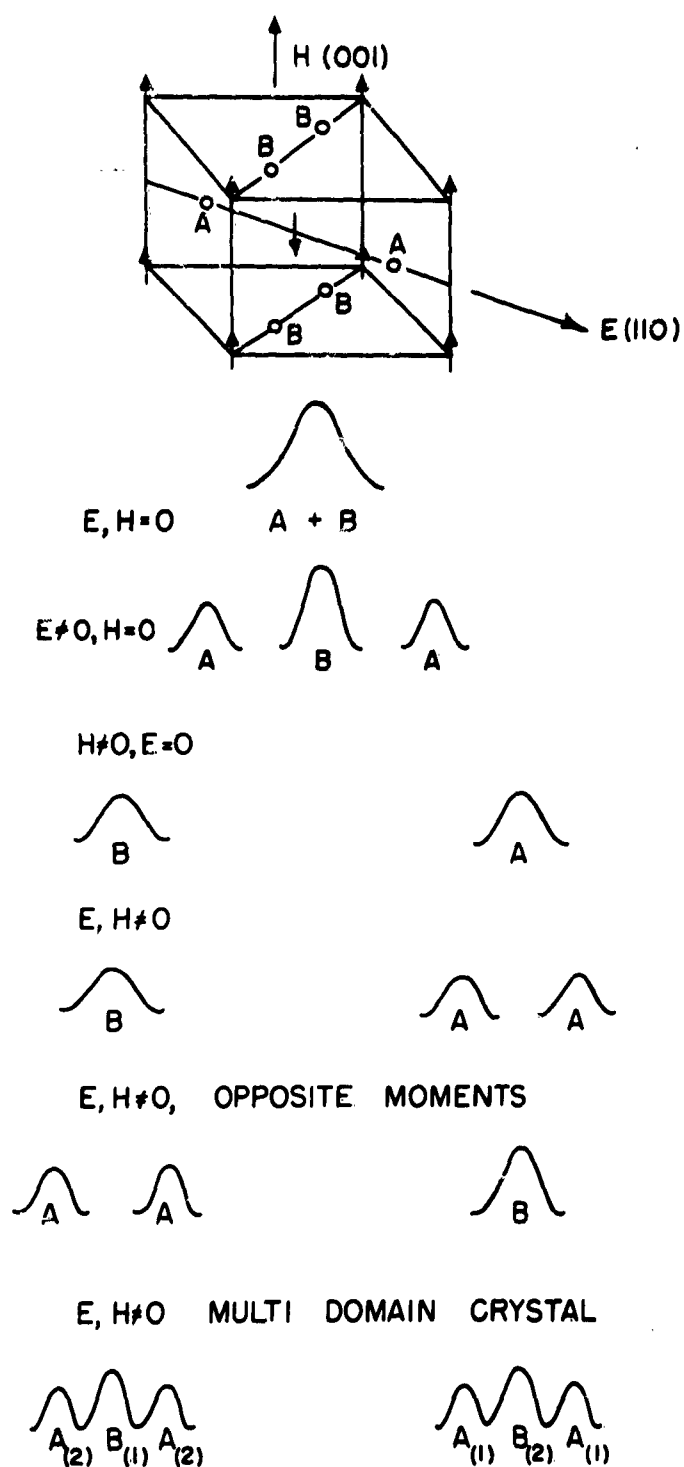
FIG. 1 THE Mn F$_2$ UNIT CELL AND THE ABSORPTION SPECTRA FOR VARIOUS COMBINATIONS OF ELECTRIC AND MAGNETIC FIELDS

The experiments in APR60 were repeated with a single crystal of MnF_2 1mm x 4.8mm x 7.9mm with the [110] direction perpendicular to the broad face. The results, shown in Fig. 2, for various combinations of fields, are traces of the absorption derivatives. The last two traces, with both electric and magnetic fields, are clearly much more like a doublet and a singlet than two triplets. The signal-to-noise level is poor because it was difficult to operate the spectrometer at a low enough level without saturating the lines. There is no evidence for more than one domain, and even with poor signal-to-noise, we can safely claim the crystal is at least 80 percent of one domain.

Absence of domain walls in perfect crystals of MnF_2 at $4.2^\circ K$ is expected on the basis of theoretical calculation of Li [4]. The large anisotropic energy of an antiferromagnetic domain wall is not compensated by a decrease in the magnetostatic energy as in ferromagnetic material. The gain in entropy is minor, and not sufficient to create a domain wall at $4.2^\circ K$.

Antiferromagnetic domains begin to nucleate and grow as soon as the crystal is lowered through the Néel point. In a small temperature decrement, however, they become thermodynamically unstable and diffusion of the walls eliminates them. The more recent experiments by Alperin, Brown, Nathans, and Pickart [5], using the scattering of polarized neutrons to detect antiferromagnetic domains, confirm these findings. These techniques, capable of probing very small areas, find multi-domains at the corners of their otherwise single domain crystal, suggesting that domain walls can be trapped by rather special arrangements of crystal imperfections, i.e., dislocations. Neutron diffraction methods are also capable of domain studies just below the Néel point.

References

1. N. Bloembergen, Phys. Rev. Letters 7, 90 (1961).

2. P. S. Pershan and N. Bloembergen, Phys. Rev. Letters 7, 165 (1961).

3. F. Keffer, T. Oguchi, W. O'Sullivan, and J. Yamshita, Phys. Rev. 115, 1553(1959).

4. Yin-Yuan Li, Phys. Rev. 101, 1450 (1956).

5. H. A. Alperin, P. J. Brown, R. Nathans, and S. J. Pickart, Phys. Rev. Letters 8, 237 (1962).

- - - - -

4. Stark Effect of the Cl^{35} Quadrupole Resonance in Molecular Crystals, N. Bloembergen and R. W. Dixon.

In most organic compounds most Cl nuclei are not at centers of symmetry. If one substitutes Cl in a hydrocarbon, this atom is covalently bonded to a carbon atom on one side, but not on the other side. Even in solid Cl_2 each chlorine nucleus is not a center of symmetry, although the center of the molecule is. After the first observation of the Stark shift in paradichlorobenzene by Armstrong, Bloembergen, and Gill [1], Dixon has observed the field effect on the pure quadrupole resonance of Cl^{35} in a series of molecular crystals. The asymmetry parameter in all these crystals is small and will be ignored.

The linear variation with E of the zero field quadrupole splitting in the case of axial symmetry with $I = \frac{3}{2}$ is given by

$$h\Delta \nu_E = \frac{1}{2}R_{zzz}\, e\, Q\, E \cos \theta = \Delta \nu_E^{max} \cos \theta \qquad (1)$$

where θ is the angle between $\vec{E}$ and the z-axis of symmetry. Note that the Kramers degeneracy of the levels $\pm \frac{3}{2}$ and $\pm \frac{1}{2}$ is not lifted by $\vec{E}$. Since the rf-magnetic field is always at right angles to E in the experimental arrangement, the normalized powder line shape due to the electric shift alone is a segment of a parabola.

$$g_E(\nu) = \frac{3}{8\Delta \nu_E^{max}} \left[1 + \left(\frac{\nu - \nu_0}{\Delta \nu_E^{max}} \right)^2 \right] \qquad \text{for} \quad -\Delta \nu_E^{max} \leq \nu - \nu_0 \leq \Delta \nu_E^{max}.$$

$$\tag{2}$$

$g_E(\nu) = 0$ otherwise.
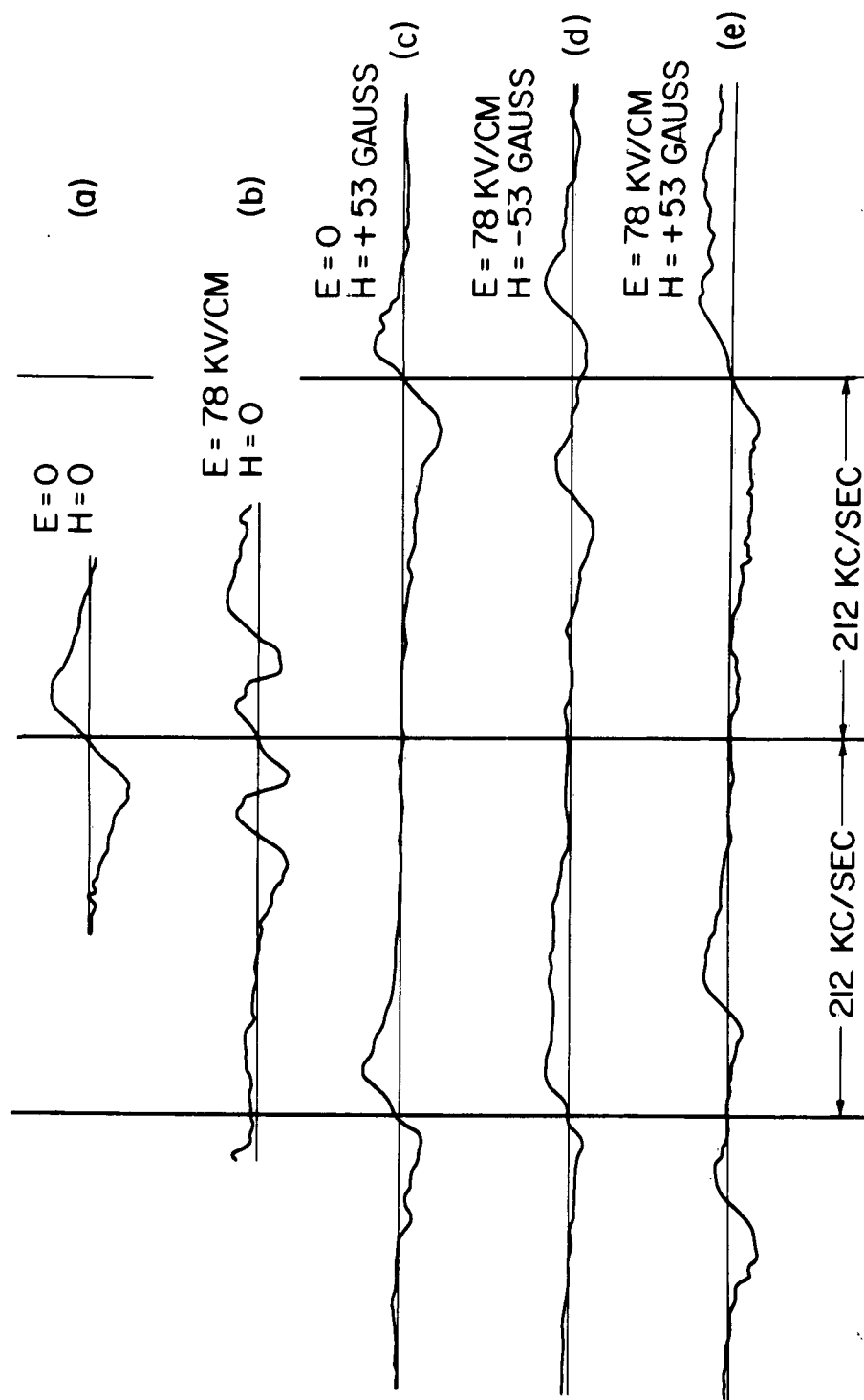
FIG. 2   RECORDINGS OF THE FIRST DERIVATIVES OF THE Mn F$_2$ ABSORPTION
SPECTRA FOR VARIOUS COMBINATIONS OF ELECTRIC AND MAGNETIC
FIELDS

This characteristic line shape has been detected in some powder samples, where the intensity was sufficient to probe the broadened line with a small modulation sweep. In general, the constant R_{zzz} can be determined from the observed increase in second moment of the line, when the electric field is applied,

$$< \Delta v^2 >_E = \frac{2}{5} R_{zzz}^2 \, E^2 (\frac{1}{2} e \, Q h^{-1})^2 \quad . \tag{3}$$

Such determinations have been made by Dixon for the compounds listed in Table I. There are only small variations of R_{zzz} in the various hydrocarbon and benzene derivatives. One might say that this reflects the fact that the C - Cl bond is essentially the same in all substances. The small amount of π - bonding in the benzene compounds is too small to have a noticeable systematic effect on the electric shift.

Actually, there was a hopeful expectation at the beginning of these experiments that the constants might be quite different, even for different resonance lines in the same compound.

They correspond to different positions in the unit cell with different Lorentz local field corrections. The experimental results imply about the same effective field at each bond. Perhaps the following picture is more accurate. The bonding orbital is so spread out that it essentially probes the average microscopic field. Furthermore, the bond is elongated. The acting component of E parallel to the bond should, therefore, be taken equal to the component of the applied macroscopic field E along the bond direction. Note that components perpendicular to the bond do not produce a linear effect. This procedure has been adopted in the present report.

The theory of the chlorine quadrupole coupling in a covalent bond is reviewed by Das and Hahn [2], who give the following simplified expression

$$q_{zz}^{Cl} = (1 - s^2 + d^2 - I - \pi) \, q_{at}^{Cl} \quad . \tag{4}$$

Here q_{at} is the gradient q_{zz} produced by the atomic p_z - orbital; s^2 is the partial s-character, d^2 the partial d-character of the hybridized chlorine orbital; I is the ionic character of the bond, and π describes the partial

double bonding via the π- orbitals. Each of these quantities, except a_{at}^{Cl}, will vary linearly with the perturbation, $- e E r$, on the bonding electron. In principle, the variations $\partial s / \partial E$, etc. can be determined by solving the determinantal problem of the linear combination of atomic orbitals by means of the Ritz variational procedure.

If one makes the assumption that the amount of d- and π - character of the C - Cl bond is very small both in aliphatic and aromatic compounds, one finds fair agreement between theory and experiment. The electric field effect can be explained with reasonable values of sp-hybridization and ionic character [3], if one takes $E_{loc} = E$ along all bond directions.

The larger electric shift in solid Cl_2 is quite interesting. The ionic character I vanishes in the Cl - Cl bond because of symmetry. One usually assumes negligible d and π- bonding, because this requires promotion to 3d and 4s orbitals which seems energetically unfavorable. Since the observed quadrupole coupling Cl_2 is very close to the value given by q_{at}^{Cl}, one arrives at the conclusion that s = 0, and that the orbital character around each Cl-nucleus is almost pure p-type. If this were true, the electric field shift should be very small. This contrasts sharply with the observation of Dixon. His provisional data indicate that there is considerable hybridization of such a nature that $s^2 - d^2 + \pi^2 \approx 0$, but $\partial / \partial E (s^2 - d^2 + \pi^2) \neq 0$. It can be shown that $\partial s / \partial E$ and $\partial d / \partial E$ have opposite signs in covalently bonded chlorine atoms. The electric shift thus leads to interesting information about the nature of bond. It constitutes another parameter that should be fitted by the assumed chemical nature of the bond.

Musher [4] has recently shown that systematic variations in the zero field quadrupole coupling of a series of di-substituted chlorobenzenes can be explained by the internal electric field produced by a polar group at the position of the C - Cl bond in another part of the same molecule. The external electric field effect lends credence to such an explanation.

Similar explanations had been given earlier to explain systematic variations of proton chemical shift in substituted hydrocarbons. The very strong internal electric fields from the polar group at the position of the

C-H bond change its ionic character. Direct effects of external electric field on the chemical shift have unfortunately not been observed because of their small size.

TABLE I
Electric field effect on the Cl^{35} quadrupole splitting R_{zzz} is evaluated from the broadening in polycrystalline samples.

Compound	ν_0 (NQR) at 77°K Mc/sec	R_{zzz} x 10^{-9} (cm^{-1})
Cl_2	54.248	7.8 $\pm$ 1.0
$CH_2 Cl_2$	35.9934	6.5 $\pm$ 0.8
$CHCl_3$	38.3081 38.2537	6.7 $\pm$ 0.3
CCl_4	40.6083	5.5 $\pm$ 1.0
$CFCl_3$	39.157	4.6 $\pm$ 0.2
$C_6 H_5 Cl$	34.6219	6.5 $\pm$ 0.5
$p\text{-}C_6 H_4 Cl_2$	34.780	6.4 $\pm$ 0.5
$C_6 Cl_6$	38.504 38.465 38.390	4.8 $\pm$ 0.3

References

1. J. Armstrong, N. Bloembergen, and D. Gill, J. Chem. Phys. 35, 1132(1961).

2. T. P. Das and E. L. Hahn , Solid State Physics, Supp. II, Edited by Seitz and Turnbull, Academic Press, New York, 1958.

3. N. Bloembergen, J. Chem.Phys. 35, 1131 (1961).

4. J. I. Musher (to be published).

- - - - -

5. Rapid Microwave Cavity Q Measurements in the Presence of Series Losses, J. P. van der Ziel.

During the work on the measurements of dielectric losses at microwave frequencies, it was necessary to measure cavity Q values rapidly and accurately. The method given below is a simplification of other reflectometer methods [1, 2], and differs only in that the impedance necessary to find the half-power points can be obtained from a single curve irrespective of the series loss. Series losses are due to the coupling system and become important in the millimeter wavelength region. In the next section the experimental method is outlined and then the theory is analyzed to simplify the procedure.

Experimental Procedure

The essential components of the reflectometer circuit used to measure cavity Q's are shown in Fig. 3. The power reflected from the cavity is compared with the incident power by means of the oscilloscope, and the amplitude of the incident signal is adjusted with the calibrated attenuator. The signal from the mixer-radio combination intensity modulates the oscilloscope trace and produces a pip when the FM klystron frequency differs from the c.w. klystron frequency by the radio frequency.

Typical oscilloscope traces are shown in Fig. 4, and explained below[2].

(a) The cavity is replaced by a short circuit. The incident and reflected traces are superposed.

(b) The cavity is replaced. The attenuation must be increased by Z_∞ to superpose the incident and reflected traces far from resonance due to the series loss.

(c) The attenuation is increased to a total of Z_0 until the incident trace just touches the bottom of the resonance curve.

(d) The attenuation $Z_{1/2}$ necessary to give the half-power points is then inserted and the frequency difference between the crossover points is measured with the radio receiver.

It will be shown in the next section that it is not necessary to replace the cavity by a short circuit, but that the impedances may be referred to the superposition of the reflected cavity and incident traces.
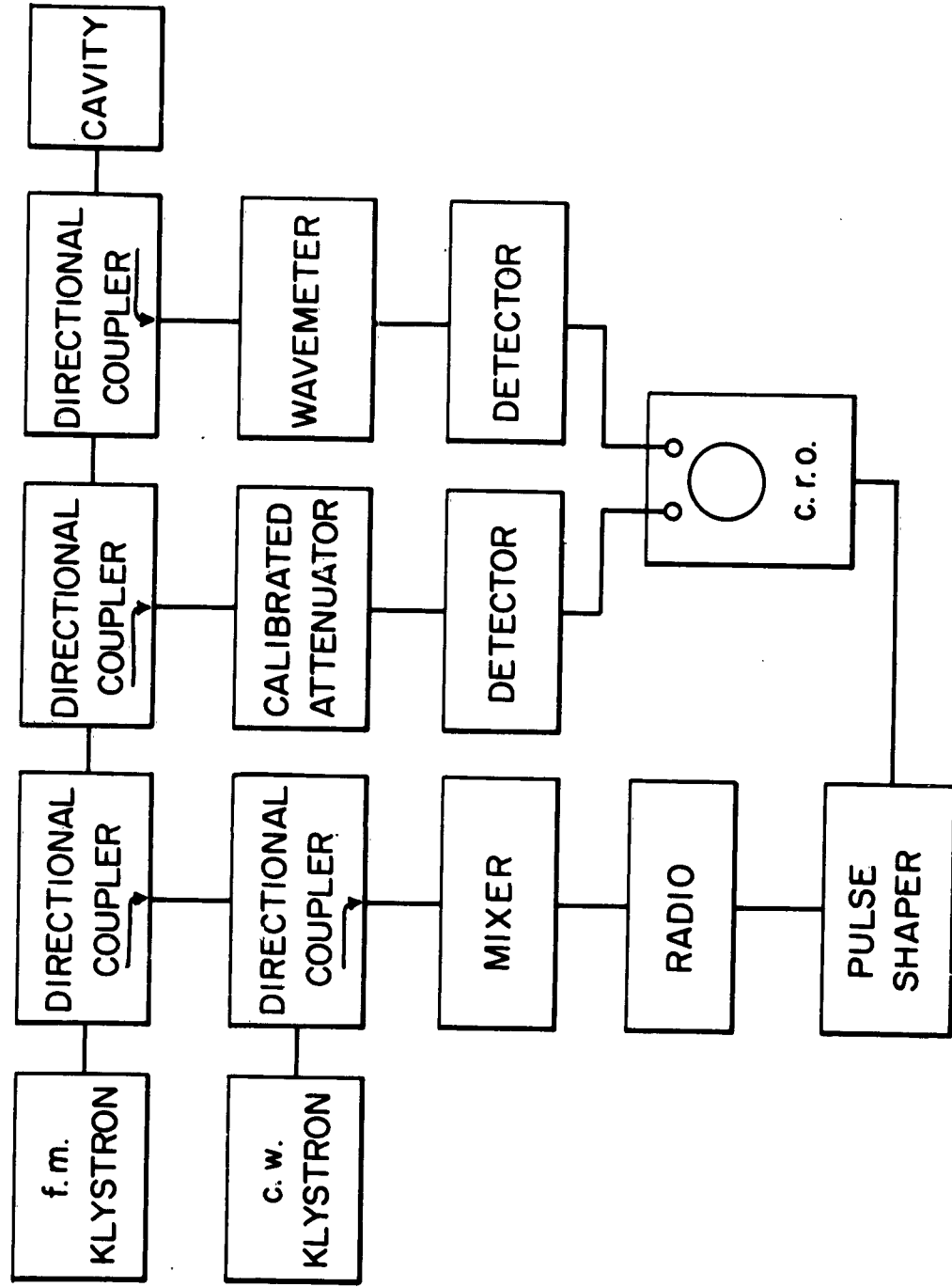
FIG. 3 CIRCUIT FOR MEASURING CAVITY Q
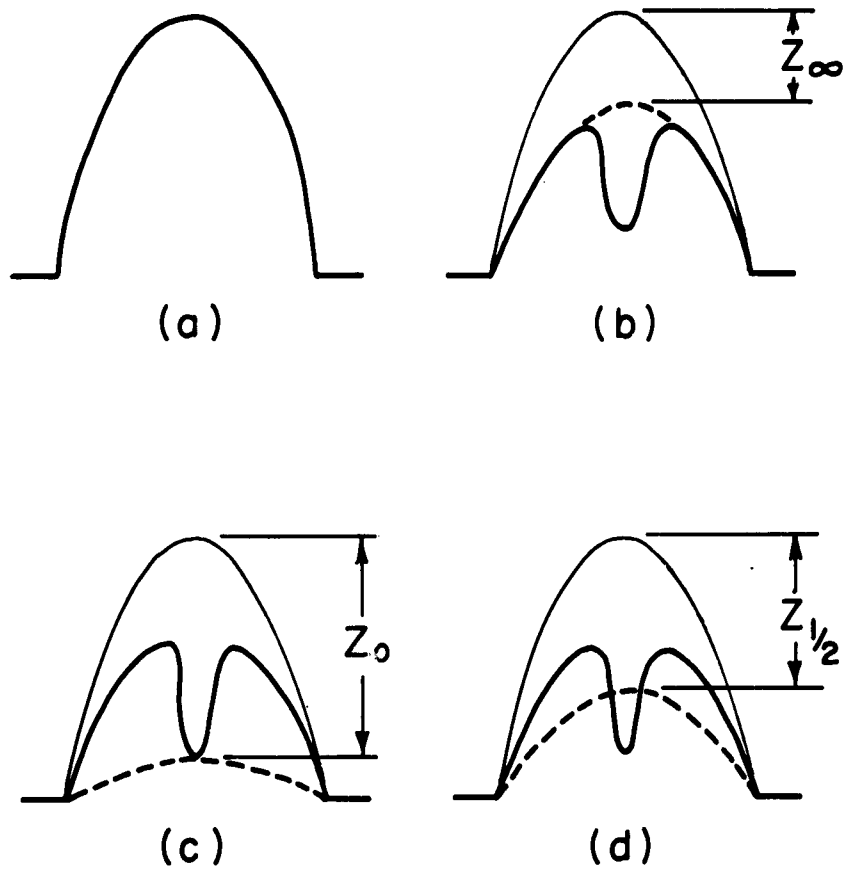
FIG. 4 RESPONSE OF THE MICROWAVE CIRCUIT AS VIEWED ON THE
        OSCILLOSCOPE

Theory

The equivalent circuit theory of microwave cavities has been known for a long time [1]. In this section, a simple relation for the half-power points of a cavity in the presence of series loss will be derived. Following standard theory [3], the cavity is assumed to be described by the equivalent circuit in Fig. 5-a. The series loss is indicated by R_s , and Y_o is the impedance of the input line. All measurements are made at the reference $a - a'$ to which the cavity impedances may be transformed as in Fig. 5-b.

The loaded cavity Q is defined as

$$Q_L = \frac{2\pi \text{ energy stored in the circuit}}{\text{energy dissipated in } Y_o, R_s \text{ and } G \text{ per cycle}} \qquad (1\text{-}a)$$

$$Q_L = \frac{f_o}{\Delta f} \qquad , \qquad (1\text{-}b)$$

where Δf is the difference between the two frequencies when the total susceptance B is equal to the total conductance

$$B_{\frac{1}{2}} = \pm \left[G + \frac{1}{R_s + \frac{1}{Y_o}} \right] \qquad . \qquad (2)$$

The reflection coefficient of the cavity as observed from $a - a'$ is

$$\rho = \frac{Y_L - Y_o}{Y_L + Y_o} \qquad , \qquad (3)$$

where Y_L is the admittance of the load referred to $a - a'$. The voltage standing-wave ratio (VSWR) is

$$S = \frac{1 + |\rho|}{1 - |\rho|} \qquad . \qquad (4)$$

The effect of series loss is to limit the reflection coefficient and VSWR to the following values far from resonance

$$\rho_\infty = \frac{1 - Y_o R_s}{1 + Y_o R_s} \qquad (5\text{-}a)$$

$$S_{\infty} = \frac{1}{Y_o R_s} \neq \infty \qquad . \tag{5-b}$$

Assuming an undercoupled cavity, the reflection coefficient and VSWR at resonance are

$$\rho_o = \frac{Y_o (G R_s + 1) - G}{Y_o (G R_s + 1) + G} \tag{6-a}$$

$$S_o = \frac{G}{Y_o (G R_s + 1)} \qquad . \tag{6-b}$$

Using 2 and 3, the magnitudes of the reflection coefficient and VSWR at the half-power points in terms of S_{∞} and S_o are

$$|\rho_{\frac{1}{2}}| = \left\{ \frac{(S_o^2 - 1)^2 + \left[(S_o - 1) + (\frac{2}{S_{\infty} + 1})(S_o - S_{\infty}) \right]^2}{2(S_o + 1)^2} \right\}^{1/2} \tag{7-a}$$

$$S_{\frac{1}{2}} = \frac{(S_o + 1)(S_{\infty} + 1) + \left\{ (S_{\infty} - S_o)^2 + (S_o S_{\infty} - 1)^2 \right\}^{1/2}}{(S_o + 1)(S_{\infty} + 1) - \left\{ (S_{\infty} - S_o)^2 + (S_o S_{\infty} - 1)^2 \right\}^{1/2}} \qquad . \tag{7-b}$$

For the case of zero series loss S_{∞}' becomes infinite and $S_{\frac{1}{2}}$ is

$$S_{\frac{1}{2}}' = \frac{(S_o + 1) + (S_o^2 + 1)^{1/2}}{(S_o + 1) - (S_o^2 + 1)^2} \tag{8}$$

which is the result given by Lawson [4].

The VSWR may be measured by means of the reflectometer. Referring the zero impedance level to correspond to an infinite VSWR, i.e., 100 percent reflection, the VSWR for imperfect reflection is given by

$$S = \frac{\text{antilog} \frac{Z_{db}}{20} + 1}{\text{antilog} \frac{Z_{db}}{20} - 1} \tag{9-a}$$
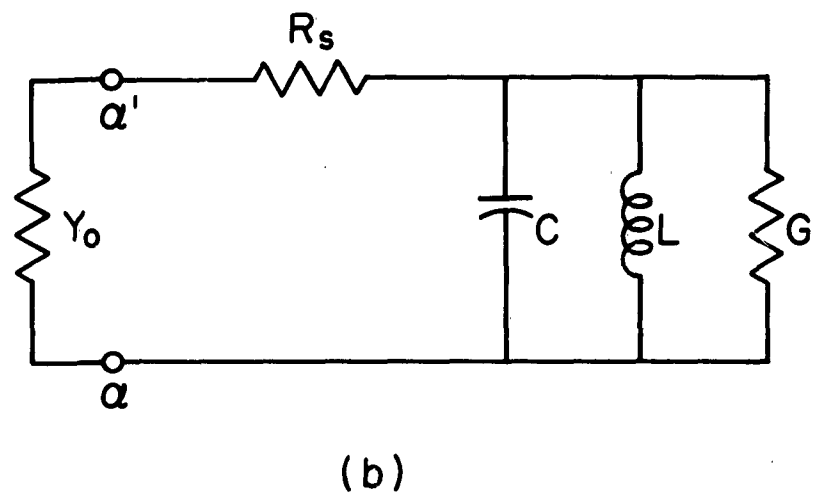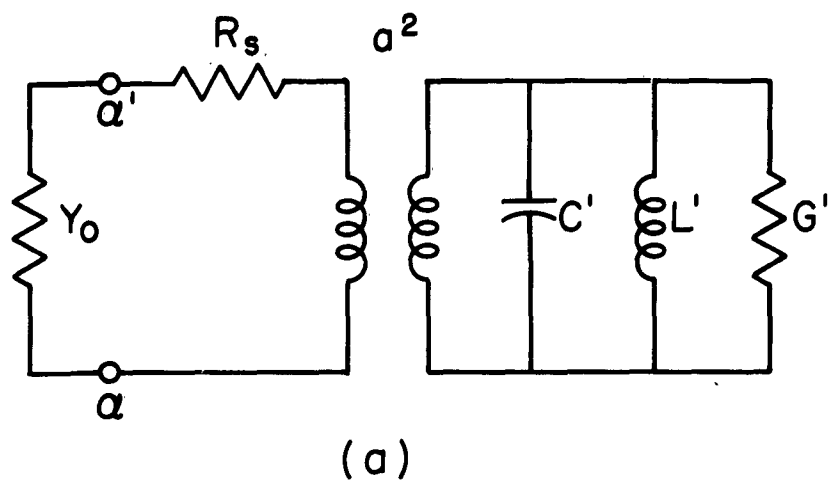
FIG. 5a   EQUIVALENT CIRCUIT OF A RESONANT CAVITY WITH SERIES LOSSES
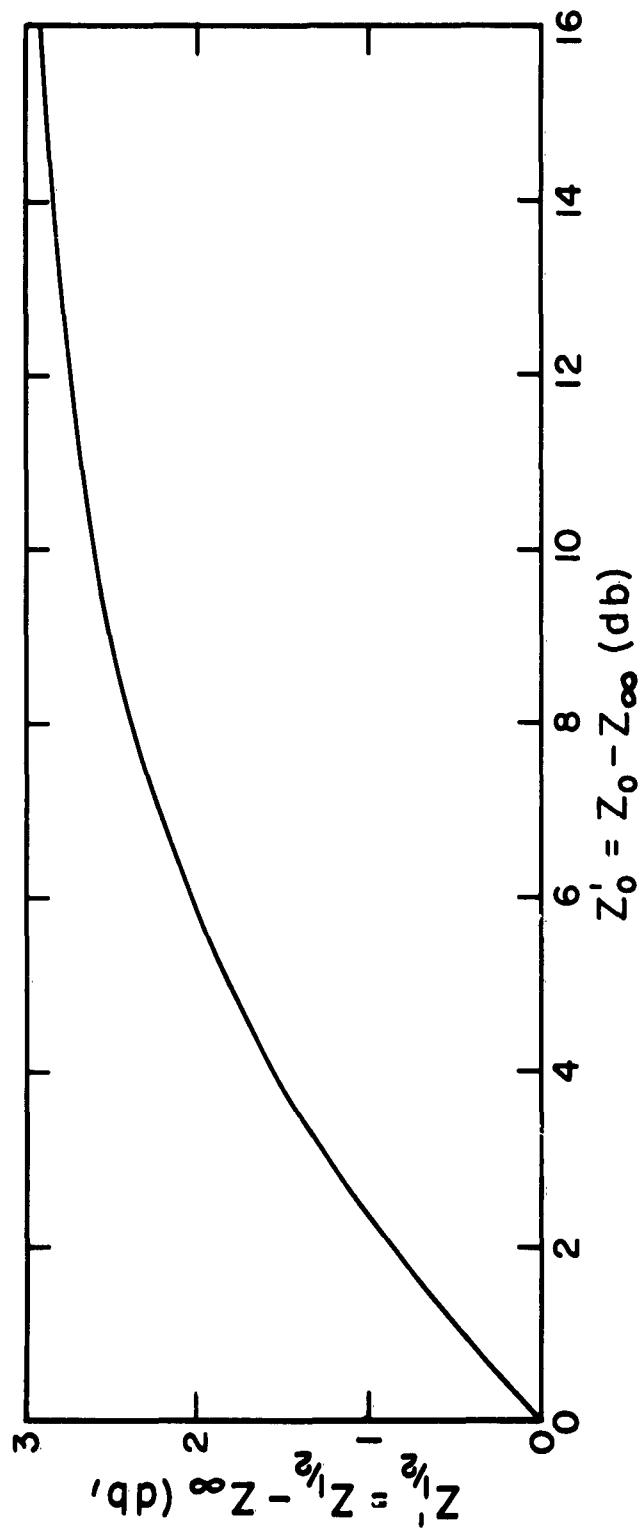
FIG. 5b REFERENCE ATTENUATION AT THE HALF-POWER POINTS AS A
FUNCTION OF REFERENCE ATTENUATION TO THE BOTTOM OF
THE RESONANCE CURVE

and

$$Z_{db} = 20 \log \frac{S+1}{S-1} \qquad . \qquad (9\text{-}b)$$

The VSWR's S_o and S_∞ in terms of Z_o and Z_∞ may be substituted in 7-b and $Z_{\frac{1}{2}}$ found from $S_{\frac{1}{2}}$ by means of 9-b. The resulting expression is

$$Z_{\frac{1}{2}} - Z_\infty = 3 - 20 \log \sqrt{\frac{(\text{antilog } \frac{Z_o - Z_\infty}{20})^2 + 1}{\text{antilog } \frac{Z_o - Z_\infty}{20}}} \qquad \text{db} \qquad . \qquad (10)$$

This important result indicates that it is not necessary to know or measure the series loss or Z_∞ , as zero impedance level is now referred to the impedance level of the cavity far from resonance instead of the short. Equation 10 is plotted in Fig. 4. It is now a simple matter to measure $Z_o' = Z_o - Z_\infty$. Set the attenuator to $Z_{\frac{1}{2}}' = Z_{\frac{1}{2}} - Z_\infty$ and measure Δf by superposing the pips from the radio on the crossover points, without having to replace the cavity by a short-circuit for each measurement.

References

1. C. G. Montgomery: Technique of Microwave Measurements, MIT Radiation Laboratory Series (1947).

2. J. O. Artman and P. E. Tannenwald, MIT Lincoln Lab. TR70 (October 1954).

3. S. C. Brown, et al., MIT-RLE Report 66 (1948).

4. J. L. Lawson, MIT Report 64-3 (May 1942).

- - - - -

6. Measurements of the Complex Microwave Dielectric Constant of Single Crystal $NaClO_3$ and $NaBrO_3$, J. P. van der Ziel.

The real and imaginary parts of the complex dielectric constant ($\epsilon = \epsilon' - i\epsilon''$) of cubic crystals of $NaClO_3$ and $NaBrO_3$ were measured at 9Gc between $77^\circ K$ and $520^\circ K$ using a standard cavity perturbation technique [1].

The results are shown in Figs. 6 and 7. The real part ϵ' was found to be identical with the low frequency (1000 cps) dielectric constants measured by Mason [2]. Measurements of ϵ' at 35 Gc. are identical to those at 9 Gc. As shown in Fig. 7, the imaginary part ϵ'' of $NaClO_3$ increases more rapidly with increasing temperature than for $NaBrO_3$. This appears to be associated with the lower melting point of the chlorate salt. The melting points of $NaClO_3$ and $NaBrO_3$ are $537^\circ K$ and $693^\circ K$ respectively [2]. From room temperature measurements at 9 Gc. and 35 Gc. it appears that ϵ'' increases linearly with frequency indicating that the major loss mechanism in this frequency range is due to the tail of the infrared lattice absorption.

References

1. H. A. Bethe and J. Schwinger, N. D. R. C. Report D1-117, Cornell University (March 1943).

2. W. P. Mason, Phys. Rev. 70, 529 (1946).

- - - - -

7. Temperature Dependence of Dielectric Loss in Ionic Crystals, J. C. Owens.

Although measurements of the dielectric constants and loss tangents of ionic crystals have been made for many years, there have been very few measurements in the microwave region, particularly as a function of temperature, and the actual mechanism of absorption is not understood. Theoretical predictions of the temperature dependence of the loss give conflicting results. For these reasons, a study has been begun in which the dielectric constant and loss of single crystals of several different alkali halides will be measured over a wide range of temperatures at frequencies around 9, 34, and 110 kMc/s, all on the low-frequency side of the reststrahlen absorption. Knowing the loss as a function of temperature, frequency, and molecular weight, it should be possible to gain insight into the actual absorption mechanism.

The only measurements to date have been made on sodium chloride around 34 kMc/s. Several different microwave circuits have been tried, for its combination of relatively large dielectric constant and very small loss tangent presents a rather difficult problem of measurement. It is necessary to
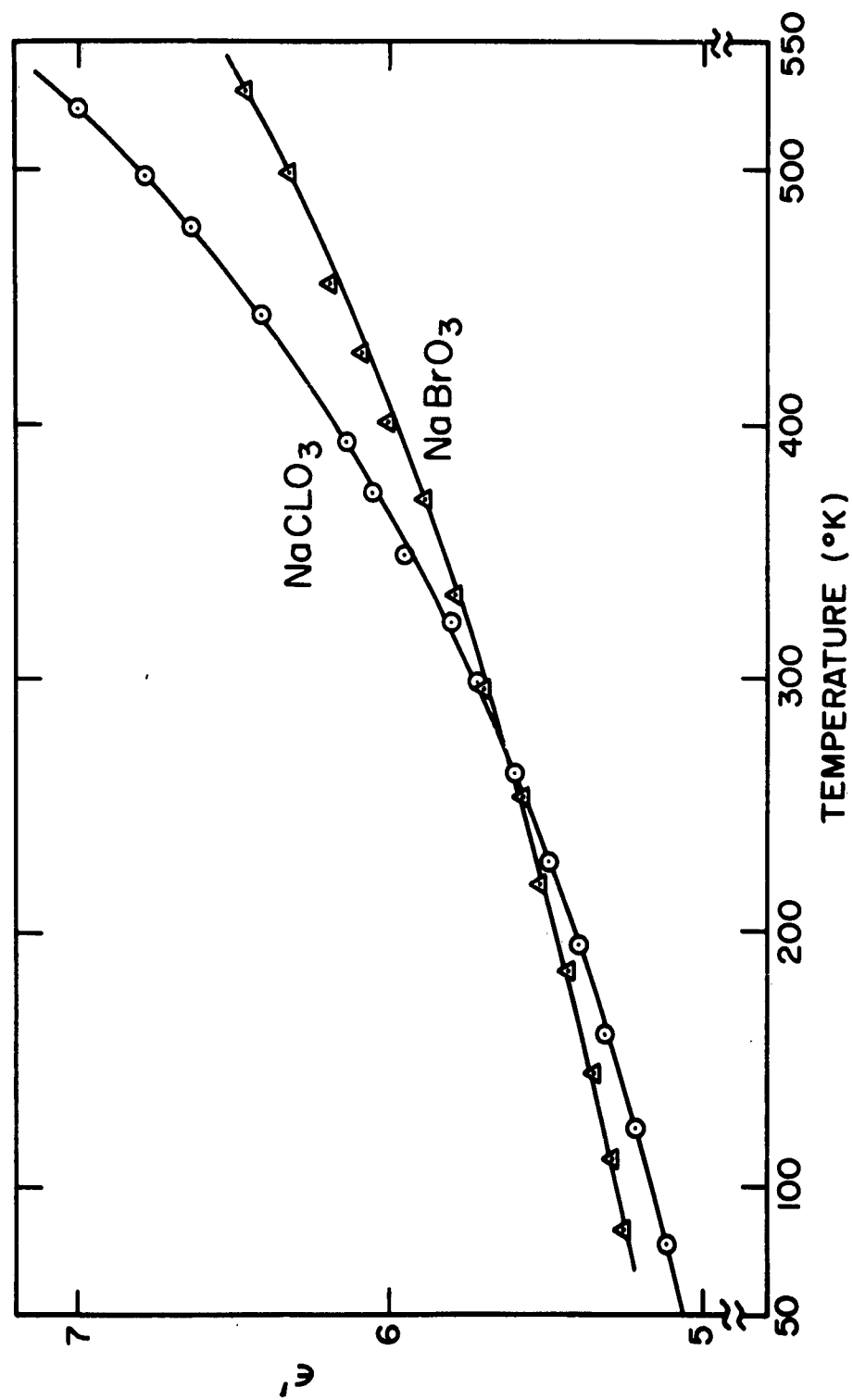
. FIG. 6 Temperature Variation of ϵ' at 9Gc for $NaClO_3$ and $NaBrO_3$
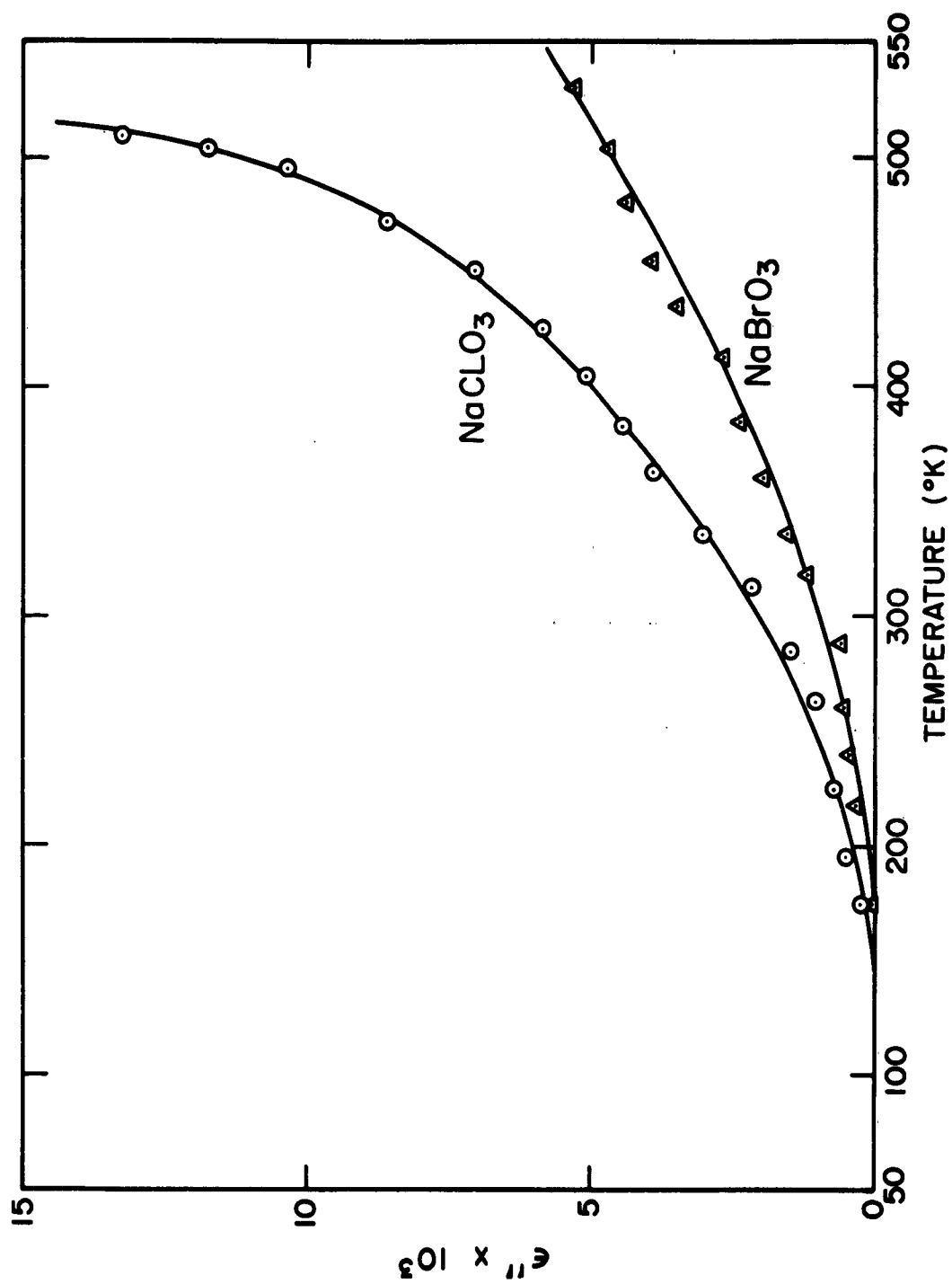
FIG. 7 Temperature Variation of ϵ'' at 9Gc for $NaClO_3$ and $NaBrO_3$

have the sensitivity of resonant cavity methods, but it was found that the usual perturbation techniques were not accurate enough. Therefore, a filled cavity is now being used. By measuring its dimensions, resonance frequency, and Q , and then correcting for wall losses, the dielectric constant and loss tangent can be found.

In this way, the dielectric constant at constant pressure of sodium chloride between - 100 and + 380°C has been found to be given by

$$\frac{\epsilon'}{\epsilon_o} = 5.930 \left(\frac{2490}{2515 - T} \right) \pm 0.2\%$$

where T is in $^\circ$C , while the loss tangent at room temperature is

$$\tan \delta = (4.3 \pm .5) \times 10^{-4} .$$

The Q measurements have been difficult to make, and sufficient accuracy and reproducibility have not yet been achieved to allow an accurate temperature dependence of the loss to be given. Nevertheless, preliminary measurements show that $\tan \delta$ is approximately proportional to $T^{2.5}$ where T is in $^\circ$K , while theoretical predictions by different authors go as T , T^2 , and T^3 [1].

Reference

1. D. W. Jepsen and R. F. Wallis, Phys. Rev. 125, 1496 (1962).

- - - - -

8. Electric Field Effects in Paramagnetic Resonance, E. B. Royce and
   N. Bloembergen.

Effects of a uniform applied electric field on the paramagnetic resonance of a transition metal ion in a diamagnetic host lattice have been observed by several workers using a variety of systems. In general, a paramagnetic ion with spin greater than one-half is influenced by the electrostatic field of its crystalline surroundings through the spin-orbit interaction. Under the action of a uniform applied electric field this interaction of the magnetic ion with its surroundings is changed, and a shift in magnetic resonance field

is observed. In the spin Hamiltonian formulation, all parameters become a function of an applied electric field.

It is useful to separate the possible effects of an applied electric field into two groups, although it may be questioned as to whether such a separation has much real meaning. In the previous annual report we considered only what may be termed the indirect effect, which arises from the dielectric polarization of the crystalline lattice. This polarization is associated with a movement of cations and anions with respect to each other, and, hence, produces a movement of the surroundings of the magnetic ion. The resulting alteration of the crystalline electric field can be calculated in a fairly straightforward manner, as previously outlined.

In addition, however, there may be a direct effect of the applied electric field on the unpaired electrons of the magnetic ion. A linear effect may exist, if the wave functions for these electrons are of mixed parity. This mixed parity, in turn, may arise as the result of the influence of a crystalline field which does not have inversion symmetry. Under certain circumstances it appears that this effect may be much larger than the indirect effect. Linear electric field effects can exist, of course, only where the magnetic ion is at a site of non-inversion symmetry [1]. If the site has inversion symmetry, there can be only a quadratic electric field effect, direct or indirect.

<u>Experimental Results</u>

Paramagnetic resonance in several materials has been investigated in the presence of an applied electric field. The experimental procedure has been outlined in the previous annual report, and only one modification has been made. Electrical leads to the evaporated silver electrodes on the sample are ultrasonically soldered in place with indium. The sample is then coated with insulating material to allow the use of electric fields of up to 200 kilovolts per centimeter across the sample. No effect was found for the resonance of Fe^{+++} in TiO_2 or for Cr^{+++} in MgO in a site of axial symmetry. An unexpectedly large effect was observed for Cr^{+++} in Al_2O_3 (ruby), and the angular dependence of this effect was investigated in detail.

The first electric field effect in paramagnetic resonance was observed by Ludwig and Woodbury for an Fe^{o} impurity in silicon [2]. Through the kindness of Dr. Ludwig, a suitable sample of iron-doped silicon was obtained, and the effect observed by Ludwig and Woodbury was confirmed qualitatively. The experiments were done at liquid helium temperature in order to have sufficient sensitivity for the small spin concentration present. Unfortunately, the spectrometer used was not designed to operate at low levels, and saturation of the spin system gave a poor sensitivity, preventing more accurate work.

In the previous annual report, the indirect effect was calculated for the resonance of Fe^{+++} in TiO_2 [3]. The effect is second-order, because the site of the iron has inversion symmetry. For an applied field of 50 kilovolts per centimeter, there should be a shift in the resonance field of one gauss, for the transition at four kilogauss and 14 gigacycles, $\theta = 90^{o}$, $\phi = 0^{o}$. The electric field was taken along the c- or y-axis. Experimentally, the effect could not be found, and an upper limit was set which is an order of magnitude smaller than the calculated effect. This work was also done at liquid helium temperature.

The calculations are based on the assumption that the ionic polarizability of the iron surrounded by oxygens of the TiO_2 lattice is the same as the polarizability of the titanium in TiO_2. Apparently, this is not the case, but rather, the iron-oxygen bonds in the TiO_2 lattice are less like the titanium-oxygen bonds and more like the iron-oxygen bonds in, say, Fe_2O_3, where the ionic polarizability is an order of magnitude smaller, as evidenced by the smaller dielectric constant.

In the previous annual report, we also calculated the indirect linear electric field effect for Cr^{+++} in an axial site in MgO [4]. The effect so calculated is just too small to be detected experimentally, and the experiments, even at liquid helium temperature, gave a negative result. In light of the anomalously large electric field effect on Cr^{+++} in ruby, however, the case of MgO was re-examined. If one assumes that the ruby theory of Artman and Murphy [5] (see below) is correct for MgO as well, one can scale the ruby results and predict an effect in MgO which is ten times larger than the minimum detectable

signal. With this calculation in mind, the experiment on MgO was repeated, giving the same result as previously. The experimental upper limit on the electric field effect is an order of magnitude smaller than the effect predicted by scaling the ruby theory of Artman and Murphy. A theory is proposed below which takes account of this discrepancy.

The major experimental effort during the last year has been devoted to the linear electric field effect of Cr^{+++} in ruby, first observed by Artman and Murphy [6].

The Cr^{+++} ions in ruby are located at sites of symmetry C_3. There are four such sites in a unit cell, related to each other in pairs by an inversion symmetry operation. These pairs are in turn related to each other by reflection in a mirror plane. The local environment of the Cr^{+++} consists of two unequal triangles of oxygen, one aligned with the crystallographic axes and one rotated about the c-axis by 4.3^o with respect to the x- and y-axes. The three-fold axis of the site is parallel to the crystallographic c-axis. The sites related to each other by mirror symmetry differ in having their second triangles rotated in opposite senses. Each of these sites is distinguished in an electric field experiment, although they are all equivalent, if only a magnetic field is applied.

The angular dependence of the electric field effect on the energy levels giving rise to the magnetic resonance may be described by the following spin Hamiltonian.

$$\mathcal{H}_s = g_{||} \beta H_z S_z + g_\perp \beta (H_x S_x + H_y S_y) + D \left[S_z^2 + \frac{1}{3} S(S+1) \right]$$

$$+ \sum_i \sum_{j \leq k} \frac{1}{2} R_{ijk} E_i (S_j S_k + S_k S_j) + \sum_{ijk} T_{ijk} E_i H_j S_k$$

The term containing T is experimentally too small to be observed. For C_3 symmetry and using the trace relation $\sum_j R_{ijj} = 0$, the tensor R has the form

	$S_1{}^2$	$S_2{}^2$	$S_3{}^2$	$\frac{1}{2}(S_2S_3 + S_3S_2)$	$\frac{1}{2}(S_1S_3 + S_3S_1)$	$\frac{1}{2}(S_1S_2 + S_2S_1)$
E_1	R_{111}	$-R_{111}$	0	R_{123}	R_{113}	$-2R_{222}$
E_2	$-R_{222}$	R_{222}	0	R_{113}	$-R_{123}$	$-2R_{111}$
E_3	R_{311}	R_{311}	R_{333}	0	0	0

$$R_{311} = -\frac{1}{2}R_{333}$$

Sites related to each other by inversion have values of R equal in magnitude but opposite in sign. Hence, under the influence of an applied electric field, resonance lines from the two sites shift in opposite directions, giving the appearance of an electrically induced splitting. By taking suitable orientations of the applied electric and magnetic fields with respect to the crystallographic axes, each of the five components of the R- tensor was experimentally evaluated together with its relative sign. The results for two sites related by mirror symmetry are $R_{111} = -.020 \pm .003$ Mc per kv/cm, $R_{222} = \pm .073 \pm .003$, $R_{333} = .179 \pm .003$, $R_{123} = \pm .04 \pm .02$, $R_{113} = -.09 \pm .02$. Further details have been reported [7], and are to be published [8].

If the coordinate system used in writing the spin Hamiltonian is rotated by 5° about the c-axis, $R_{111} = 0$, as would be the case for C_{3v} symmetry. However, R_{123} should vanish simultaneously with R_{111}, and it, in fact, does not. From this we conclude that the true symmetry of the site is C_3, and that both oxygen triangles contribute to the electric field effect. The triangle rotated by 4.3° is dominant. This is in agreement with the theory to be presented.

For Gd^{+++} in Al_2O_3, Geschwind and Remeika [9] have found strong preferences for occupation of certain of the four sites in the unit cell, whereas for Cr^{+++}, no evidence for such behavior is found from the electric field experiments. This is not surprising, since the Cr^{+++} ionic radius is more comparable to the Al^{+++} ionic radius than is the Gd^{+++} ionic radius.

Theoretical Considerations - Cr^{+++} in Ruby

The electric field effect in ruby consists phenomenologically in a perturbation of the term $D[S_z^2 + \frac{1}{3}S(S+1)]$ in the usual spin Hamiltonian. In order to understand the origin of this electric field effect, one must first understand the D-term. In the hands of Tanabe and Sugano [10], the crystal field theory has had considerable success in explaining the optical spectrum of Cr^{+++} in ruby. The splitting of the optical ground state is then obtained by a perturbation calculation using the off-diagonal elements of the spin-orbit interaction and the low symmetry part of the crystalline field. Unfortunately, these calculations have yielded values of the splitting of the optical ground state which are smaller than observed, and this is just the D-term of the spin Hamiltonian. Nevertheless, it is possible to construct a theory of the electric field effect using the crystal field formulation. In the perturbation calculation, one replaces elements such as $(g|V^g_{crys}|g')$ by $(g|V^u_{crys}|u)(u|eEr|g')/(W_u - W_g)$. The results of such a calculation are in only fair agreement with experiment. Artman and Murphy have called attention to the importance of the odd terms in the crystalline potential, V^u_{crys}, and have shown that in the original calculations, one should have included terms such as $(g|V^u_{crys}|u)$ $(u|V^u_{crys}|g')/(W_u - W_g)$. They have carried out the perturbation theory in detail including such terms, and they find fair agreement with experiment, both for the electric field effect and for the value of D in the spin Hamiltonian. Their numerical values assumed for some of the parameters seem a bit unreasonable, however.

This calculation is contradicted by experiment on two points. Firstly, on the basis of a point-charge model, it is difficult to understand why, of the two oxygen triangles surrounding the metal ion, one should be so dominant in producing the odd terms in the crystal field, as evidenced by the angular dependence of the electric field effect. The aluminum- or chromium-oxygen distances differ by only 10 percent in the two triangles. A covalent interaction, on the other hand, could be more sensitive to distance, and this indicates that one should take covalency effects into account more explicitly in the theory.

Secondly, the axial site for Cr^{+++} in MgO consists of an eight-fold coordination of nearest neighbor oxygen ions in a cubic arrangement. The axial field arises from a next nearest neighbor magnesium vacancy. If one assumes that the theory of Artman and Murphy accounts for the D-term in this case, also, one predicts an electric field effect an order of magnitude larger than experiment. On the other hand, there can be no covalent bonding to a next neighbor; so again, the assumption that the odd terms in the crystalline potential, and, hence, the electric field effect, arise from covalent effects will explain the experimental results.

Because of the inadequacy of the point-charge crystal field model in dealing with the electric field effect in the two cases mentioned above, a molecular orbital calculation was performed on the complex CrO_6^{-9} . The geometrical arrangement of the complex was taken the same as the arrangement in ruby. It was hoped that such an approach would take covalent effects into account more explicitly, although the model is surely a crude one. Machine calculations were performed by L. Lohr of the Department of Chemistry, Harvard University. He finds that the covalent bonding of the chromium is much more strongly to one triangle, namely the triangle which is rotated 4.3° and which has a 10 percent smaller oxygen-chromium distance. This means that the electric field effect will be dominated by this triangle, in agreement with the experimental results on the angular dependence. Also, the admixture of wave functions of odd parity into the ground state is sufficient to account for the observed electric field effect. Furthermore, this mixing of wave functions makes the spin-orbit interaction sufficiently anisotropic to account for the size of the D-term in the absence of applied electric field, as was originally suggested by Tanabe and Sugano.

Thus, it appears that the electric field effect on the magnetic resonance of Cr^{+++} in ruby can be accounted for by covalent effects. In other words, what one is seeing is the polarization of the covalent bonds in the presence of an applied electric field. It may be noted that Sugano [11] has pointed out that a molecular orbital approach is the more appropriate way to handle the cubic field splitting, and this is confirmed by Lohr, whose calculations give both the correct sign and magnitude for the cubic and trigonal field splittings.

Permanent Electric Dipole Moments

The observed electric field effect should not be confused with the possible existence of an intrinsic electric dipole $P = 2\xi\beta S$, which would give rise to a term in the Hamiltonian $- 2\xi\beta S \cdot E$. β is the Bohr magneton, and ξ is a pseudo-scalar. A major consequence of such a term is that the Kramers degeneracy would be lifted by an applied electric field or by any electrostatic potential of odd symmetry, such as the odd terms in the crystalline potential. The effect of such a term on paramagnetic resonance has been calculated by Sachs and Schwebel [12], who predict a line shift of the order $\lambda (W_g - W_u)^{-1} 2\xi\beta$ $|e^{-1} V^u_{crys} + E_{applied}|$. Browne [13] has experimentally attempted to detect such an effect using an externally applied electric field, with negative results.

The term $e^{-1} V^u_{crys}$, however, is much larger than any applied field, and a scheme has been devised to check the existence of a permanent electric dipole using this fact. In ruby, the apparent splitting of the resonance line is produced by the sum of the ordinary electric field effect discussed previously and the effect of a permanent electric dipole moment acted on by the crystal field. If either the applied electric or magnetic field is reversed, the relative signs of these two terms change, allowing them to be separated.

Preliminary experiments of this type have placed an upper limit on the electric dipole moment of the electron which is only two times larger than the best limit set by the electron beam experiments of Nelson, et al. [14]. It is hoped that this upper limit can be reduced by an order of magnitude using this effect.

References

1. N. Bloembergen, Science 133, 1363 (1961).

2. G. W. Ludwig and H. H. Woodbury, Phys. Rev. Letters 7, 240 (1961).

3. D. L. Carter and A. Okaya, Phys. Rev. 118, 1485 (1960).

4. J. E. Wertz and P. Auzins, Phys. Rev. 106, 484 (1957).

5. J. O. Artman and J. C. Murphy, Bull. Am. Phys. Soc. II, 7, 196(1962). First International Conference on Paramagnetic Resonance, The Hebrew University, Jerusalem, Israel, 1962 (to be published).

6. J. O. Artman and J. C. Murphy, <u>Bull. Am.</u> <u>Phys.</u> <u>Soc. II,</u> <u>7</u>, 14 (1962).

7. E. B. Royce and N. Bloembergen, <u>Bull. Am. Phys. Soc. II,</u> <u>7</u>, 200 (1962).

8. N. Bloembergen and E. B. Royce, First International Conference on Paramagnetic Resonance, The Hebrew University, Jerusalem, Israel, 1962 (to be published).

9. S. Geschwind and J. P. Remeika, <u>Phys. Rev.</u> <u>122</u>, 751 (1961).

10. Y. Tanabe and S. Sugano, <u>J. Phys. Soc. Japan</u> <u>13</u>, 880 (1958). See also references therein: S. Sugano, M. Peter, <u>Phys. Rev.</u> <u>122</u>, 381 (1961), and D. S. McClure, <u>J. Chem. Phys.</u> <u>36</u>, 2757 (1962).

11. S. Sugano, <u>J. Appl. Phys. Supp.</u> <u>33</u>, 303 (1962).

12. M. Sachs and S. Schwebel, <u>Annals of Physics</u> <u>8</u>, 475 (1959).

13. M. E. Browne, <u>Phys. Rev.</u> <u>121</u>, 1699 (1961).

14. D. F. Nelson, et al., <u>Phys. Rev. Letters</u> <u>2</u>, 492 (1959).

- - - - -

9. Stark Effect on NQR in $NaClO_3$, F. A. Collins.

The theory and initial measurements of the Stark effect on the NQR of chlorine compounds were discussed at length in Annual Progress Report No. 60.

A spin Hamiltonian describing the effect in $NaClO_3$ is:

$$\mathcal{H} = \gamma \, \underline{H} \cdot \underline{I} + \frac{e^2 Qq}{4I(2I-1)} \left[3 I_z^2 - I(I+1) \right]$$

$$+ \, \underline{\underline{Q}} \cdot \underline{\underline{R}} \cdot \underline{\underline{E}} \qquad \text{with } I = 3/2 \, .$$

Here the first two terms are the usual Zeeman and axial quadrupole terms, and

$$\underline{\underline{Q}} = \text{quadrupole tensor spin operator}$$

$$= Q_{ij} = \frac{eQ}{6I(2I-1)} \left[\frac{3}{2} (I_i I_j + I_j I_i) - \delta_{ij} I(I+1) \right]$$

$$\underset{\sim}{E} = E_k \quad = \text{electric field}$$

$$\underset{\sim}{R} = R_{ijk} = \text{proportionality tensor to be measured .}$$

If the applied magnetic field is parallel to the quadrupole axis or zero, only R_{zzz} gives diagonal matrix elements in the last term, and so shows up in first-order perturbation theory. Fairly large magnetic fields perpendicular to the quadrupole axis are necessary to measure the other four independent components of $\underset{\sim}{R}$ in the C_3 symmetry of the chlorine site in $NaClO_3$. Then, after solving the secular problem for the first two terms of the Hamiltonian, these other terms contribute to the diagonal elements for the transformed matrix.

Single crystals of $NaClO_3$ are now on hand, and R_{zzz} has been measured for them giving a tentative value of $+.222 \, c/s$ shift for $E_z = 10^4$ volts/cm. The plus (+) sign is referred to the face of the crystal which assumes a plus (+) piezoelectric voltage in compression for a levorotatory crystal. As is seen from the above, the question of the sign of the components of $\underset{\sim}{R}$ requires careful attention.

Preparations have been completed for measuring the remaining components of $\underset{\sim}{R}$ using a magnetic field of 16 kilogauss, the field and the spectrometer being locked to the same frequency standard.

- - - - -

10. Temperature Dependence of Paramagnetic Resonance Lines, I. Svare and G. Seidel.

We have continued measurements of resonance line shapes at 30 kMc/s and down to $0.4^\circ K$ using a ^3He cryostat. For these lowest temperatures where $kT < h\nu$, almost all spins are in the lowest energy state, and this will influence the effects of spin-spin interaction. McMillan and Opechowski [1], and others have modified the theory of resonance line moments to take account of the differences in spin-level populations at low temperature. They show that an exchange interaction $\mathcal{H}_{ex} = \underset{ij}{\Sigma'} A_{ij} \vec{S_i} \vec{S_j}$ between non-identical spins i and j will give the lines a temperature-dependent shift. This we have observed in $NiSiF_6 \cdot 6H_2O$ as reported in Annual Progress Report No. 60.

We have now studied lineshape changes at low temperature in three other crystals.

(A) In $Nd(C_2H_5SO_4)_3 \cdot 9H_2O$ the Nd^{+++} ions of effective spin 1/2 are arranged so that each spin interacts strongly only with two neighbors. With the external field along the crystalline axis we then see the line split in three peaks that correspond to the four possible arrangements of the two neighbors as indicated below:
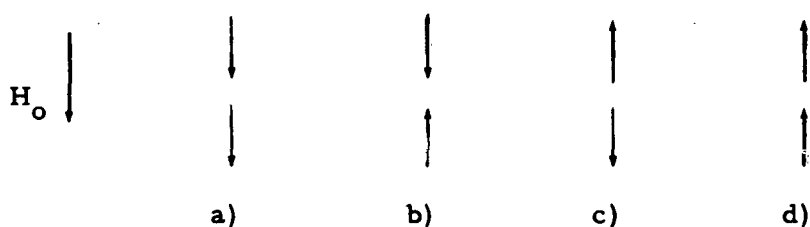
At $T \to \infty$ the arrangements a) - d) are equally probable. a) and d) will give dipolar shifts in opposite directions, while b) and c) do not shift the resonance, and, therefore, the middle peak is twice as strong as the side peaks.

How the lines change at low temperature is shown in Fig. 8. The intensity of each peak is in agreement with the temperature-dependent probability for the corresponding neighbor arrangement. The changes in first and second moments of the lines can be explained from dipolar interaction, if we distinguish properly between "like" and "unlike" neighbors. Spin-flip terms $S_{+i}S_{-j}$ have to be truncated out of the interaction Hamiltonian unless the spins are like and resonate at the same frequency. In the case of $Nd(C_2H_5SO_4)_3 \cdot 9H_2O$ the arrangement of the neighbors determines whether two spins are like or not.

For complete explanation of the peak separation it seemed necessary to assume a very small antiferromagnetic exchange $A = 6.10^{-19}$ erg with the two nearest neighbors.

(B) $K_2Cu(SO_4)_2 \cdot 6H_2O$ has two ions per unit cell. Each spin has two like nearest neighbors $6.14\overset{o}{A}$ away and four unlike neighbors at $7.55\overset{o}{A}$, and there is a likelihood of exchange to all six spins. First moment shift will

give information about the exchange between unlike spins only, and we find $A = -1.4 \cdot 10^{-18}$ erg . This is a ferromagnetic interaction.

Hyperfine interaction in copper broadens the resonance lines, and it may be questionable whether spins of nuclear quantum number $m = 3/2$ can flip freely with spins of $m = -3/2$. Only if some restriction is placed on the spin-flips within the hyperfine-broadened line can the first moment shifts be completely explained. Then we can tentatively give the exchange between like nearest neighbors as $A_1 = -10 \cdot 10^{-18}$ erg .

These estimates of exchange strengths are in agreement with measured Curie temperatures of 0.035° to 0.055° K .

(C) $CuSO_4 \cdot 5H_2O$ also has two ions per unit cell, but the exchange is so strong that the lines overlap below room temperature, and we could not calculate useful line moments. Below 1° K we saw the line split up into a number of separate components. This can probably be explained as magneto-static Walker modes within the magnetized sample.

Some of these results were reported by G. Seidel at the International Conference on Paramagnetic Resonance in Jerusalem, 1962, and will appear in the Proceedings. We are preparing more complete accounts to be published elsewhere. Lineshape measurements on other crystals continue.

Reference

1. M. McMillan and W. Opechowski, Can. J. Phys. 38, 1168 (1960).

- - - - -

11. Spin-Lattice Relaxation of Paramagnetic Ions in Diamagnetic Garnets,
    C. Y. Huang, G. Seidel, and I. Svare.

A conventional pulse saturation method has been used to measure spin-lattice relaxation times of rare-earth ions in diamagnetic garnets. The paramagnetic ions reported here are Dy^{3+}, Nd^{3+} and Yb^{3+} substituted in small concentrations.

The sample is placed in a microwave cavity at 8.7 kMc/s and saturated with 1/2 watt power for a time ranging between 10^{-5} and 10^{-4} sec by means of a klystron externally modulated by a pulser. The recovery of the absorption
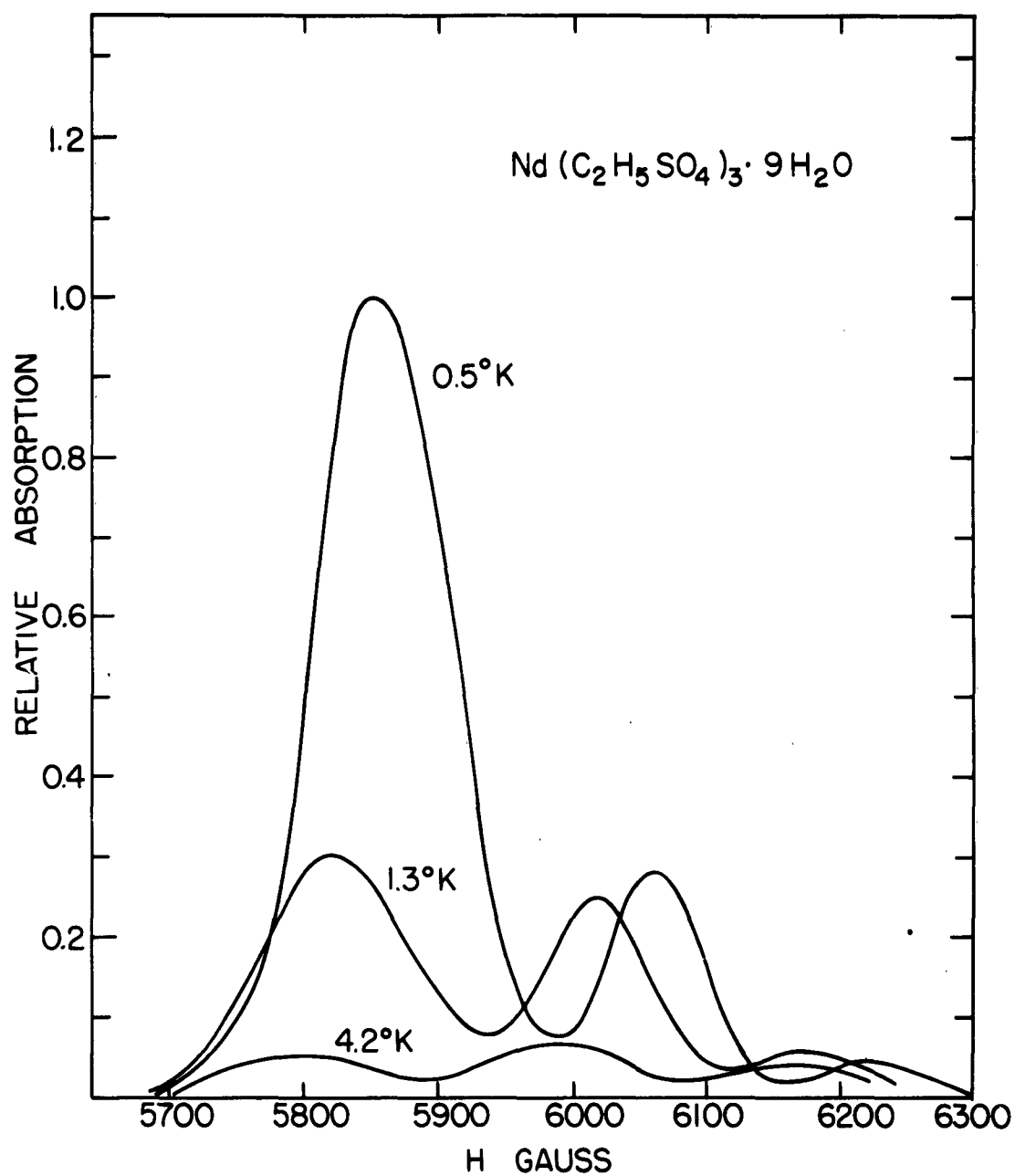
FIG. 8 Resonance Lineshape in $Nd(C_2H_5SO_4)_3 \cdot 9H_2O$ as a Function of Temperature

is then monitored by a low power microwave signal using superheterodyne detection. Because of the limited amount of saturating power available, relaxation times shorter than 5×10^{-6} second are difficult to determine. In a few cases, linewidth measurements provide additional information of relaxation times in the 10^{-9} second range.

Since the first excited state of the lowest J multiplet is presumed to be $550 \, cm^{-1}$ above the ground state, Kramers doublet for Yb^{3+} in yttrium gallium garnet (Y Ga G), the relaxation time for this ion was expected to be long. Two samples, 0.1 percent and 1 percent Yb, were measured.

For the 0.1 percent concentration, relaxation time below $20^{\circ} K$ can be expressed by the relation

$$\frac{1}{T_1} = 33T + 1.8 \times 10^{-7} T^9 \, sec^{-1} \quad .$$

This temperature dependence agrees with predictions for a Kramers salt at low temperatures, when the energy splitting to the first excited state is large. The first term on the right-hand side is the result of the single phonon, or direct processes, while the second arises from Raman processes. The estimated values of T_1 are longer than those given by the above expression by a factor of 10^2 in the range where the direct process dominates. Moreover, a theoretical estimate of the relaxation time due to the Raman process is in even poorer agreement with experiment.

The measurements of the 1 percent Yb sample agree well with those of the 0.1 percent sample in the Raman process region, but deviate at low temperatures. The deviation presumably arises from an additional contribution to the relaxation from exchange coupled pairs.

Measurements have been made of Er having a nominal 1 percent concentration in YAlG, Lu Al G, Y Ga G, and LuGaG . The results can all be fit by the following equation with varying accuracy:

$$\frac{1}{T_1} = AT + B \exp(-1.44 \, \Delta / T)$$

where the second term accounts for the Orbach process. As shown in the

accompanying table, the energy splitting Δ of the first excited state agrees
with that obtained by the optical spectra analysis.

The relaxation time of Dy^{3+} in a 1 percent concentration in Y Ga G
and Y Al G has been measured. The best interpretation of the data shows
that the relaxation is composed of the direct and the Orbach processes. The
T_1 of Dy in Y Ga G seems to indicate that impurities may be affecting the
results. The listed coefficients, then, may not represent the coupling of a
single Dy^{3+} ion to the lattice.

The T_1 of Nd^{3+} in 1 percent concentration in Y Ga G has been de-
termined. The relaxation time can be approximated reasonably well by the
sum of a term linear in T and an exponential term. The coefficients are
listed in the accompanying table.

$$\frac{1}{T_1} = AT + B \exp(-1.44 \, \Delta / T)$$

Ion	Garnet	A $(^{\circ}K \, sec)^{-1}$	B $(sec)^{-1}$	Δ cm^{-1}	Δ (optical) cm^{-1}
Er^{3+}	Y Al G	20	$3.2 \cdot 10^6$	20	22.1
	LuAl G	10	$6 \cdot 10^7$	36	36.7
	Y GaG	70	$1.1 \cdot 10^9$	46	44.3
	LuGaG	50	$1.4 \cdot 10^9$	47	49.7
Dy^{3+}	Y Al G	10	$2.4 \cdot 10^9$	53	
	Y GaG	440	$1.1 \cdot 10^7$	14	
Nd^{3+}	Y GaG	17	$9 \cdot 10^{10}$	85	
Yb^{3+}	Y GaG	$\frac{1}{T_1} = 33T + 1.8 \times 10^{-7} T^9$			

12. Microwave-Optical Experiments in Ruby, M. G. Cohen.

The purpose of this experiment as indicated in Progress Report No. 60 is to measure the relative optical transition probabilities for the Zeeman components of the R-lines in ruby, and compare the results with those predicted theoretically and partially verified by Sugano and Tanabe. Also, it is desired to verify the expected change in the optical absorption spectrum when the populations of the ground state levels are changed by microwave absorption.

Both parts of the experiment can be carried out simultaneously as follows. Record the optical absorption spectrum with the microwaves off. Then, turn on the microwave power at a resonance frequency for one of the ground state microwave transitions and record the optical spectrum again. In the first case:

$$I_j = I_o \, e^{-k_j n_j \overline{l}}$$

where

I_j = light intensity transmitted at maximum absorption for j^{th} transition

I_o = light intensity transmitted far from any transition

k_j = product of constants and relative transition probability

n_j = population of jth ground state level

$\overline{l}$ = average length of crystal that a light wave traverses

If the ratio of $\dfrac{k_1 n_1 \overline{l}}{k_2 n_2 \overline{l}}$ is known, then $\dfrac{k_1}{k_2}$ is known only if the populations n_1 and n_2 are known. This is controlled by the Boltzmann distribution, and computation requires an accurate knowledge of the temperature. However, when microwave power is on and saturating transition from $1 \rightarrow 2$, then $n_1 = n_2$ and thus k_1/k_2 is known immediately, once $\dfrac{k_1 n_1 \overline{l}}{k_2 n_2 \overline{l}}$ is known. Using some of the transitions where k_1/k_2 is known, the experimental system can be checked and then used to determine other relative transition probabilities using the microwave-optical interaction.

The experimental equipment can be described under three main headings: low-temperature apparatus, microwave spectrometer, and optical spectrometer.

Low-Temperature apparatus. A Hofman cryostat with a sapphire window at the bottom of the helium chamber has been purchased. This dewar will hold ordinary helium for several hours, but the bubbling at the window due to incident room-temperature radiation disperses the light beam almost completely. It is, therefore, necessary to work below the λ-point, with the helium in the non-bubbling superfluid phase. It turned out that the window had a superleak, i.e., a leak to superfluid helium. The liquid leaking into the vacuum chamber vaporized and ruined the thermal insulation. The resulting heat leak drove off the helium after only twenty minutes of operation. The problem was solved by attaching an Ultek ion pump to the dewar vacuum jacket and pumping constantly. The amount of helium leaking out is minimized by throttling the Kinney pump and keeping the helium vapor pressure just below 37 mm Hg. The number of superfluid atoms is very small just below the λ-point and, hence, the leak rate is small. The dewar holds superfluid helium for several hours with this arrangement.

Microwave spectrometer. A magic-T bridge with klystron stabilized on the sample cavity has been successfully operated at room temperature and liquid nitrogen temperature to give microwave resonance absorption curves for all the allowed transitions in ruby. The sample is large, about 20 percent of the length of the cavity, and the mode excited is not a simple one. However, the Q is high enough (~ 3000) to see strong signals. At helium temperature, the signal becomes weak and distorted as expected. Milliwatts of power easily saturate the ruby transitions at $2^{\circ}K$ where T_1 is of the order of 100 milliseconds.

Optical spectrometer. The Jarrell-Ash 1-meter Ebert spectrometer is the heart of the optical system. Two factors have prevented its optimum use in the region of the red lines. The first is the variation in focusing on the exit slit which occurs as the grating is rotated. If the instrument were ideal and were focused at the Hg green line in 11th order, rotating to 6934Å in the 8th order would not change the focus. However, the instrument is not

perfect and some change does occur, thereby degrading the resolving power. Previously, the instrument was tuned at 5461Å in 11th order. Now it will be tuned at 2537Å in the 22nd order. This corresponds to a grating angle which is very close to the angle for 6934Å in 8th order and, hence, the loss of focus will be minimized.

The more serious and less easily controlled problem involves the heavy vibration due to the construction on the floor above the spectrometer room. The proving-ring slit assembly is a very delicate mechanism and its vibrations are visible under a microscope when the air hammers are at work up above (two new floors are being added to the laboratory building). This vibration results in a change of slit adjustment and loss in resolution. The heavy pounding also moves the large collimating mirror, spoiling the focusing. Hopefully, this phase of the construction work will be completed in the near future. It is imperative that the instrument be working very close to the optimum performance as the spectral width that can be tolerated is only $.05 \, cm^{-1}$. This requires very small slit widths - ~ 10 microns. The high resolving power is required not to see the Zeeman splittings which are $\sim .8 \, cm^{-1}$, but to avoid errors in the strength of the absorption due to the spectral width of the instrument approaching the actual width of the absorption line. In a good ruby at $2^{\circ}K$, this latter is about $.1 \, cm^{-1}$. Samples from good Linde disc boules have been obtained in concentrations of $.05 \% \, Cr$ and $.005 \% \, Cr$. The spectrometer has been tuned up, but the continued vibrations from the roof make it difficult to say whether it remains so. The improvements made it possible to see the ground state splitting on the R_1 line at $77^{\circ}K$. This splitting is $.38 \, cm^{-1}$ and the two components exhibit widths of $\sim .25 \, cm^{-1}$, so they are easily resolved. With the end of construction, the instrument will be adjusted again, at which time it is hoped that the true linewidth can be observed at $2^{\circ}K$.

The small slit widths limit the light intensity, so a phase-sensitive light-detection system has been built to optimize the signal-to-noise ratio. The light incident on the ruby is chopped by a disc driven by a synchronous motor. The motor is driven in phase with an oscillator which also provides the reference signal for a lock-in detector. The ac signal from the photo-multiplier at the exit slit is amplified and put into the lock-in signal channel.

The output will be recorded on a Leeds and Northrup recorder which will arrive next month. Noise will be further minimized by reducing the dark current in the phototube using liquid nitrogen. The dewar for this purpose is being perfected.

Some optical absorption spectra have been recorded for R_1 and R_2 at $2^\circ K$, but the spectrometer adjustment did not allow for observing the true width of the levels, though the Zeeman splitting could be clearly seen. This should be corrected soon, at which time experimenting will begin with the combined microwave-optical apparatus.

- - - - -

13. Faraday Effects in Rare-Earth Ions, Y. R. Shen.

A general expression of electric susceptibility tensor, involving matrix elements of dipoles and multipoles is derived by using density matrix methods. The result is applied to the special case of rare-earth ions. Ordinarily, only the first-order terms (due to electric dipole transitions) and the second-order terms (due to electric quadrupole, magnetic dipole transitions, and crystal effects) need to be taken into consideration. Far away from resonance lines, the first-order terms are much larger than the second-order terms, but near resonance lines (forbidden lines) the latter become comparable to the former. The imaginary parts of the off-diagonal components of the susceptibility tensor are linearly proportional to the Faraday rotations. Experiments are to observe the rotations about the forbidden lines in the rare-earth ions. Calcium fluoride crystals, with various kinds of doping, have been used because of their simple cubic structures. Since the charge compensation situation is complicated in these doped crystals, the lines are all inhomogeneously broadened. We observed dispersion-like curves for rotations about these lines.

Among the rare-earth ions, Eu^{+++} is particularly simple for having a single ground state. We found that, theoretically, the first-order rotation in this ion is due primarily to the perturbation effect of the Zeeman energy, which mixes in the next higher states to the ground state. The rotation is proportional to the magnetic field and has no saturation phenomenon. Experiments will be done to prove the theory.

14. Interactions Between Light Waves in a Nonlinear Dielectric, J. A. Armstrong, N. Bloembergen, J. Ducuing, and P. S. Pershan.

A detailed discussion of this work is presented in the Cruft Laboratory Technical Report No. 358, March 20, 1962. The following is an abstract of that report.

The induced nonlinear electric dipole and higher moments in an atomic system, irradiated simultaneously by two or three light waves, are calculated by quantum mechanical perturbation theory. Terms quadratic and cubic in the field amplitudes are included . An important permutation symmetry relation for the nonlinear polarizability is derived and its frequency dependence is discussed. The nonlinear microscopic properties are related to an effective macroscopic nonlinear polarization, which may be incorporated into Maxwell's equations for an infinite, homogeneous, anisotropic, nonlinear, dielectric medium. Energy and power relationships are derived for the nonlinear dielectric which correspond to the Manley-Rowe relations in the theory of parametric amplifiers. Explicit solutions are obtained for the coupled amplitude equations, which describe the interaction between a plane light wave and its second harmonic or the interaction between three plane electromagnetic waves, which satisfy the energy relationship $\omega_3 = \omega_1 + \omega_2$, and the approximate momentum relationship $\vec{k}_3 = \vec{k}_1 + \vec{k}_2 = \Delta\vec{k}$. Third harmonic generation and interaction between more waves is mentioned. Applications of the theory to the dc and microwave Kerr effect, light modulation, harmonic generation, and parametric conversion are discussed.

- - - - -

15. Light Waves at the Boundary of Nonlinear Media, N. Bloembergen and P. S. Pershan.

A full report of this work is given in Cruft Laboratory T. R. No. 367. The abstract of that report is presented here.

Solutions to Maxwell's equations in nonlinear dielectrics are presented which satisfy the boundary conditions at a plane interface between a linear and nonlinear medium. Harmonic waves emanate from the boundary.

Generalizations of the well-known laws of reflection and refraction give the
direction of the boundary harmonic waves. Their intensity and polarization
conditions are described by generalizations of the Fresnel formulas. The
equivalent Brewster angle for harmonic waves is derived. The various con-
ditions for total reflection and transmission of boundary harmonics are dis-
cussed. The solution of the nonlinear plane parallel slab is presented which
describes the harmonic generation in experimental situations. An integral
equation formulation for wave propagation in nonlinear media is sketched.
Implications of the nonlinear boundary theory for experimental systems and
devices are pointed out.

- - - - -

16. Experimental Studies of Nonlinear Optical Phenomena, J. Ducuing,
    J. A. Armstrong, and N. Bloembergen.

The study of nonlinear optical effects requires light beams of ex-
tremely high peak power. These high peak powers are available in especially
constructed optical masers. We have designed, constructed, and successfully
operated a high power laser using the so-called Q-spoiling technique of
Hellwarth and McClung [1]. This involves the use of a resonance cavity formed
by the back face of the laser crystal and an external mirror. A high speed
switch—in this case an electro-optic shutter—is interposed between the laser
crystal and the external mirror and is used to provide the rapid change in
cavity Q which results in short, high powered pulses.

Using this high powered laser we have undertaken an experimental
program designed to detect the nonlinear boundary effects which occur at the
surface of highly polished nonlinear dielectrics, such as KDP . These
effects have been discussed theoretically by Professors Bloembergen and
Pershan in Cruft Laboratory Technical Report No. 367. At present we are
attempting to detect the specularly "reflected" second harmonic of ruby laser
light incident in an almost plane wave on the surface of a KDP crystal.

Reference

1. Hellwarth and McClung, J. Appl. Phys.

17. Microwave Modulation of Linear Electro-Optic Effect in KDP, R. A. Myers
     and P. S. Pershan.

     The past year has seen success in many aspects of the electro-optic
microwave frequency light modulator. Since the experiment has been described
in previous reports, only a brief description of our present scheme will be
presented, followed by a summary of the results to date and an analysis of
present experiments.

     A. Experimental. A light source is focused onto the microwave Kerr
cell [1] consisting of (in order) a variable aperture, a Glan-Thompson prism,
a silver-plated crystal of KDP (potassium dihydrogen phosphate) in a suitable
holder, a crossed G-T prism, and another variable aperture. The emergent
light is focused onto a detector in the dark room with a long focal-length lens
and a mirror. The microwave source is synchronized to the light—which is
commonly pulsed or chopped— by a photo-diode trigger and the variable delay
of a Tektronix 545A oscilloscope. The signal is displayed in a manner suitable
to the detector employed. Table I summarizes the various sources, rf gen-
erators, and detectors used.

          B. Results to Date.

                    1. Effective rotations of the plane of polarization by micro-
                        waves greater than 3° at 13. 5 Gc and 5° at 16. 5 Gc have
                        been observed.

                    2. All four sources in Table I have been modulated.

                    3. Dependence of the intensity of the modulated light on the
                        microwave power has been measured, and the linear
                        relation has been verified.

                    4. Dependence of the intensity of the modulated light on the
                        angle between the light polarization and the crystallo-
                        graphic $\hat{a}$-axes has been measured, and the predicted
                        sin 2θ function has been observed.

                    5. By means of a gated integrator, microwave modulation
                        has been detected with pulses of less than 500 mW peak

power. This corresponds to a peak rotation of less than 9' ; for our system, this is a modulation depth of approximately 5%. (It should be noted that with crossed nicols we only consider 10^{-4} of the incident light intensity. Thus, the modulation depth here observed is less than 5×10^{-6} of the initial intensity.)

6. The angular distribution of the modulated light has been observed both photographically and by direct visual observation. This appears to be approximately uniform for all directions in the acceptance cone of the Kerr cell.

C. Present Experiments. Recent theoretical work [2] has led to great interest in nonlinear effects in solids. Particularly promising are experiments involving the mixing of different optical frequencies in highly polarizable media. These experiments may be discussed in terms of a dielectric constant which is itself a function of the electric field

$$\underset{\approx}{\epsilon} = \underset{\approx}{\epsilon_0} + \underset{\approx}{\beta} \vec{E} + \underset{\approx}{\gamma} \vec{E} \vec{E} + \ldots \tag{1}$$

hence

$$\vec{D} = \underset{\approx}{\epsilon} \vec{E} = \underset{\approx}{\epsilon_0} \vec{E} + \underset{\approx}{\beta} \vec{E} \vec{E} + \underset{\approx}{\gamma} \vec{E} \vec{E} \vec{E} + \ldots \tag{2}$$

The present study is a special case in which one of the fields $\vec{E}_1$ is at an optical frequency (say, that of the Hg^{198} green line) and another $\vec{E}_2$ is at a microwave frequency. It is clear from the form of Eq. 2 that the frequency spectrum of $\vec{D}$ will have frequency components at all the frequencies $\omega_L, \omega_M,$ $\omega_L \pm \omega_M$, ... insofar as the tensors β , γ ... are non-zero. As a simple analysis shows*, spectral resolution of the microwave modulated light (with, say, a Fabry-Pérot interferometer of convenient spacing) should then reveal

- - - - - - -

*One must be careful, in such an analysis, not to neglect the change in wave-vector that must accompany the change in frequency induced by the modulation. Ditchburn [3], for example, gives an erroneous derivation of sidebands by omitting these changes in wave-vector.

a signal at the sideband frequencies. Preliminary marginal indications of such an effect are now being investigated with the magnetron source.

References

1. P. S. Pershan and R. A. Myers, Cruft Lab. Annual Progress Report No. 60, p. 14. (1961).

2. J. A. Armstrong, N. Bloembergen, J. Ducuing, and P. S. Pershan, _Phys. Rev._ (to be published).

3. R. W. Ditchburn, "Light, " New York, Interscience (1959), p. 390.

TABLE I

I. LIGHT SOURCES

A. General Radio Strobotac

B. Hg^{198} 2.450 Gc Electrodeless Discharge Lamp

C. Trion Ruby LASER

D. American-Optical 30-Watt Incandescent Lamp

II. MICROWAVE SOURCES

A. Varian VA 64F Klystron: 200 Watts at 13.5 Gc

B. Bomac BLM-030 Magnetron: 600 Watts at 16.0 - 16.5 Gc

III. DETECTORS

A. RCA 6810A Photomultiplier

     1. Direct CRO display (with cathode-follower for short pulses)

     2. Recorder display following transistorized gated integrator

          a. Directly

          b. Through Jarrell-Ash one-meter spectrometer

B. Polaroid Camera

     1. Direct photograph of light transmitted by Kerr cell

     2. Photograph of 5461Å Fabry-Pérot , interference fringes (with interference filter for fore-prism)

- - - - -

18. Microwave Maser Spectrometer, S. Dmitrevsky.

The aim of the project described below is the development of a high
sensitivity EPR spectrometer utilizing maser techniques. The instrument
can be built in one of the two configurations given below:

(1) A bridge EPR spectrometer driven by a klystron source and em-
ploying a low noise maser preamplifier followed by a conventional
superheterodyne receiver.

(2) A marginal maser oscillator coupled to the sample cavity.

Configuration 1 has the advantage of greater simplicity inasmuch as
it is using components (source, bridge, maser preamplifier) the adjustment
of which for optimum system performance can be carried out independently.
The usefulness of this configuration, however, is contingent on the condition
that noise sources other than the noise of the signal oscillator impose the limit
on the sensitivity. Should the signal oscillator noise become dominant, it
would be necessary to replace the signal oscillator with a maser oscillator.
The system then would consist of a maser oscillator, spectrometer bridge,
and maser amplifier. Noting that both masers would operate at the same fre-
quency, the natural development would be to confine the two masers in one
cavity, which would result in a device of configuration 2 as designated
earlier.

Work has been started on the klystron-maser amplifier. The frequency
chosen was 9 kMc/s . It is mandatory that the bridge be capable of a high
degree of balance, because of a relatively low power handling capacity of a
maser oscillator and the enhancement of sensitivity by high energy storage in
the sample cavity. The equipment designed and built utilizes a magic tee, the
symmetric arms of which are connected to two identical cavities. One cavity
will serve as the sample, the other, as the reference cavity. Provisions
have been made for the external adjustment of the resonant frequencies and
coupling coefficients of the two cavities. Preliminary tests of the balance of
the bridge have indicated balances slightly in excess of 60 dB . This figure
may be improved, since the full range of balance controls could not be used
in the first tests.

The maser section of the device has been built and cold tested, and is due to be put into operation on the arrival of the klystron pump.

The principal question requiring our attention when the complete device is assembled will be the effect of the source noise. It should then be possible to decide which of the two modes of operation—maser amplifier, or marginal oscillator, is the more profitable. The mechanical modifications required for the change of operation are small, and it is hoped that they do not cause undue delay.

- - - - -

III. AUTOMATIC CONTROL[*]

Personnel

Prof. A. E. Bryson, Jr.
Assoc. Prof. R. E. Kronauer
Asst. Prof. Y. C. Ho
Asst. Prof. K. S. Narendra
Mr. P. Drew
Mr. R. M. Goldwyn
Mr. R. Grief

Mr. R. Gross
Mr. S. Johnson
Mr. L. E. McBride, Jr.
Mr. R. McLaughlin
Mr. F. K. Minami
Mr. D. N. Streeter
Mr. K. Tait

III A. Control Systems[*]

1. Determination of Lock-On Time for an Automatic Phase Control Loop,
   R. McLaughlin and R. E. Kronauer.

This work has been completed and the report is being prepared for publication. In addition to the time integrals taken from analog computer studies, analytic formulas were derived, one for the probability of failure to lock-on in the long time (small probability)limit, and another for all other probabilities. Certain numerical constants in these formulas required the computer integrals for their evaluation.

- - - - -

2. Performance Criteria for Control Systems with Random Excitation,
   F. Minami and R. E. Kronauer.

Performance criteria for randomly excited systems are typically limited to the minimization of quadratic integrals or summations. Experience with systems excited deterministically has cast doubt on mean-square-error criteria and alternatives have been used. This study is aimed at: (1) examining whether the experience with deterministic input has been colored by the fact that the test conditions may not match those under which the system will actually be used, and (2) finding criteria for randomly excited systems which correspond to the alternative criteria which have been developed for the deterministic input. Under (1), results have shown that the choice of a

- - - - - - -

reasonable power spectral distribution for a random input can lead to known
desirable system parameters with a mean-square-error criterion. Under
(2) it appears that a useful variety of alternative criteria can be devised from
the input-error correlation function.

- - - - -

3. Analysis of a Rapid-Acting Adaptive System, P. Drew and R. E. Kronauer.

Analysis of parameter-perturbation adaptive systems (e. g. , Rideout
and McGrath, IRE, PGAP, February 1961; Krasovskii, Proc. First Meeting
on Automatic Control, Moscow, 1960) usually assumes frequency separations
between various control variables. For rapid adaptation, it appears desirable
to violate these assumed separations. Our present work examines the effects
of such violations on the rapidity, stability, and accuracy of adaptation, and
on the asymptotic value of control system error. It appears that both stability
conditions and increases in asymptotic error provide limits on adaptation
time. Both random and deterministic inputs are being considered.

- - - - -

III B.   Optimal Programing of Multivariable Control Systems[*]

1. Optimal Programing of Multivariable Control Systems in the Presence of Noise, A. E. Bryson, Jr.

This is a brief review of the current status of optimal programing theory as applied to multivariable control systems in the presence of noise. Open-loop programing of control variables for a noise-free nonlinear system is discussed first, followed by a description of closed-loop gain programing for a linearized version of the same type of system. Optimal filtering of noisy measurements is then reviewed for linear time-varying systems. A combination of these techniques promises to provide optimal control for a wide class of systems and performance indices.

Optimal Programing for Nonlinear Systems (Noise-Free).   The solution of optimal programing problems on computers may now be considered practical and straightforward through the use of gradient (steepest-ascent) techniques developed within the last few years [see references 1-7]. The type of problem that can be solved is as follows.

Given: A physical system governed by:

$$\dot{x} = f (x , u , t)$$

where:

$x(t) = n$ by 1 matrix of state variables

$u(t) = q$ by 1 matrix of control variables

$x(t_o)$ given

$f(x, u, t) = n$ by 1 matrix of known functions (nonlinear)

- - - - - - - -

Find: u(t) to maximize

$$\phi[x(t_1), t_1]; t_1 > t_o$$

with terminal constraints

$$\psi[x(t_1), t_1] = 0$$

where

$\phi(x,t)$ is pay-off function (given)

$\psi(x,t)$ is an r by 1 matrix of given functions, $r \leq n-1$.

Solution: Calculus of variations using steepest-ascent numerical
calculations

This is an open-loop control system with programed control variables,
u(t) . This is not a feasible type of control to use in many systems, due to
errors in the determination of initial conditions and parameters of the system.
However, if the "path" is used as a nominal path and small perturbations are
considered around it, a linear feedback control system with programed gains
can be synthesized that will bring the system very close to the desired termi-
nal conditions.

Neighboring-Optimum Feedback Control (Noise-Free).   A simple
approach to this problem is what might be called "minimum incremental effort"
control. It is a straightforward application of a quadratic performance index
to the system linearized around the optimum path of the previous section. This
is discussed with several examples, in references 8 and 9. A slightly more
sophisticated approach is used in references 10 and 11 where the performance
index is the same one used in the original nonlinear problem; here a true
neighboring-optimum is found using the second variation. An outline of the
type of problem solved by this latter technique is:

Given: u(t) that minimizes $\phi[x(t_1), t_1]$ with $\psi[x(t_1), t_1] = 0$

and given $x(t_o)$, for $\dot{x} = f(x, u, t)$

Find: $\delta u(t)$

such that $u(t) + \delta u(t)$

minimizes $\phi[x(t_1), t_1]$ with $\psi[x(t_1), t_1] = 0$

and given $x(t_o) + \delta x(t_o)$ for $\dot{x} = f(x, u, t)$.

Solution: $\delta u(t) = -\Lambda(t, t_o) \delta x(t_o)$

where $\Lambda(t, t_o)$ is pre-calculated from second variation

Note 1: The concept is readily extended to continuous measurement

of $\delta x(t)$, $\rightarrow \delta u(t) = -\Lambda(t) \delta x(t)$.

Note 2: $\delta x(t)$ due to $\delta u(t)$ governed by linear equations:

$$\frac{d}{dt}(\delta x) = F(t)\delta x + G(t)\delta u \; ; \; F_{ij} = \left(\frac{\partial f_i}{\partial x_j}\right)_{nom.} \; , \; G_{ij} = \left(\frac{\partial f_i}{\partial u_j}\right)_{nom.}$$

Optimal Estimation for Noisy Time-Varying Linear Systems. In references 12-14, a practical filter was developed for time-varying linear systems with Gaussian random noise in the system and in the measurements. The procedure may be regarded as keeping track of the mean values and covariances of a multivariable Gaussian distribution in a Markov process. An easy way to understand the optimal estimation procedure is to consider only one step of a discrete process where either (1) a set of measurements is made or (2), a set of discrete forcing functions is applied. First, consider the improvement in the estimate as the result of a set of measurements:

Given: (1) A priori estimate of state variables and covariances:

$\epsilon[x] = \bar{x}$ (an n   vector)

$\epsilon[(x - \bar{x})(x - \bar{x})^T] = \bar{P}$ (an n x n symmetric matrix)

(2) A set of measurements and covariances:

$\epsilon[z] = \bar{z}$ (a p   vector)

$\epsilon[(z - \bar{z})(z - \bar{z})^T] = \bar{R}$ (a p x p symmetric matrix)

where $z = Hx$

Find: maximum likelihood estimate $\hat{x}$, that minimizes

$$\phi = \frac{1}{2}\tilde{z}^T \overline{R}^{-1}\tilde{z} + \frac{1}{2}\tilde{x}^T \overline{P}^{-1}\tilde{x} \quad ,$$

where $(\tilde{\ }) = (\hat{\ }) - (\overline{\ })$.

Answer: $\hat{x} = \overline{x} + PH^T \overline{R}^{-1}(\overline{z} - H\overline{x})$

$$P^{-1} = \overline{P}^{-1} + H^T \overline{R}^{-1} H$$

where $P = \epsilon[(x - \hat{x})(x - \hat{x})^T]$.

Next, consider the degradation in the estimate as the result of a set of forcing functions:

Given: (1) A priori estimate of state variables and covariances

$$\epsilon[x] = \overline{x}$$

$$\epsilon[(x - \overline{x})(x - \overline{x})^T] = \overline{P}$$

(2) A set of forcing functions and covariances:

$$\epsilon[u] = \overline{u}$$

$$\epsilon[(u - \overline{u})(u - \overline{u})^T] = \overline{Q}$$

where $\Delta x = Gu$

Find: revised estimate of state variables and covariances after application of forcing function.

Answer: $\hat{x} = \overline{x} + G\overline{u}$

$$P = \overline{P} + G\overline{Q}G^T$$

where $P = \epsilon[(x - \hat{x})(x - \hat{x})^T]$

If we now apply the above to a discrete process with a transition matrix $\Phi_{n, n-1}$ that describes the transition from the state at the $(n-1)$st step to the nth step, we have the following:

Stochastic Controller for Discrete Measurements and Discrete Forcing Functions

$$
\hat{x}_n = \begin{cases}
\Phi_{n,n-1}\,\hat{x}_{n-1} & \text{if ordinary point} \\[2ex]
\Phi_{n,n-1}\,\hat{x}_{n-1} + K_n(\bar{z}_n - H_n\,\Phi_{n,n-1}\,\hat{x}_{n-1}) & \text{if measurement made} \\[2ex]
\Phi_{n,n-1}\,\hat{x}_{n-1} + G_n\,\bar{u}_n & \text{if forcing function applied}
\end{cases}
$$

$$
P_n = \begin{cases}
\Phi_{n,n-1}\,P_{n-1}\,\Phi_{n,n-1}^T & \text{if ordinary point} \\[2ex]
\left[(\Phi_{n,n-1}\,P_{n-1}\,\Phi_{n,n-1}^T)^{-1} + H_n^T\,\bar{R}_n^{-1}\,H_n\right]^{-1} & \text{if measurement made} \\[2ex]
\Phi_{n,n-1}\,P_{n-1}\,\Phi_{n,n-1}^T + G_n\,\bar{Q}_n\,G_n^T & \text{if forcing function applied}
\end{cases}
$$

$$
K_n = P_n H_n^T \bar{R}_n^{-1} \quad, \quad \text{gain in optimal estimator}
$$

In the limit, as the process and the measurements become continuous, the results of reference 14 are obtained. Instead of a transition matrix, we then have differential equations.

$$
\dot{x} = F(t)\,x + G(t)\,u \quad .
$$

In place of covariance matrices we have the correlation matrices $\bar{R}(t)$ and $\bar{Q}(t)$ that serve to describe the "white noise" in the measurements and in the forcing functions respectively:

$$
\epsilon\{z(t)\} = \bar{z}(t) \quad,
$$

$$
\epsilon\left\{[z(t) - \bar{z}(t)][z(\tau) - \bar{z}(\tau)]^T\right\} = \bar{R}(t)\,\delta(t-\tau) \quad,
$$

where $z = Hx$, and

$$
\epsilon[u(t)] = \bar{u}(t) \quad,
$$

$$
\epsilon\left\{[u(t) - \bar{u}(t)][u(\tau) - \bar{u}(\tau)]^T\right\} = \bar{Q}(t)\,\delta(t-\tau) \quad .
$$

The optimal filter then becomes:

$$\dot{\hat{x}} = F\hat{x} + G\bar{u} + PH^T \bar{R}^{-1} (\bar{z} - H\hat{x}) \quad ; \quad x(t_o) = \bar{x}_o$$

$$\dot{P} = FP + PF^T - PH^T \bar{R}^{-1} HP + G\bar{Q}G^T \quad ; \quad P(t_o) = \bar{P}_o$$

where

$$\epsilon \quad [x(t_o)] = \bar{x}_o$$

$$\epsilon \left\{ [x(t_o) - \bar{x}_o][x(t_o) - \bar{x}_o]^T \right\} = \bar{P}_o \quad .$$

Reference 15 discusses the estimation problem from the point of view of maximum likelihood estimation which, in turn, is a type of "least square" fitting.

Combination of Optimal Filter and Closed-Loop Gain Programming. In reference 16 it is shown that, for quadratic performance indices, the combination of the optimal filter and the closed-loop optimal gain programming technique (noise-free)produces optimal control for linear systems in the presence of noise. There is reason to believe this combination will be optimal for a more general class of performance indices. Using the nomenclature of the previous sections the control system is given by

$$u(t) = - \Lambda(t)\hat{x}(t)$$

$$\dot{x} = Fx + Gu$$

$$\dot{\hat{x}} = F\hat{x} + Gu + PH^T \bar{R}^{-1}(\bar{z} - H\hat{x}) \ ; \quad \hat{x}(t_o) = \bar{x}_o$$

$$\dot{P} = FP + PF^T - PH^T \bar{R}^{-1} HP + G\bar{Q}G^T \quad ; \quad P(t_o) = \bar{P}_o$$

where $\Lambda(t)$ is a set of pre-calculated time-varying gains determined from noise-free control considerations regarding $\hat{x}(t)$ as though it were the exact value of $x(t)$. Note $P(t)$ may be pre-calculated and the time-varying gains $K(t) = PH^T \bar{R}^{-1}$ stored in a memory for use during operation of the control system (see Fig. 1). Obviously, this system can also be combined with the neighboring-optimum feedback scheme described above.

References

1. H. J. Kelley, "Gradient Theory of Optimal Flight Paths, " J. Am. Rocket Soc., Vol. 30, pp. 947-953 (Oct. 1960).

2. A. E. Bryson, W. F. Denham, F. J. Carroll, and K. Mikami, "Lift or Drag Programs that Minimize Re-Entry Heating,"Inst. Aerospace Sciences, Annual Meeting, January 1961; J. Aerospace Sci., Vol. 29, No. 4, pp. 420-430 (April 1962).

3. A. E. Bryson, "A Gradient Method for Optimizing Multi-Stage Allocation Processes, " Proc. Harvard University Symposium on Digital Computers and their Applications, April 1961 (to be published).

4. A. E. Bryson and W. F. Denham, "A Steepest-Ascent Method for Solving Optimum Programming Problems, " J. Appl. Mech. (Trans. ASME, Series E), pp. 247-257 (June 1962). (Also Raytheon Co. ,Report BR-1303, August 10, 1961).

5. K. Mikami, C. T. Battle, R. S. Goodell, and A. E. Bryson,"Three-Dimensional Trajectory Optimization Study, " USAF Document ASD-TDR-62-295, Parts I, II, and III, May 1962. (Also Raytheon Co., Report BR-1759).

6. A. E. Bryson, K. Mikami, and C. T. Battle, " Optimal Lateral Turns for a Re-Entry Glider,"Aerospace Eng. (April 1962).

7. G. Leitman (Editor), Optimization Techniques, Academic Press, August 1962. (See particularly Chap. 6 by H. J. Kelley, "Method of Gradients.")

8. A. E. Bryson and W. F. Denham,"Multivariable Terminal Control to Minimize Mean Square Deviation from a Nominal Path, " Proc. Inst. Aerospace Sci. Symposium on Vehicle Systems Optimization, November, 1961, Garden City, New York. (Also Raytheon Co., Report BR-1333,Sept. 20, 1961.)

9. A. E. Bryson and W. F. Denham, "A Guidance Scheme for Supercircular Re-Entry of a Lifting Vehicle,"J. Am. Rocket Soc., Vol. 32, No. 6, pp. 894-898 (June 1962).
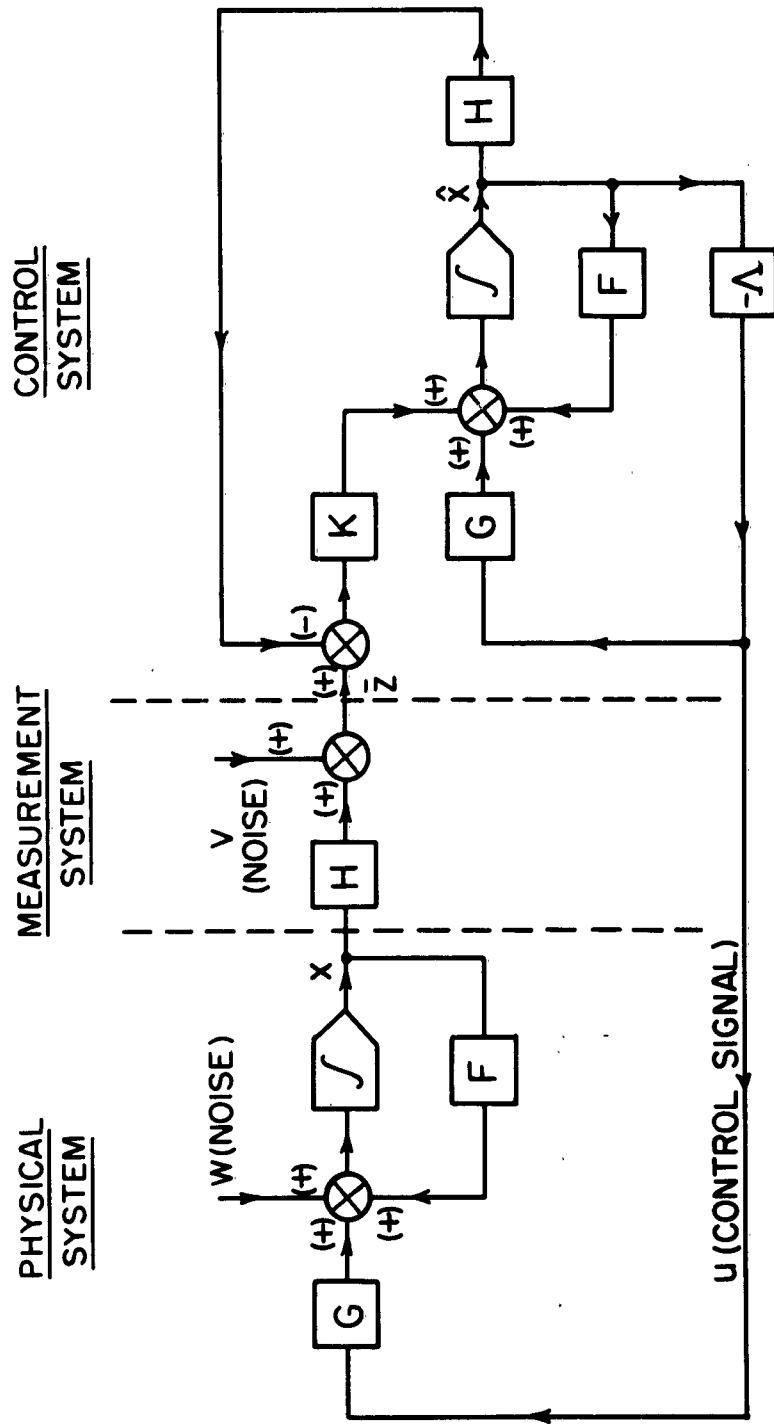
FIGURE 1

10. H. J. Kelley, "Guidance Theory and Extremal Fields, " Presented Nat. Aerospace Electronics Convention, May 14-16, 1962, Dayton, Ohio.

11. J. V. Breakwell and A. E. Bryson, "Neighboring-Optimum Terminal Control for Multivariable Nonlinear Systems, " to be presented at Soc. Indus. and Appl. Math. Conference on Control, Boston, Massachusetts, November 1962.

12. P. Swerling, "A Proposed Stagewise Differential Correction Procedure for Satellite Tracking and Prediction, " J. Astro. Sci.(Autumn 1959).

13. R. E. Kalman, "A New Approach to Linear Filtering and Prediction Problems, " J. Basic Eng.(Trans. ASME Series D), Vol. 82, pp. 34-45 (1960).

14. R. E. Kalman and R. S. Bucy, "New Results in Linear Filtering and Prediction Theory,"J. Basic Eng. (Trans. ASME, Series D) Vol. 83, pp. 95-108 (1961). (See also RIAS Tech. Report 61-1 for elaboration.)

15. A. E. Bryson and M. Frazier, "Smoothing for Linear and Nonlinear Dynamic Systems, " Proc. Conference on Optimum Systems Synthesis, Wright-Patterson Air Force Base, Ohio, September 11-13 (1962).

16. T. F. Gunckel and G. F. Franklin, "A General Solution for Linear Sampled-Data Control Systems,"J. Basic Eng. (Trans. ASME) (to be published).

- - - - - - -

III C. Optimal Control for Dynamic Systems[*]

1. Study of the Optimal Control of Dynamic Systems, Y. C. Ho

The study of optimal control systems has received much attention in the past year. A comprehensive study of the problem for general linear systems was completed under a doctoral dissertation (Cruft Lab. Tech. Reports Nos. 335 and 340) in which the well-known bang-bang control problem was first solved in complete generality via a successive approximation method. The study also revealed close connection between the methods of nonlinear programing and those of the calculus variations. Extension of the method obtained in Cruft Lab. Tech. Report No. 340 has been made to more general nonlinear systems with inequality constraint on the state variable (to appear in J. of Math. Analysis and Application).

- - - - -

2. Investigator, Y. C. Ho

The effort of the investigator for the past year has been devoted to the systematic study of computational algorithms for the solution of optimal control problems. Briefly, we consider:

(1) <u>Systems</u>. It is assumed that the dynamic system is governed by

$$\dot{\underline{x}} = \underline{f}(\underline{x}; \underline{u}; t)$$

(2) <u>Performance criterion</u>.

$$J = \lambda(\underline{x}(t_1)) + \int_{t_o}^{t_1} L(\underline{x}; \underline{u}; t) \, dt$$

- - - - - - -

(3) <u>Constraints</u>.

(a) $\underline{\psi}\,(\underline{x}(t_1)\,,\,t_1\,) = \underline{d}$

(b) $\underline{g}\,(\underline{x};u;t) \leqslant 0$

The optimal control or programing problem is then defined as, "Given (1), determine $\underline{u}(t)$ for $t_o \leqslant t \leqslant t_1$ such that (2) is optimized subject to (3). " In Cruft Lab. Tech. Report No. 335 we first detailed a method to solve the problem when (1) and (3a) are linear, (2) is quadratic, and (3b) is a linear function of u only (the generalized bang-bang control problem). It was later shown that this method can be directly extended to handle nonlinear cases with (3b) as a nonlinear function of the state $\underline{x}$ only. This result is to be published by J. of Math. Analysis and Application later this year. We have also demonstrated that the computational solution of the above problem is basically a problem in mathematical programing . . The general case where (3b) is several functions involving $\underline{x}$ and $\underline{u}$ separately can be identified and solved using techniques developed in mathematical programing areas (see Cruft Lab. Tech. Report No. 347).

The use of penalty functions in the computational solution of optimal control problems has also been investigated and reported in Cruft Lab. Tech. Report No. 368.

III D. Topics in Automatic Control[*]

1. Multivariable Systems, K. S. Narendra and R. M . Goldwyn.

In Cruft Lab. Tech. Report No. 342 (June 1961), "Application of Matrix Methods to the Optimum Synthesis of Multivariable Systems Subject to Constraints, " will be found material discussed in the previous annual report. During the past year this was revised for presentation and publication at the Winter General Meeting of the AIEE in New York.

- - - - -

2. Multivariable Systems, K. S. Narendra and L. E. McBride, Jr.

Work has been essentially completed on a comparison of the different modes of the representation of a multivariable system, i. e., by a matrix of transfer functions or by a set of first-order differential equations. The mode of representation depends on the nature of the problem and the constraints involved. The relative merits of the several methods as well as their inherent limitations have been considered. Concepts such as "controllability, " "observability, " "structure, " and "interaction" which are peculiar to multivariable systems are examined to form the basis for the comparison. This work will appear in Cruft Lab. Tech. Report No. 356.

- - - - -

3. Adaptive Control, D. N. Streeter and K. S. Narendra.

The work to be described below will appear in Cruft Lab. Tech. Report No. 359. The report deals with control systems that exhibit a capacity to learn, in the sense of meaningful self-alteration based on experience. The relation between learning, adaptation, and self-organization in control systems and in animals is discussed. A system capable of synthesizing its controllers without explicit knowledge of the process or the spectra of the inputs is detailed. The synthesis is based on the cross-correlation between a signal representing

- - - - - - -

the desired output and the various components of the tentative input signal.
The system, in a general way, exemplifies the principles of learning by Mr.
A. L. Samuel in programing a computer to play checkers. Results of
computer simulation of the system are presented.

– – – – –·–

4. Time-Varying Systems, K. S. Narendra

The synthesis of feedback systems having time-varying plants is being
considered. Stability is being examined using the methods of Liapunov.

IV. COMMUNICATIONS AND NETWORKS

Personnel

Asst. Prof. D. W. Tufts   Mr. J. Hopkins
Dr. H. J. Riblet   Mr. J. Huang
Dr. A. A. Pandiscio   Mr. N. Johnson
Mr. T. Baker   Mr. Y. Ohashi
Mr. T. Fine   Mr. D. Shnidman

1. Study of an Automatic Phase Control Loop, A. A. Pandiscio and T. Baker. Nonr -1866(16).

Several methods have been developed for determining the pull-in and pull-out frequency ranges for various filter configurations in first, second, and higher-order automatic phase control loops. These results must still be compared with analog and digital computer solutions and data from an experimental model.

- - - - -

2. Avalanche Transistor Pulse Circuits, A. A. Pandiscio and J. Huang. Nonr-1866(16).

In the last Quarterly Status Report, an experimental method for determining transistor switching parameters based on the charge control concept was mentioned. This technique is particularly pertinent to switching characteristics, since the parameters are derived under similar large signal conditions.

If a transistor (PNP, for example) is turned on into a short circuit load, i.e., no change of collector voltage, the charge control analysis defines the following emitter, base, and collector time constants:

$$\tau_E = \frac{Q_B}{I_E} \quad , \quad \tau_B = \frac{Q_B}{I_B} \quad , \quad \tau_C = \frac{Q_B}{I_C} \quad .$$

The total base stored charge Q_B includes Q_{VE}, the charge associated with charging the emitter depletion layer capacitance. Q_{VE} is usually a small fraction of Q_B in alloy junction transistors, but may be large in graded

base ones. If Q_{VE} is neglected, τ_C as well as τ_E (for $\alpha \simeq 1$) are identical with the mean transit time across the base and τ_B with the mean lifetime of minority carriers. For low level injection, and assuming a 6 dB per octave fall-off of common emitter current gain magnitude at high frequency, τ_C is equal to the reciprocal of gain-bandwidth product commonly denoted by ω_T. τ_C is, therefore, the most important parameter characterizing transistor high-frequency performance, and its measurement does not involve the 6 dB per octave approximation.
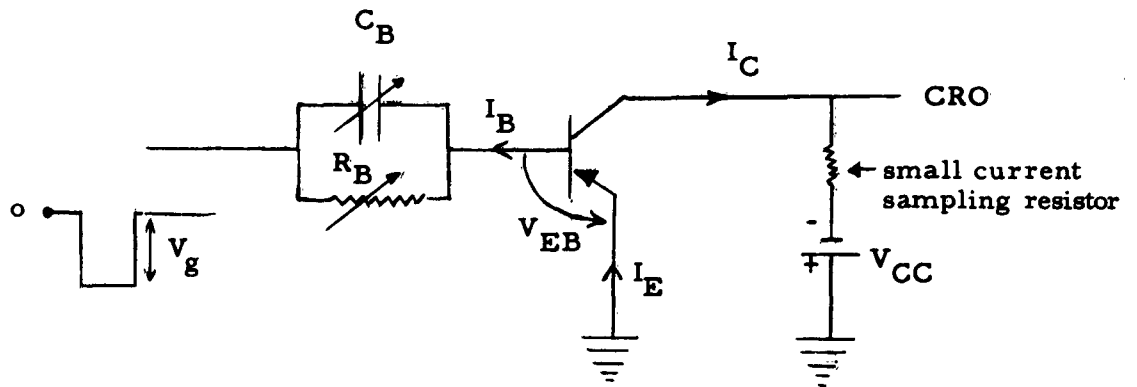
FIGURE 1

The circuit of Fig. 1 is the basic circuit for the measurement of τ_C, τ_B, and the dc common emitter short circuit current gain β. The input is a fast rise square wave with amplitude V_g. R_B is set so that $I_B = \dfrac{V_g}{R_B}$, giving

$$\beta = \frac{I_C}{I_B} = \frac{I_C R_B}{V_g} \qquad . \tag{1}$$

C_B is adjusted so that the output square wave exhibits neither overshoot nor undershoot. We then have $Q_B = C_B V_g = I_C \tau_C$

$$\tau_C = \frac{C_B V_g}{I_C} \qquad\qquad (2)$$

and

$$\tau_B = C_B R_B \qquad . \qquad\qquad (3)$$

The large signal collector depletion layer capacitance C_{av} is defined as the average of the small signal depletion layer capacitance C_c over the collector voltage excursion from V_{BC1} to V_{BC2}

$$C_{av} = \frac{1}{V_{BC1} - V_{BC2}} \int_{V_{BC1}}^{V_{BC2}} C_c\, dV_{BC} = \frac{Q_{VC}}{V_{BC1} - V_{BC2}} \quad , \qquad (4)$$

where Q_{VC} , exactly analogous to Q_{VE} , is the charge necessary to displace the collector depletion layer capacitance as the result of the change of collector-base junction voltage. The presence of a load resistance R_L in the collector circuit of Fig. 1 can cause such a change during the "turn on" process. The measurement of C_{av} consists first in choosing R_L so that

$$V_{BC2} = V_{BC1} - R_L I_C \qquad .$$

The stored charge Q_{B1} is then obtained from the relation

$$Q_{B1} = C_{B1} V_g = I_C \tau_C + Q_{VC} \qquad . \qquad\qquad (5)$$

R_L is then halved, while R_B is decreased by an amount sufficient to double the collector current, so that the collector voltage is again V_{BC2}. C_B is adjusted for a square wave output and Q_{B2} is given by

$$Q_{B2} = C_{B2} V_g = 2I_C \tau_C + Q_{VC} \qquad . \qquad\qquad (6)$$

Combination of Eqs. 5 and 6 yields

$$Q_{VC} = (2 C_{B1} - C_{B2}) V_g \qquad ,$$

and, consequently, we have

$$C_{av} = \frac{(2C_{B1} - C_{B2})V_g}{V_{BC1} - V_{BC2}} \qquad (7)$$

Figure 2 shows the stored charge profiles in the base of an alloy junction transistor for the two-step measurements to obtain C_{av} .
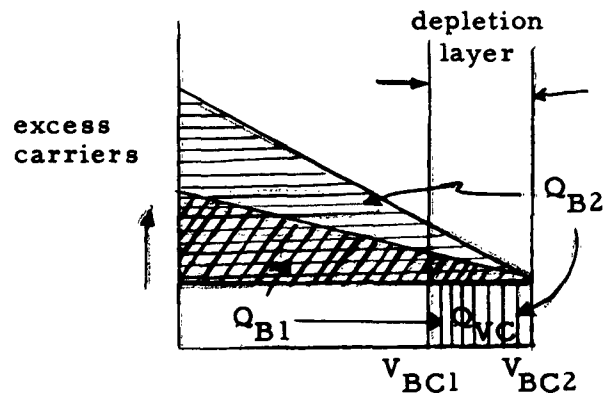
FIGURE 2

It should be noted that in the above analysis the saturation current I_{CO} is ignored, since it is very small compared to the switch on current I_C . The forward biased emitter-base junction voltage V_{EB} can be neg- lected only when V_g is sufficiently large. If the extrinsic base or collector resistances are not negligible, corrections have to be made to the measured collector junction voltage V_{BC} .

- - - - -

3. Automatic Phase Control Loop, T. Baker.   Contract Nonr-1866(16).

The automatic phase control loop has been considered primarily as a device for synchronizing a sinusoidal oscillator.   The loop as shown in Fig. 3 consists of a local oscillator whose frequency is variable around a "free-running" value, a phase discriminator whose output is a sinusoidal function of the phase difference between the input synchronizing signal and the oscillator output signal, and a linear (or, possibly, nonlinear) low-pass filter which attenuates the unwanted high frequency noise in the loop.   This system has been analyzed in some detail when the input signal is sinusoidal and the filter has one of several configurations.
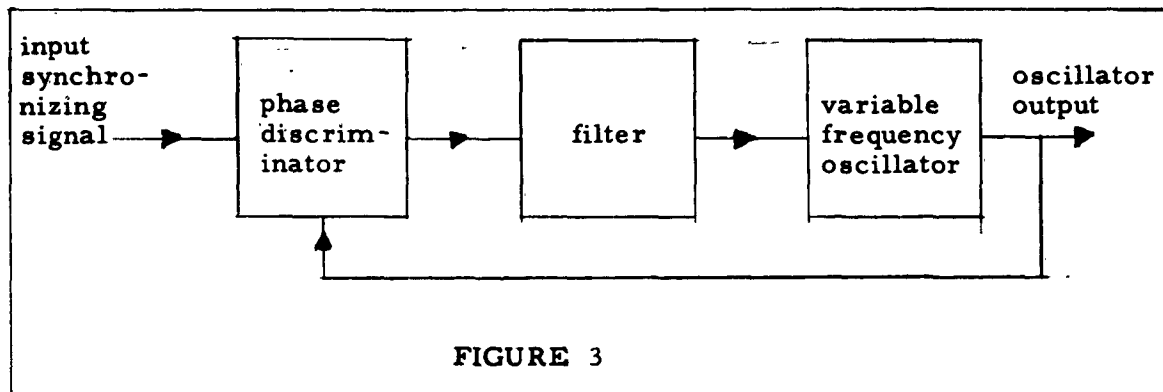
FIGURE 3

The loop equation is

$$\frac{d\phi(t)}{dt} + \omega_c N(p) \sin\phi(t) = \omega_o \tag{1}$$

where:

$\phi(t)$ is the instantaneous phase difference between the input and output signals

ω_c is the "characteristic frequency" of the open loop—the product of all gains and sensitivities

$N(p)$ is the expression, in operator form $(p = \frac{d}{dt})$, of the differential equation relating the input and output of the filter

ω_o is the frequency difference between the free-running oscillator and the synchronizing signal

The filter configurations of Fig. 4 have been considered in analyzing Eq. 1.

$$N(p) = 1$$

$$N(p) = \frac{1}{1 + \frac{p}{\omega_f}}$$

$$N(p) = \frac{1 + p\frac{\beta}{\omega_f}}{1 + \frac{p}{\omega_f}}$$

$$\omega_f = \frac{1}{RC}$$

$$\omega_f = \frac{1}{RC}$$

FIGURE 4a   FIGURE 4b   FIGURE 4c
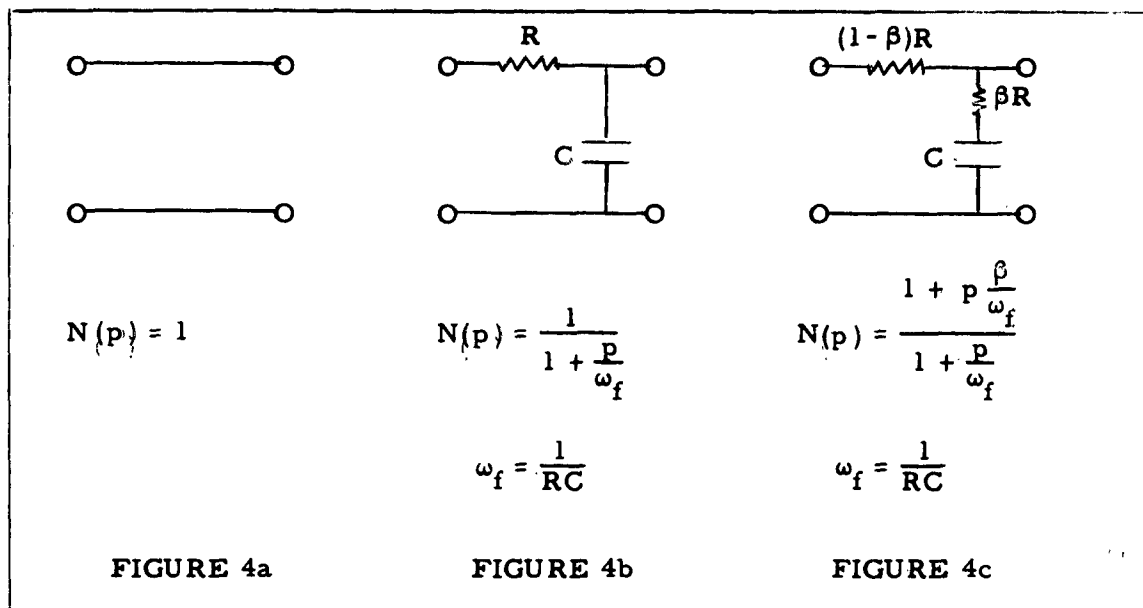
When the filter is all-pass, as in Fig. 4a, Eq. 1 is of first-order, and has an analytical solution. If $\omega_o < \omega_c$, then $\phi(t)$ approaches a constant value, $\sin^{-1}\frac{\omega_o}{\omega_c}$, or that value shifted by some multiple of 2π , depending on the initial phase. If $\omega_o > \omega_c$, then ϕ increases somewhat linearly (with a periodic modulation), so that the output of the phase discriminator, $\sin\phi$, has a "beat frequency" $\sqrt{\omega_o{}^2 - \omega_c{}^2}$. Thus, the oscillator has a "pull-in" range $|\omega_o| < \omega_c$ wherein it "locks." to the synchronizing input. For other filters, the loop equations have no exact analytical solutions, since the equations are of higher order. For example, for the low-pass filter of Fig. 4a, the loop equation is

$$\frac{1}{\omega_f} \frac{d^2\phi(t)}{dt^2} + \frac{d\phi(t)}{dt} + \omega_c \sin\phi(t) = \omega_o \qquad .$$

The determination of pull-in ranges for different values of filter parameters and initial phase and frequency conditions has been investigated using experimental and approximate techniques. The results will appear in a forthcoming report.

- - - - -

4. Parametric Amplification, J. Hopkins. Contract Nonr-1866(16).

A general review of literature in the field of parametric amplification was undertaken to help determine the specific line along which effort might be directed profitably. The program adopted comprises further examination of the broadband operating characteristics obtained with parametric amplifiers consisting of varactor diodes terminated in bandpass filter structures. The basic inspiration for this work was found in papers by Hermann and Seidel [1], and by Matthaei [2].

A lower-sideband varactor diode parametric amplifier may be thought of as a negative resistance (resulting from the time-varying component) with an associated constant capacitance, C_o . A simple analysis indicates that amplification is obtained only when the input and output impedances , $z(j\omega)$, seen by the negative resistance are almost entirely real; yet these impedances include C_o as a terminating element, and for such a case, the integral

$$I_z = \int_0^\infty \text{Re } z(j\omega) \, d\omega$$

is very restricted. For example, if C_o appears as a shunt termination [2, 3],

$$I_z = \pi / 2 C_o \quad .$$

Thus, since gain is a function of $\text{Re } z(j\omega)$, to obtain an amplifier of broad bandwidth and fairly uniform gain, it is necessary to constrain z to be almost purely real over the desired bandwidth with prescribed (frequency dependent) value. This requires a bandpass filter structure between C_o and the final load, or source, impedance (which is generally resistive). Due to the rather involved relationship between amplifier gain and load (and source) impedance, detailed design of the essential filter characteristics for given gain uniformity and bandwidth present a challenging problem. It is this subject which has been chosen for investigation.

Much study was devoted to analysis and possible extension of the design methods of Matthaei, based on conventional filter synthesis techniques, and to those of Herrmann and Seidel, dealing directly with the gain function as

related to filter parameters. Because no satisfactory solution has emerged
from this research to date, it appears that experimental work will be neces-
sary to gather information on the pumped varactor diode as a circuit element.
Plans are being made for the construction of a C-band degenerate amplifier,
which will have an operating frequency of 5.4 Gc pumped at 10.8 Gc , with
particular preliminary interest in impedance measurements.

References

1. G. F. Herrmann and H. Seidel, " Circuit Aspects of Parametric Amplifiers,"
   Part 2, pp. 83-90, WESCON Convention Record (1959).

2. G. L. Matthaei, " A Study of the Optimum Design of Wide-Band Parametric
   Amplifiers and Up-Converters, " Trans. IRE, Vol. MTT-9, pp. 23-38(1961).

3. H. W. Bode, Network and Analysis and Feedback Amplifier Design (New
   York, D. Van Nostrand Co., Inc., 1945), pp. 280-281.

- - - - -

5. Communication Theory

A. Optimum Pulse Communication, D. W. Tufts.

The design of optimum pulse signals and receivers was considered
from the point of view of least mean-square-noise interference and interpulse
interference. It was discovered that there exists a unique, linear receiver
which minimizes noise interference while constrained to eliminate completely
interpulse interference over a block of N pulses. The receiver can be real-
ized in the form of a matched filter followed by a tapped-delay line. This
work is discussed in Cruft Lab. Tech. Report No. 345, July 20, 1961.

A more effective method of reducing interference in pulse systems will
be found in Cruft Lab. Tech. Report No. 355, February 5, 1962. In this
report, interpulse interference, noise interference, and timing jitter are all
considered on an equal basis by minimizing total interference in a mean-
square sense.

- - - - -

B. Non-Stationary, Nonlinear Noise Experiment, D. W. Tufts and

D. Shnidman.

Nonlinear operations on periodic signals plus stationary noise produce non-stationary random processes. It is difficult to study such processes analytically. Hence, an experimental setup was constructed to simulate a nonlinear radar receiver. Data will be taken during the subsequent period.

- - - - -

C. Interpolation of Random Signals, D. W. Tufts and N. Johnson.

A study of methods of interpolating samples of random signals was begun. The tools of numerical analysis and communication theory have been used and related. Numerical methods for calculating optimum-least-squares interpolatory functions have been developed.

- - - - -

V. MICROWAVE APPLICATIONS

OF FERROMAGNETIC AND FERROELECTRIC MATERIALS

Personnel

Assoc. Prof. R. V. Jones	Mr. T. Penney
Dr. A. Dymanus	Mr. M. Shabana
Dr. Y. Obata	Mr. A. Smith
Mr. J. Comly	Mr. F. Sandy
Mr. D. Hannon	Mr. R. Tancrell
Mr. F. Molea	Mr. R. Temple
Mr. C. Nowlin	Mr. R. Tulloss

1. Dielectric Measurements on Ferroelectric Materials, F. Sandy. Contract AF19(604)-5487.

The microwave utilization of the highly nonlinear dielectric constants of ferroelectric substances has often seemed very tempting indeed. In view of these nonlinearities, one can imagine a whole host of devices in which the phase (or time delay) of a transmitted signal would be controlled by an external electric field. Electric field control, of course, has the dual advantages of rapid response time and low power dissipation. However, the anomalously high dielectric losses of common ferroelectrics have thus far made all such valuable devices impractical. The reduction of these losses is the question of central concern in ferroelectric utilization. Until quite recently, even the basic nature of ferroelectric loss mechanisms has been poorly understood.

In order to gain some insight into these loss mechanisms, Mr. Sandy has been investigating the microwave dielectric properties of Rochelle salt type ferroelectrics. The choice of this particular ferroelectric system for study was colored by a number of circumstances. Firstly, large, high quality, pure crystals of Rochelle salt may be grown easily from water solution. Secondly, the simple expedient of deuturation dramatically alters the dynamic response of Rochelle salt. Thirdly, these crystals pass through their phase transformations in a convenient temperature range, that is, near room temperature. Fourthly, as a covalently bonded material, Rochelle salt might be expected to exhibit loss characteristics quite distinct from those observed in ionically bonded materials such as barium and strontium titanates. Since

some of these ionic compounds are being extensively studied in industrial laboratories, it appeared that careful work on the Rochelle salt system might constitute a more unique contribution to the field.

In the last year or so there have been significant developments in the dynamic theory of ferroelectricity. The English crystallographer, W. Cochran, has postulated that the onset of ferroelectricity (or antiferroelectricity) may be viewed as the unstable growth of certain optical mode phonons or lattice vibrations. In his first paper Cochran derives the dispersion relationships for "barium titanate-like" crystals starting from a free energy function which is quadratic in the lattice displacements and the atomic polarizations, i.e., the free energy contains terms of the form (lattice displacement) x (atomic polarization) as well as the usual terms. The derived dispersion relations relate the vibrational frequencies of the various phonon modes to their corresponding wave numbers. Due to the anharmonicity of lattice vibrations, the dispersion relationships will be strongly temperature dependent. For a certain set of conditions, Cochran shows that frequency of one of the zero wave number (infinite wavelength) optical phonons goes to zero at some temperature, T_c. At the temperature, T_c, the crystal would be unstable against the growth of this phonon mode. Since an optical phonon of infinite wavelength carries a net polarization, the state of the crystal below T_c corresponds to ferroelectricity. Cochran's model gives an elegant picture of at least some of the dielectric loss in ferroelectric crystals, since the frequency of the unstable optical mode must move down from its normal infrared range into the vicinity of the microwave band. Thus, as the ferroelectric approaches T_c the optical phonon may suck up an increasing amount of microwave energy. Cochran's contentions have been at least partially verified by far infrared measurements on barium titanate. Below T_c the loss is undoubtedly associated with complex domain processes.

In a later paper, Cochran discusses a more general model of ferroelectricity and, in particular, crystals of the Rochelle salt types, i.e., crystals piezoelectric above T_c. Mr. Sandy's preliminary results on the temperature dependence of the dielectric loss of Rochelle salt are in general agreement with the predictions of this theory (see below). An unimaginative,

tentative consideration of the Cochran theory[*] seems to cast a pessimistic
pall over the prospects of microwave ferroelectric devices, since the high loss
appears to be an intrinsic characteristic of the phenomenon. However, it is
too early to make any categorical judgments. Careful measurements of the
intrinsic losses must be made first.

Most of Mr. Sandy's time thus far has been spent on developing reliable
techniques for measuring the losses in high dielectric constant material- a
non-trivial microwave measurements problem. It was clear from his first
measurements that earlier work on Rochelle salt was seriously in error. After
much experimentation, which has been described in previous quarterly reports,
two quite reliable techniques (producing mutually consistent data) have been
evolved. In one method the real and imaginary parts of the dielectric constant
are determined from VSWR measurements on a waveguide section containing
an E-plane slab of the crystal. In the other method, the dielectric constants
are found from measurements on a coaxial line terminated by a capacitor
loaded with the ferroelectric. Both methods have particular advantages, but
both suffer (as do almost all dielectric measurements) from the problem of
the air gap between the dielectric surface and the adjacent metallic surface.
This gap acts as a small capacitance in series with the large capacitance of
the dielectric and thus masks the dielectric measurement (i.e., $C_{total} = C_{gap}/$
$(1 + C_{gap} / C_{dielectric}) \simeq C_{gap}$). However, with considerable care, Mr..
Sandy has been able to reduce the effects of the "air gap errors. "

During the last quarterly period, measurements using the coaxial unit
have been made at 9.45 and 10.77 GMc/s on several Rochelle salt samples.
There have been significant variations in the results from sample to sample
and, to a lesser degree, between runs on the same sample. These variations
may be due to small sample irregularities, or possibly strain and damage
produced in the sample during the measurements. Until the source of these

- - - - - - -

[*]Several other workers have proposed ideas similar to those treated by Cochran.
However, the many ramifications of the lattice instability theory are most
clearly illuminated in his works. (Reference: Advances in Physics, 36, 387
(1960) and 37, 401, (1961).)

fluctuations is definitely established and, if possible, removed, it is difficult
to assess the accuracy of the measurements. However, the following figure
may be considered as a typical result.
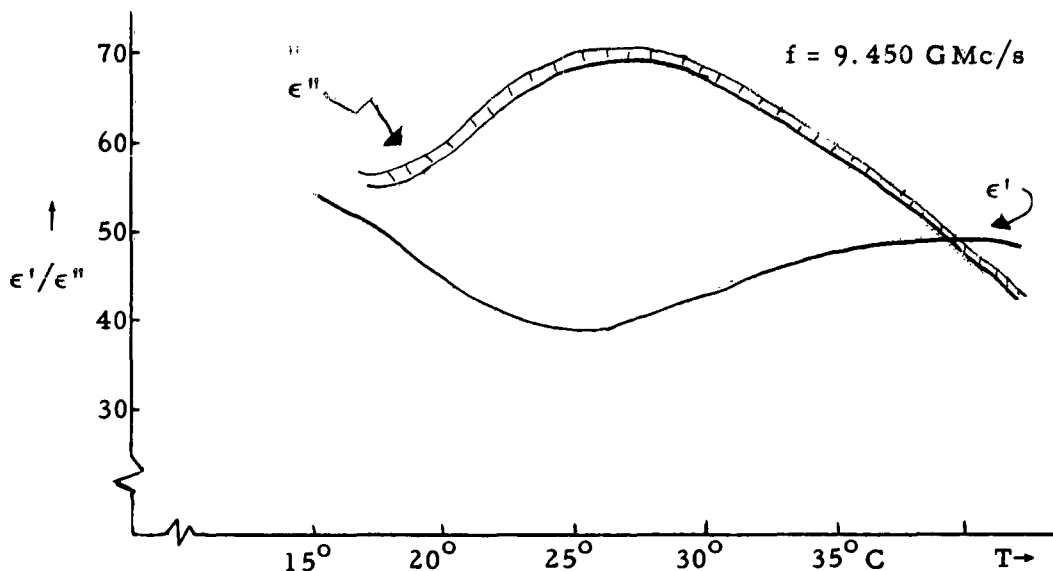
Note that ϵ'' comes to a single broad maximum slightly above the Curie
temperature, and ϵ' has a distinct minimum at, or slightly above this point.
As mentioned in the previous quarterly report, this minimum in ϵ' was not
observed in the earlier work of Akao and Susaki, but is consistent with the
theory of Cochran discussed above.

In the presence of an unstable harmonic mode, required by this theory,
one would expect that frequency dependence of ϵ' might have a dispersion-like
shape and that ϵ' would drop to a large negative value when the measuring
frequency is in the vicinity of the resonance frequency of the mode. Since this
resonance frequency is lowest at T_c , one might expect a dip in ϵ' at the
Curie temperature. For the highly anharmonic binding of active hydrogen
atoms in Rochelle salt, the negative values of ϵ' may still be expected but the
magnitude of the negative peak and the shape of the frequency dependence will
be difficult to predict. The slow drop in ϵ with frequency observed below
10 GMc/s indicates that the resonance in Rochelle salt will be extremely broad
and will require measurements into the K-band range. For these high frequen-
cies it will be necessary to use the waveguide method.

2. Capacitively-Driven Microwave Modulators, A. B. Smith. Contract AF 19(604)-5487.

As noted above, capacitively-operated microwave control devices would offer several distinct practical advantages over the conventional inductively-driven ferrite phase shifters and modulators. In particular, the capacitive devices could be driven faster and at vanishingly small power. Ferroelectric devices are one possibility. However, it is at least conceptually possible that the magnetoelastic properties of ferrimagnetic insulators may also be used for this purpose. The ferromagnetic resonance frequency of any magnetic material is a direct function of the magnetocrystalline anisotropy which in turn is a function of the state of strain of the substance. Thus, an applied strain will displace the resonance frequency and alter the microwave properties of any ferrite. This effect may have practical importance, if the magnetoelastic displacement of the resonance can be made comparable with the linewidth of the resonance. In preliminary experiments on several types of ferrimagnetic materials this condition has been obtained.

One may conceive of at least two general types of device configurations:

(a) A magnetic sample, e.g., a sphere of YIG, might be clamped in a "vise" of piezoelectric material, e.g., quartz. Then an electric field applied to the quartz will cause a "squeezing" of the YIG. In this way, the electric field will change the dispersive and absorptive properties of the microwave cavity containing the YIG and quartz one might expect at X-band, by a shift of 2 oersteds in the resonance field compared to a linewidth of 0.4 oersted.

(b) A second type of configuration would take advantage of the properties of a magnetic material which is itself piezoelectric. Such a material is the compound $Ga Fe O_3$. In this case, the electric field would produce the strain directly in the magnetic material and an additional transducer would not be required. Devices using such materials would be fast and efficient. Unfortunately, $Ga Fe O_3$ would not be very useful for this purpose, since it has an exceedingly

broad resonance linewidth. However, other materials having the dual properties of ferromagnetism and piezoelectricity will undoubtedly come to light in the course of time.

The work carried out thus far on this project has been related to the former type of configuration and has largely involved a study of the magnitude of the magnetoelastic effect. In much of this, Rochelle salt transducers have been used. In order to obtain good mechanical contact, the Rochelle salt is grown on the YIG sphere. In the last report, experiments were described which involved such YIG spheres with Rochelle salt crystals surrounding them. By applying a voltage to the Rochelle salt, it was possible to strain the YIG and thereby to change its ferrimagnetic resonance frequency. The change in resonance frequency thus produced would cause a change in the transmission of a microwave cavity containing this Rochelle salt-YIG combination. Microwave modulation could thus be achieved.

Certain difficulties were experienced in achieving an appreciable amount of modulation with this arrangement. Most important, the apparent ferrimagnetic linewidth of the sphere was increased by an order of magnitude by the microwave losses of the Rochelle salt. Because of this effect, work on this Rochelle salt-YIG modulator was not continued during this report period. Instead, another construction was investigated which it seemed could be more readily developed into a useful modulator. The Rochelle salt-YIG modulator might still warrant more investigation later, after a workable modulator of the other type has been constructed. The Rochelle salt-YIG type of construction may offer a higher acoustical resonance frequency than other possible structures, and hence be desirable for this reason. Perhaps other materials such as ADP or piezoelectric ceramics might replace the Rochelle salt.

Most of the time of this report period was spent on a modulator construction in which the YIG sphere and a piece of piezoelectric material are both retained in a quartz tube. The end of the tube containing the YIG is closed off, then inserted through a hole in the wall of a microwave cavity and clamped into position. A steady pressure is applied to the piezoelectric material which protrudes from the other end of the tube. This construction allows the piezoelectric to be located outside the cavity where its losses will not affect the microwave circuit.

Modulators of this type have been constructed and a small modulator effect has been noted. Because of lost motion in the various parts which clamp the quartz tube and piezoelectric in place, the amount of modulation observed is an order of magnitude smaller than would be expected. Since the piezoelectric lengthens by only a microinch when voltage is applied, part of this motion is easily lost. The degree of polish on mating surfaces and the exactness of fit seem to become very important when small motions of this type are involved. A modified modulator will be constructed which, it is hoped, will exhibit a useful amount of modulation.

Until this report period, all modulator designs had utilized YIG. During this period, some measurements were made to determine whether some other material might be more suitable. Measurements were made on three other materials which have relatively narrow linewidths. The largest change in anisotropy field for a given uniaxial pressure in the easy direction in $Ni_{.95}$ $Co_{.05} Fe_2 O_4$ was 4 times the largest value yet observed in YIG; $Ni_{.9} Co_{.1}$ $Fe_2 O_4$ had six times the YIG value and $Zn_2 Y$ had only .28 times the YIG value. Despite these large figures for the nickel cobalt ferrites , their larger linewidths more than offset, as far as modulator sensitivity is concerned, any advantage gained by the greater pressure dependence. However, these larger linewidth materials might be useful in modulators designed to handle power levels.

Investigation was also begun during this period on a different method of achieving microwave modulation utilizing piezoelectric and ferrimagnetic materials. Twisting a ferrimagnet in a dc magnetic field alters its resonance frequency due to the angular dependence of the anisotropy fields. Hence, it should be possible to construct a modulator in which a piezoelectric transducer provides a twisting motion to a ferrimagnet. "Bender" or "twister, " "bimorph"(i. e. , two-layer) transducer structures would very likely be necessary to impart sufficient motion to the ferrimagnet. No pressure need be applied to the ferrimagnet as in the constructions previously studied. A modulator using such a bender transducer is being constructed. The major disadvantage of this construction will probably be its low acoustic resonance frequency.

Until this report period, all modulator configurations involved the use of a microwave cavity. Measurements with .025" YIG spheres show, however, that wide-band modulators without cavities may be practical. With these spheres in standard X-band rectangular waveguide, attenuations of several db are experienced at resonance. Reducing the height of the guide and using somewhat bigger spheres should make possible useful attenuations in a broad-band structure.

- - - - -

3. Gallium Ferrite Systems, C. Nowlin. Contract AF19(604)-5487

In 1959 J. P. Remeika of the Bell Telephone Laboratories discovered that compounds of the composition $Ga_{1+x}Fe_{1-x}O_3$ exhibit both the properties of ferromagnetism and piezoelectricity. The crystal structure of these compounds is new and has yet to be completely determined. Mrs. Wood of the Bell Telephone Laboratories has determined that the crystals are orthorhombic with probable space group C_{2v}^9 and that the dimensions of the unit cell are (in Ångstrom units) 8.75 x 9.40 x 5.07 with eight formula units per cell. Since there are only ferric ions present in these compounds, it is surprising that they are not antiferromagnetic rather than ferromagnetic. The magnetic structure of these materials is undoubtedly quite complex.

In view of the device potentialities of piezoelectric-ferromagnetic materials (e. g., see above), a detailed study of the magnetic properties of Ga Fe O_3 was undertaken in this laboratory. One facet of this study involved ferromagnetic resonance measurements which were carried out by Dr. A. Dymanus, and which have been described in a forthcoming technical report. A second facet has involved magnetometer and piezoelectric measurements by Mr. C. Nowlin. The work, thus far, may be summarized as follows:

(a) Crystal growth:

1) The growth of crystals with composition $Ga_{1-x}Fe_{1+x}O_3$ ($-1 \leq x \leq +1$) has been attempted. The orthorhombic structure is found in the range $-0.4 \leq x \leq +0.4$ (approximately). Outside of this range rhombohedral crystals of the $\alpha - Fe_2O_3$

(hematite) are found. Such crystals exhibit classical "weak ferro-magnetism" and are not piezoelectric (see later comments in this report).

2) The growth of crystals with Al^{3+} substitutions has also been attempted. Again for small amounts of Al^{3+} the orthorhombic structure is stable. However, for large concentrations, the rhombohedral structure again prevails.

(b) X-ray analysis:

The cell dimension of the crystals of varying compositions has been determined from x-ray analysis. In the aluminum substituted compounds a distinct superstructure has been noted. This superstructure seems to be associated with a thermal ordering which has also been found in the magnetic measurements.

(c) Piezoelectric measurements:

A highly sensitive piezoelectric detector has been designed and constructed. This detector, which is essentially a marginal oscillator, has been used to evaluate the piezoelectric constants of the various crystals grown. Typical crystals over the whole compositional range have two strong interaction constants (about double the strength of quartz) and high acoustical Q's. There seems to be no significant variation in the interaction strength over the entire range. The samples for magnetic measurements are selected on the basis of high acoustical Q's. In this way the the confusing effects of flux inclusions and second phases are avoided.

(d) Magnetic measurements:

Extensive measurements of the magnetic moment of these gallium ferrite crystals have been made in the temperature range from $4^{\circ}K$ to about $400^{\circ}K$. Roughly speaking, the Curie temperature and the normalized, low temperature saturation moment vary linearly with the compositional parameter x . This

normalized saturation moment (i. e., the moment per ferric ion
present in the crystal) has a value, again roughly speaking, of
one Bohr magneton. Of course, each ferric ion should have an
individual moment of five Bohr magnetons. The high tempera-
ture susceptibilities have a "Curie-Weiss-like" behavior with a
Curie constant in agreement with the five Bohr magneton value.
Thus, as might be expected, the ordered magnetic state of
$Ga Fe O_3$ is not that of a totally aligned ferromagnet, nor does
an uncompensated antiferromagnetic configuration, such as found
in the garnet and spinel ferrites, seem reasonable. Given the
fact that the known space group allows only four equivalent posi-
tions, it is difficult to conceive of a distribution of identical
ferric ions which would give ferromagnetism.

Most of the characteristics of this material may be accounted for
by assuming a weak ferromagnetism-like model. In such a model
it is assumed that the magnetic moments are constrained by the
magnetic symmetry to lie in directions other than the easy direc-
tion of magnetization. In this way, even an antiferromagnetic
configuration may have a projected permanent moment along the
easy direction. The detailed consequences of this model are
being explored.

During the last quarter, much progress has been made in the
study of the ternary system composed of $Al_2 O_3$, $Fe_2 O_3$, and
$Ga_2 O_3$. As already noted, compounds of the form $Ga_{2-x} Fe_x O_3$
($.7 \leqslant x \leqslant 1.4$) were first grown by Remeika and were shown to be
ferromagnetic and piezoelectric. We have found that the addition
of aluminum to the system to form $Al_y Ga_{2-x-y} Fe_x O_3$ does
not affect the piezoelectric or ferromagnetic properties of the
material even when y is as large as 0.2. Present work is
being directed towards determining the limits on x and y in
the general formula, if the resulting material is to be piezoelec-
tric and ferromagnetic.

X-ray studies on the compound $Al_{.2} Ga_{.8} Fe O_3$ show the presence of a superstructure in the ordered material. It is not known whether the superstructure is present in all the piezoelectric-ferromagnetic compounds and the aluminum acts merely as an indicator, or if the aluminum itself causes the superstructure, but the presence of a superstructure in an ordered sample of a material of this type ties in very well with the changes in magnetic moment brought about by heat treatments.

The magnetic moment of $Al_{.2} Ga_{.8} Fe O_3$ per ferric ion is about the same as that for $Ga Fe O_3$, but the ferromagnetic Curie temperature is increased from $300^\circ K$ for $Ga Fe O_3$ to $325^\circ K$ for $Al_{.2} Ga_{.8} Fe O_3$.

Crystals of the form $Ga_{2-x} Fe_x O_3$ have been studied in considerable detail. It has been found that the expected order-disorder phenomenon does exist. Apparently, the virgin crystal is ordered if the growing temperature is lowered below $500^\circ C$ before the crystals are removed from the oven.

Quenching from $900^\circ C$ reduces the magnetic moment by 20 percent. Heating in a furnace at $500^\circ C$ for several days will restore the moment to 96 percent of the original value. Further effort is being directed towards finding a more precise ordering temperature and towards study of long-term soaking at temperatures slightly above $500^\circ C$.

- - - - -

4. Ferromagnetic Resonance in Metals, J. Comly, T. Penney, and R. Tancrell. Contracts Nonr-1866(16) and AF19(604)-5487.

A program has been initiated which will use the techniques of microwave absorption to explore the theories of metallic magnetism. A generalized microwave spectroscopy of the ferrimagnetic insulators has revealed a vast amount of information on the details of the magnetic interaction in these

materials. This generalized spectroscopy includes not only ordinary ferro-
magnetic resonance absorption, but also more exotic techniques such as
magnetostatic modes, parallel pumping, and magnetoacoustical effects. How-
ever, the use of these techniques in conjunction with metallic magnetism has
been on a modest scale. The reason for this neglect is not the lack of interest
in the subject, but the obvious problems associated with the skin effect in
metals. Nevertheless, in carefully designed experiments several workers
have been able to make valuable inferences from experiments with metals.

The experiments being undertaken in this laboratory will involve two
types of metallic materials, viz., metallic films (J. Comly and T..Penney)and
metallic whiskers (R. Tancrell). In the metallic films the skin-depth problem
is negligible, but the films exhibit many properties which have little to do with
the bulk properties of perfect metals. On the other hand, whisker growth
provides a convenient means of obtaining highly perfect metallic specimens,
but here the problem of skin effects must be faced head-on. Clearly, both
materials have disadvantages. Ordinary ferromagnetic resonance and parallel
pump experiments are to be attempted on metals from both the 3d and 4f
transitional groups.

- - - - -

5. Theoretical Interpretations of Ferromagnetic Resonance, Y. Obata.
Contracts Nonr-1866(16) and AF19(604)-5487.

During an earlier phase of the activites of this contract, an extensive
amount of ferromagnetic resonance data was obtained on the rare-earth iron
magnetic garnets. When the garnets contain only S-state magnetic ions
(viz., Fe^{3+} and Gd^{3+}), the experimental data may be explained on the basis
of a simple theoretical model. This model is based on the known properties
of individual S-state ions subjected to local crystalline potentials and under
the influence of strong magnetic fields, which represent the effects of the
exchange interaction. Earlier technical reports, issued under this contract,
have shown this model to be highly satisfactory.

Efforts to extend this "individual ion" model to the garnets containing non-S-state magnetic ions (i.e., all garnets, except YIG and GdIG) have encountered difficulties. The non-S-state ions are subject to much stronger local crystalline fields, and, as a consequence, their behavior will be more sensitive to the details of this interaction. These details may be obtained by studying the paramagnetic resonance spectrum of dilute amounts of rare-earth ions in non-magnetic host crystals, such as YGaG or YAlG. A further complication arises from the fact that exchange interaction in these garnets appears to have a considerable anisotropy, which may be deduced from optical experiments on the magnetic crystals. Thus, the exchange interaction cannot be represented by a simple Weiss molecular field. These optical experiments, however, reveal a rich amount of detail on the energy levels of rare-earth ions in the magnetic crystals.

Dr. Yukio Obata has been trying to form a synthesis of existing x-ray paramagnetic resonance, and optical data on the garnets which would explain the temperature dependence of the magnetic field required for resonance and the resonance linewidth.. He has been successful in explaining the data on YbIG which is probably the most studied—and most puzzling—case. Dr. Obata's explanation differs considerably from a model proposed by Kittel and associates. Their model required an anomalously short rare-earth spin-lattice relaxation time in order to account for the resonance measurements. The strength of the spin-lattice interaction is supposed to damp out the gyromagnetic character of rare-earth-ion motion and to "quench" the angular momentum. Van Vleck has suggested that this quenching comes, not from the damping of the rare-earth motion, but, rather, from an appropriate enumeration of the energy levels of the rare-earth ion. Dr. Obata's calculations are a follow-up on this suggestion which appears to be the correct interpretation of the behavior of rare-earth garnets.

- - - - -

6. Magnetic Measurements, C. Nowlin and F. Molea. Contract AF19(604)-5487.

During the last two years Mr. Nowlin has developed a vibrating sample magnetometer of great sensitivity and versatility. The magnetometer was primarily developed in conjunction with the activities of the $GaFeO_3$ (No. 4) project discussed above. However, it has also been used extensively as a valuable adjunct to efforts of other projects. For example, a whole series of magnetic garnets have been carefully measured at low temperatures. These measurements have been invaluable in working out some of the details of the resonance behavior of the garnets. The original magnetic moment measurements of Pauthenet were quite crude and indicate only the general character of the temperature-dependent data. A composite set of garnet data will be set forth in a future technical report.

At present Mr. Nowlin is carrying out a study of the magnetic moment of $\alpha - Fe_2O_3$ -like compounds. This study has been an outgrowth of the work on $GaFeO_3$. As mentioned above, outside of the growth range of the orthorhombic $Ga_{1+x}Fe_{1-x}O_3$ crystals one finds rhombohedral crystals similar in character to hematite, $\alpha - Fe_2O_3$. These crystals exhibit weak ferromagnetism. The transition temperatures of the crystals vary significantly with changing gallium concentration. It has also been found that hematite-like structures and weak ferromagnetism are found with aluminum substitution into $\alpha - Fe_2O_3$. The interpretation of the magnetic properties of these compounds is directly relevant to the understanding of the magnetism of piezo-electric $GaFeO_3$. However, measurements on the hematite-like compounds are important in their own right, since much theoretical effort has been devoted to explaining the nature of their weak ferromagnetism.

- - - - -

7. Paramagnetic Resonance of Impurities in Ferroelectric Host Crystals, D. Hannon. Contract AF19(604)-5487.

Some of the key difficulties in the understanding of ferroelectricity arise from the lack of knowledge concerning the relative displacements of the

various ions within the unit cell. Several earlier theories of the phenomenon
have been based upon the erroneous interpretations of x-ray measurements.
In the case of barium titanate, for example, it was supposed that there was
a large change in the relative displacement of titanium and oxygen ions at the
Curie temperature. This result strongly influenced several proposed pictures
of the ferroelectric state. Most of these pictures seem to be invalid now,
since later, more refined, x-ray measurements have shown that the changes
in the relative displacements of the ions are much smaller than at first sup-
posed. In order to construct an adequate theory of ferroelectricity, one would,
ideally, like to know the scale and the symmetry of the potential distribution
at each ion site in the crystals of interest. Unfortunately, x-ray and neutron
diffraction experiments cannot give, unambiguously, a sufficiently accurate
picture of these potential distributions.

At least in certain particular cases, electron spin resonance may be
used to explore these local field configurations. The ESR spectrum of any
ion is, of course, quite sensitive to the details of its electrical environment.
The effects of these crystalline fields are expressed in terms of a "spin
Hamiltonian" which is appropriate to the particular paramagnetic ion and the
symmetry of its environment. Thus, paramagnetic impurities grown into
ferroelectric crystals can be used as probes of the local electric fields. For
example, in the case of barium titanate, ferric ions substitutionally replace
titanium ions while rare-earth ions replace barium ions. ESR experiments
on doped $Ba\,Ti\,O_3$ indicate, at least tentatively, that the distortion of the
oxygen octahedron containing the titanium ion is critical to the ferroelectric
transition.

Some two years ago, Mr. Hannon embarked on a program to study
ferroelectricity by means of these paramagnetic probes. The first stage in
his work has been the construction of a high sensitivity ESR spectrometer.
If the impurity concentration can be kept low, then the host crystals will most
closely approximate the unperturbed ferroelectrics, and the ESR lines will
not be broadened by the dipolar interaction. This spectrometer has been com-
pleted. The second phase of Mr. Hannon's program has consisted in seeking

out the material in which ESR experiments might make the most significant contribution. In order to explore the local crystalline fields with great sensitivity, one would like to use a paramagnetic ion which has strong spin-lattice interaction. However, the resonance of such an ion may be observed only at low temperatures due to the consequent short spin-lattice relaxation times. If one is then to observe the changes in crystalline fields on ordering, the Curie temperature of the ferroelectric host must be in the low temperature range. The properties of several such materials have been under study.

During this last quarter work on bismuth titanate was continued. The EPR of Gd^{3+} in bismuth titanate has been recorded, but the number and width of the resonance lines have made analysis difficult. Photographs demonstrating domain patterns in bismuth titanate were taken using a Vickers microscope. Although EPR experiments in bismuth titanate crystals containing Mn^{2+}, Cr^{3+}, and Fe^{3+} were attempted, no resonances were observed.

Preparations for an interesting experiment have also been in progress. In this experiment the resonance spectrum would be monitored as the host crystal passes from ferroelectric to antiferroelectric condition. Tungsten trioxide has such a transition occurring at approximately $-10^{\circ}C$. Attempts to grow single crystals of WO_3 have been encouraging. Small platelets of WO_3 grown in the laboratory exhibit domain patterns, but the condition of larger pieces is unclear. It appears likely that x-rays will be needed to determine the amount of ordering in the more bulky pieces of WO_3. Doped crystals of WO_3 have also been grown, and the resonance spectrum of these will be investigated shortly.

Fang and associates have reported a group of ferroelectric compounds whose chemical formula can be written $Bi_4 Ti_3 O_{12} nP$ where n is some small integer or a simple fraction and P denotes perovskite compounds such as $Ba TiO_3$, $Pb TiO_3$, and $Bi Fe O_3$. Bismuth titanate (n = 0) is already being investigated here. Preparation of doped single crystals of $Ba_2 Bi_4 Ti_5 O_{18}$ (n = 2; P = $Ba TiO_3$) is being pursued, and appears encouraging. This family of compounds has a layered perovskite structure, and may prove useful as host crystals for ESR experiments.

8. Microwave Characteristics of Molecular Afterglows, R. Temple and
R. V. Jones. Contract AF19(604)-5487.

A short-term project was being undertaken to study the microwave
device potentialities of gyromagnetic low density gas plasmas. During the
course of this program the propagation constants and high power character-
istics of steady state plasmas are to be measured. A complete gas flow and
microwave system has been constructed. Plasmas resulting from the long-
living afterglow of molecular nitrogen and the optical excitation of helium and
argon have been under study.

During the early part of this quarterly period a superheterodyne
resonance detection system using a frequency stabilized local oscillator was
developed. The greater sensitivity of this system over the previous video
system permitted measurements to be made down to a power level at least
20 db below the onset of high power nonlinear effects. Data taken with this
system firmly established the low power flat region of the curve. Measure-
ments have been made over a total power range of 45 db The general char-
acter of the power dependence of the width of gyromagnetic dispersion is in-
dicated in the following figure.

$\Delta H \propto \sqrt{P}$

$\ln(\Delta H/\Delta H_o)$

Break Point

Relative Power Level (db)
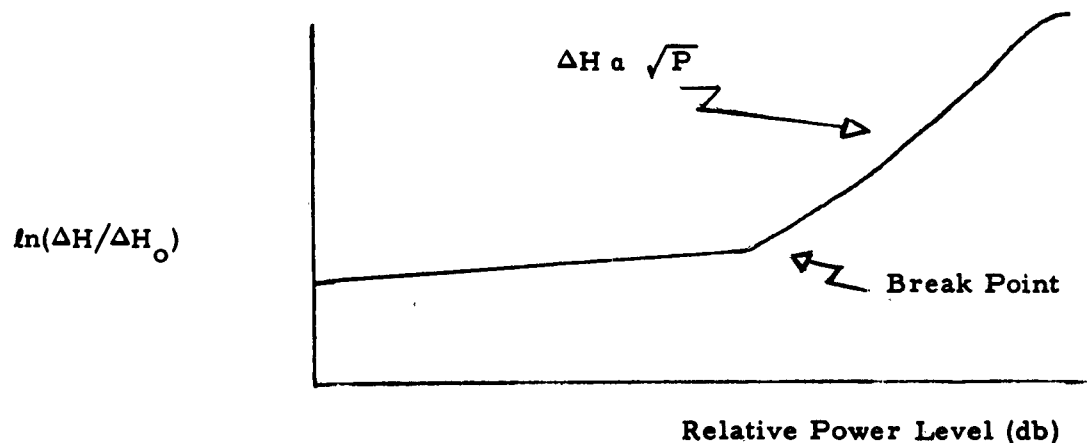
The dispersion line shapes and also the absorption curves as plotted
by the Sanborn recorder were found to be substantially asymmetric. A dis-
persion curve plotted from data taken point by point with a wavemeter was

also found to be asymmetric. Thus, the signal klystron frequency stabilization system, the microwave discriminator, and the recorder could not have been responsible for the asymmetry. Since, theoretically, the circular cavity used in the TE 111 mode had two degenerate resonances and this degeneracy could be removed by the presence of a plasma in a magnetic field, a distortion in the cavity resonance due to these two no longer degenerate resonances might have been responsible for the asymmetry. To test this possibility a circular cavity in the TE 012 mode was set up in an absorption spectrometer and the derivative of the absorption curve was obtained. This was also found to be asymmetric. The sensitivity of the absorption system was poor and the noise level was very high.

To improve the physical circular symmetry of the set up using the cavity in the TE 111 mode, and also to eliminate the right angle bends in the quartz tube and the problem of putting sleeves on these bends, a 5/8" hole was bored in the center of the pole pieces of a 3 1/2" electromagnet.

Recordings have been made using the 3 1/2" magnet system of both the dispersion and absorption of the measurement cavity as a function of magnetic field about the field required for electron cyclotron resonance. Nitrogen, helium, and argon have been measured at pressures from .5mm to 5mm of mercury over a power level range of 45 db , and with a variety of gas flow conditions. The major part of this data has been plotted in the form of dispersion linewidth versus power level curves (as above). Linewidths range from 40 to 140 gauss in the low power region to 1000 to 2000 gauss in the high power region. The remainder of the data provided plots of line-width and electron density versus gas flow rates for several pressures and gases. Typical electron densities for obtaining linewidth versus power level data are between 10^7 and 10^8 electrons per cc . Maximum electron density measured in nitrogen was over 10^9 electrons per cc .

Two independent calculations of microwave electric field strength in the cavity versus incident power level were made. The first calculation gave an average electric field throughout the cavity from energy storage and Q considerations. The second method involved measuring the power level at

which helium gas in the cavity ionized initially. The results of these two methods were in much closer agreement than could be expected.

A simple experiment with a shutter inside the quartz tube containing the plasma proved conclusively that both helium and argon were being ionized optically by an upstream discharge. When the shutter was open, light was allowed to pass down the quartz tube from the discharge region to the measurement cavity, and a measurable electron density was present. When the shutter was closed, the light was blocked, and the electron density was negligible.

Several attempts have been made to correlate the microwave measures with simple theories of low density plasmas. The first calculation made was a simple check on the power level at which one would expect the linewidth versus power level curve to break out of the flat region and start increasing. This power level was determined by equating the energy gained by an electron in a mean free path to the thermal energy of an electron at room temperature. The value for the energy gained in a mean free path was obtained from the linewidth in the low power region, which gave the mean free time, and the electric field versus power level calibration mentioned previously. Agreement with experiment was only approximate, experimental points being scattered between two orders of magnitude on each side of the predicted power level.

A calculation of low energy collision probabilities determined from linewidths in the flat region yielded values ranging from 20 to 50 for nitrogen, 23 to 58 for helium, and 9 to 30 for argon.

Studies of linewidth versus power curves revealed fairly generally (as noted above) that in the high power region linewidth was proportional to the square root of power level or directly proportional to the microwave electric field in the cavity.

Following Chapman and Cowling, an integral for the electron velocity distribution was obtained for the case of a strong alternating electric field perpendicular to a steady state magnetic field. An approximation was made to the shape of the collision probability versus electron velocity curves for nitrogen, helium, and argon. With this approximation the integral for

electron velocity distribution was done analytically, but the results were too complicated to interpret meaningfully. Numerical integrations of the collision probability curves yielded approximate power laws of velocity in the exponent and also showed the region over which they were valid. It was still not possible to do analytically the integral for the average electron velocity.

A functional argument showed that the linewidth was proportional to the electric field to the $\frac{n-2}{n}$ power of velocity in the exponent. A calculation based on doing the integral analytically in the limits of both large and small linewidth yielded the same result. If n is large, linewidth will be proportional to the electric field. Only for argon is n large over a wide range of electron velocities. For nitrogen, n is large over just a small region, and, for helium, n is never greater than 4.

VI. ELECTROMAGNETIC RADIATION

Personnel

Prof. R. W. P. King[*]
Asst. Prof. H. J. Schmitt[*]
Asst. Prof. T. T. Wu[†]
Dr. F. A. Hinchey
Dr. K. Iizuka
Dr. W. F. Pickard
Dr. S. Prasad
Dr. S. S. Sandler
Dr. S. R. Seshadri
Dr. J. Shefer
Dr. T. Soejima
Mr. R. Burton

Mr. C. L. Chen
Mr. J. G. Fikioris
Miss D. Gooch
Mr. A. Jayne
Mr. R. B. Mack
Mr. J. M. Myers
Mr. B. Rama Rao
Mr. W. A. Saxton
Mr. K. Sivaprasad
Mr. T. F. Tao
Mr. H. S. Tuan
Mr. H. Whiteside

1. Theoretical and Experimental Studies of Antennas and Arrays in a Parallel-Plate Region, B. Rama Rao. Contract AF19(604)-4118.

   A. **The Impedance and Current Distribution of a Cylindrical Antenna in a Parallel-Plate Region.**

   Closed form expressions for the current distribution and impedance of an antenna have been obtained by expressing the current on the antenna as a Fourier series in terms of waveguide modes. The divergence difficulty encountered in waveguide probe investigations has been avoided by using in the integral equation a rigorous kernel, taking into account the finite diameter of the antenna instead of a "filamentary" kernel. Experimental verification of the theory has been made and the theoretical and experimental results are found to agree well.

   The impedance of the antenna has also been obtained by a variational method using a trial function for the current of the form $I = A + B \cos k (h-z)$. The theoretical results agree quite well with experiment up to $k_o h = 3.8$, but deteriorate thereafter.

- - - - - - -

[*] Dr. Schmitt was at Eidgenoessiche Technische Hochschule in Zürich as a John Simon Guggenheim Memorial Fellow for six months during the period covered by this report.

[†] Alfred P. Sloan Foundation Fellow.

Several interesting features connected with the property of the antenna have been observed, and they will be discussed in a technical report which is now in preparation.

B. Coupled Antennas in a Parallel-Plate Region.

The current distribution, self-impedance, and mutual-impedance of a pair of antennas in a parallel-plate region have been obtained by a Fourier series method. Experimental investigations to verify the theory have been completed. The theoretical results are being computed for comparison.

C. Wave Propagation along an Array of Rods in a Parallel-Plate Region.

The purpose of the project is to investigate theoretically and experimentally the phase velocity of propagation along a periodic structure consisting of an array of rods in a parallel-plate region.

An approximate expression for the propagation constant has been obtained by a variational method. A more sophisticated method of solving the problem using conventional antenna theory is being attempted.

Numerous difficulties, mainly of a mechanical nature, were encountered in designing a suitable experimental model of the array, which permits the spacing, height, and diameter of the elements to be varied easily. A prototype model has at last been designed which seems to satisfy all requirements. It consists of a "sandwich" assembly carrying approximately 50 rods between two $\frac{1}{4}$ inch Dural plates measuring 6 feet by 1 inch. The two plates have an H-shaped slot at their center and the rods are held in position by means of a clamp and a colet which slides along the slot. After adjusting the height and spacing between elements, the slots are covered by heavy 5 mil aluminum foil. The phase velocity of propagations and the current amplitude at the base of the antenna are measured by a shielded loop probe which is mounted on a sliding panel. The experimental equipment has been completed, and preliminary measurements are now underway.

- - - - -

2. Surface Waves on Periodic Structures, J. Shefer. Contract AF19(604)-4118.

The characteristics of a new type of transmission line (see Fig. 1)
consisting of an array of parallel conducting cylinders were investigated. This
type of array has been used extensively in endfire antennas, but has not been
examined as a transmission line. By means of a relatively simple matching
network, efficient excitation of a surface wave on the periodic structure is
obtained. The frequency response has been found to be flat within 3 db over
a 20 % frequency range in X-band for several combinations of cylinder lengths
and spacings (see Fig. 2). Total insertion losses are less than 3 db and are
largely independent of the length of the periodic structure (see Fig. 3). The
conducting elements were embedded in styrofoam.

The effects of bends and twists in the line have also been investigated.
It has been shown that a guided wave on this periodic structure can follow a
circular path having 1.5λ radius of curvature with very little loss. The plane
of polarization can easily be rotated through an angle of 90° by inserting a short
twisted section.

By terminating this type of transmission line with short circuits at both
ends, a discrete series of transmission maxima is observed in accordance with
Floquet's theorem on periodic structures. Since the resonance peaks correspond
to a high Q-factor, the dispersion characteristics of the line are obtained with
very good accuracy. This type of transmission line may offer advantages where
light weight is of prime importance.

A paper on this work was presented in May, 1962 at the URSI Meeting in
Washington, D. C. A scientific report, "Periodic Cylinder Arrays as Trans-
mission Lines, " is being prepared for publication.

- - - - -

3. Experimental and Theoretical Study of Probes for Measuring Fields,
   H. Whiteside. Contract Nonr-1866(32).

This project is a study of the capabilities and limitations of probes
used for the measurement of the magnetic component of the electromagnetic
field.

Physical probes differ from an ideal probe in three ways: finite size, the presence of a connecting transmission line, and response to unwanted modes. A probe of finite size can only measure an average field, not the field at a point. The transmission line may be excited and produce an unwanted scattered field at the probe. In addition, the currents on this line flow into the probe and provide extraneous excitation. The usual magnetic probe is a loop which can support not only a magnetic dipole mode, but an unwanted electric dipole mode of oscillation as well.

To test various probes it is necessary to have a known reference field. The near-zone field of a half-wave electric dipole (actually a unipole over a conducting image plane) was chosen as being a theoretically well-known field of the desired characteristics. To produce this reference field indoors a complete "free space" room has been constructed with an aluminum ground screen as one wall. Using an electric dipole probe, for which the behavior is well understood, the actual electric field was measured and compared with the theory to determine the quality of the reference field, which proved quite adequate for our purposes.

The effect of the transmission line has been studied experimentally by measuring the scattering to an auxiliary probe. It has been found that this scattering can be materially reduced by loading the outside of the line with high-impedance choke sleeves. The upper sleeves are fixed in length at $\lambda/4$, but the one nearest the probe can be tuned for minimum coupling to a given probe.

Loop probes of diameters between $.01\lambda$ and $.125\lambda$ have been tested in the standard field, studying the relative magnitude of the unwanted electric dipole mode as a function of diameter, wire size, load resistance, and load location for circular and square loops with both single and double loads. The agreement with theory is quite adequate, except that in all cases the response of the probe to the desired magnetic mode is about 10% less than expected. The use of a double load with the two load currents subtracted at the receiver produces an output which discriminates against the unwanted electric mode successfully, especially for loops larger than $.03\lambda$ diameter. Typically, the error (unwanted) signal is reduced by a factor of 10 in current (a factor of 100 in power) compared to the desired signal. This part of the investigation was presented in a paper entitled " The
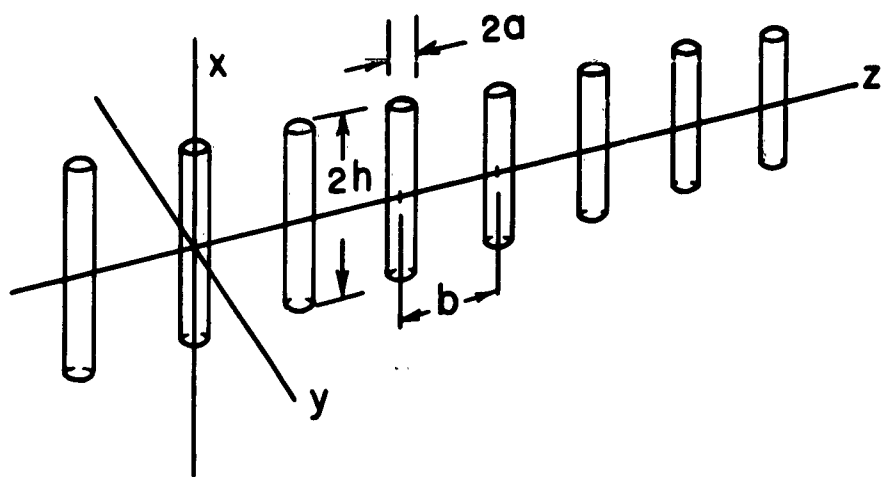
FIG. 1 ARRAY OF CONDUCTING CYLINDERS
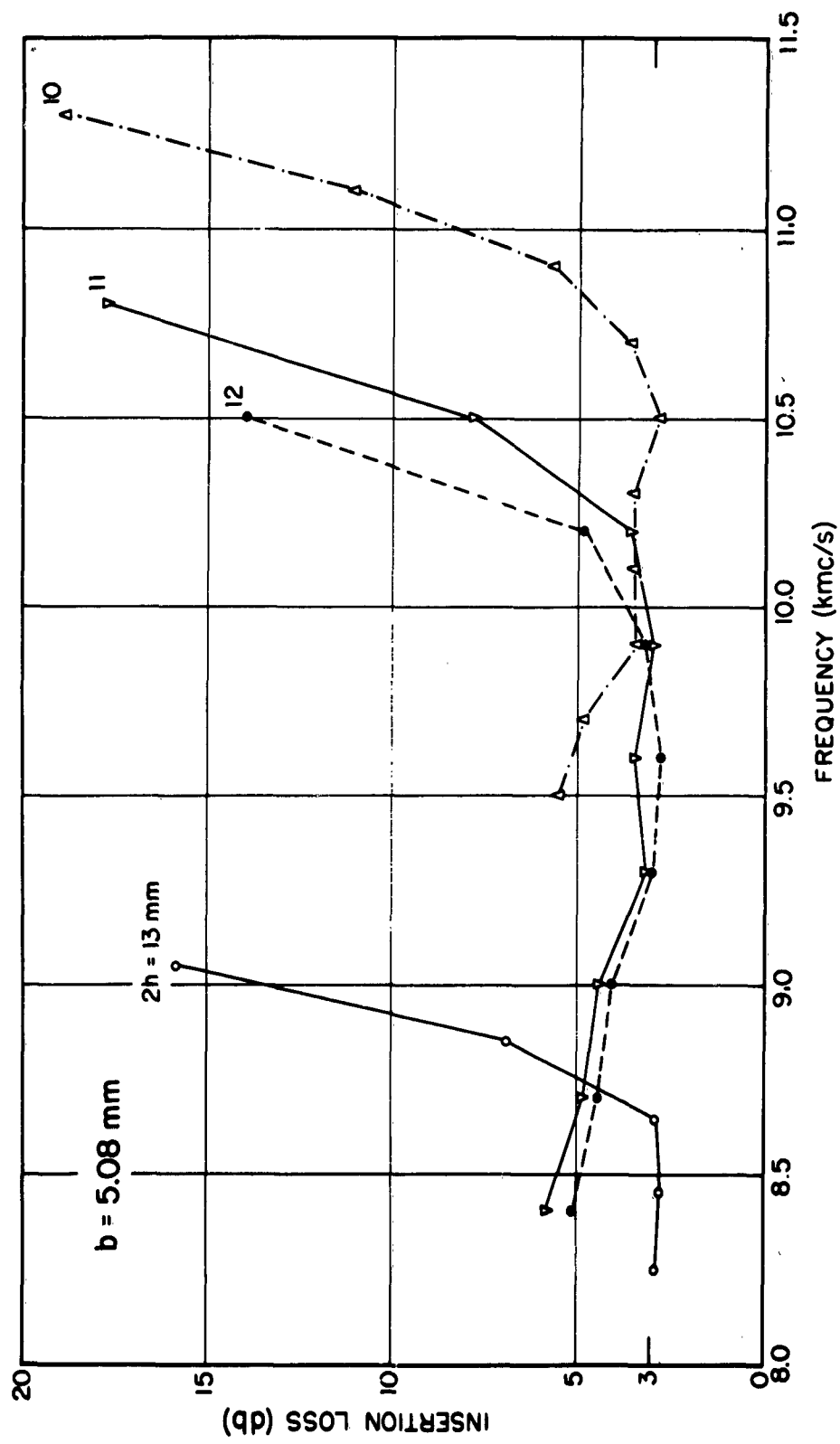
FIG. 2 INSERTION LOSS OF PERIODIC STRUCTURE

11.5 kmc   ⟵   8.2 kmc
f

L = 10.6 cm   L = 25 cm   L = 50.4 cm
N = 21   N = 51   N = 101
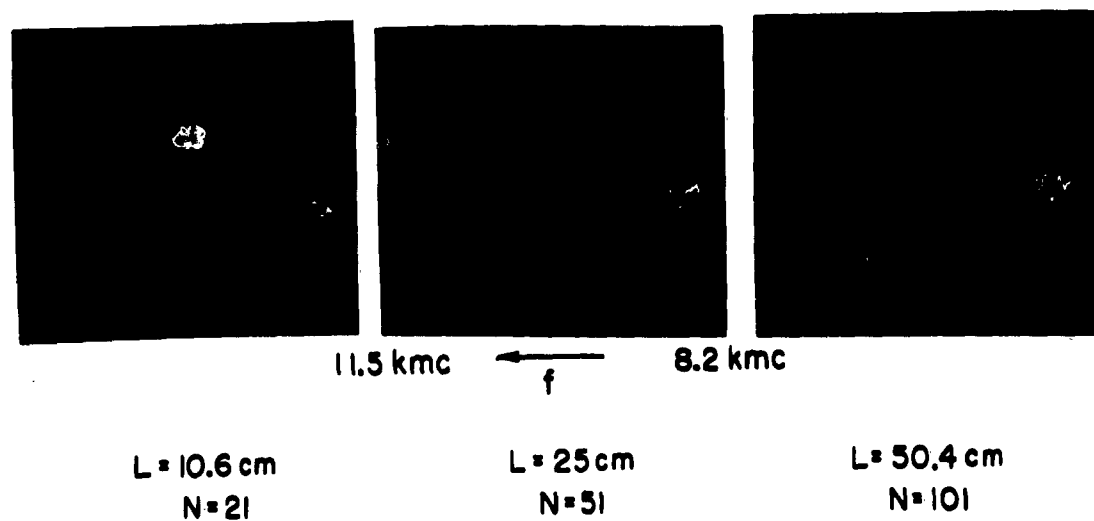
FIG. 3   TRANSMISSION ON LINEAR ARRAY VS. LENGTH OF ARRAY

Receiving Loop as a Probe in the Electromagnetic Field, " at the 1962 URSI Spring Meeting in Washington, D. C.

Current investigations are pursuing the application of the newly developed probes to difficult measurement situations where it is suspected that existing measurements are in error due to the presence of the electric dipole mode.

- - - - -

4. Surface Waves along Dielectric and Ferrite Rods, T. F. Tao. Contract AF19(604)-4118.

During the past year, two problems have been studied. The first one is the continuation of the study of the surface wave propagation along a cylindrical ferrite rod. The second one is a study of the junction between a circular waveguide and a dielectric-rod surface waveguide. Progress in each is described in the following:

Problem One. Surface Wave along a Cylindrical Ferrite Rod.

The HE_{11} - mode surface wave (X-band) along a longitudinally dc magnetized cylindrical ferrite rod has been studied. The quantities being measured are the guided wavelength, the radial field distribution, and the longitudinal attenuation of the surface wave as a function of the longitudinal dc magnetic field. The results indicate the ferrite rod supports two HE_{11} surface-wave modes simultaneously. They are identified as the positive and negative circularly-polarized wave. Their differences are best shown when the longitudinal dc magnetic field is increased. For the negative circularly-polarized wave, its guided wavelength decreases, its radial field distribution shrinks (i.e., the surface wave is more tightly bound), but the attenuation remains practically constant. For the positive circularly-polarized wave, its guided wavelength increases, its radial field distribution spreads out (i.e., the surface wave is less tightly bound), and the attenuation increases.

The ferrite used is Raytheon R-151 Mg-Mn ferrite. Three rods with different radii have been measured. It is planned to take measurements on a new type of ferrite.

The conventional theoretical study of electromagnetic wave propagation in ferrite media depends on the.the tensor permeability due to Polder, who assumed that the ferrite was saturated. The previously reported variations of the guided wavelength, radial field distribution, and attenuation occur around and before the saturation of the ferrite; hence, no theoretical study is possible with available theory for this experimental work.

Problem Two. Junction between a Circular Waveguide (TM_{01} Dominant Mode) and a Dielectric-Rod Surface Waveguide (TM_{01} Surface Wave Mode)

The mode analysis of the conventional closed waveguide is well developed. The mode analysis of the open waveguide, however, has only recently been carried out by Angulo and Chang (see reference 1), and is briefly mentioned in references 2 and 3. The correctness of their analysis has not been verified experimentally.

In this problem, a dielectric rod, which supports a TM_{01} surface wave, is considered as an open waveguide. Using the mode analysis for open wave-guides, the junction admittance between a conventional TM_{01} closed waveguide and this open surface waveguide has been studied. The theoretical result will then be checked by experiments. It is hoped that it will be possible to establish the correctness of the mode analysis for an open waveguide.

The method of analysis is as follows: (1) Find the complete set of eigen-functions for both waveguides. (2) Set up a variational expression for the input admittance of the junction by using these mode functions. (3) Use the Ritz method to express the electric field of the aperture, which is the trial function used in the variational expression, by expanding it into the mode functions of the closed circular waveguide. (4) Express the admittance in terms of a ratio of two determinants.

The theoretical results have been computed. The experimental setup has been completed. Measurements will be started soon.

References

1. Angulo and Chang, Brown University Scientific Report 1391/6 , 1957.

2. Felson and Marcuvitz, Polytechnic Institute of Brooklyn, MRI, R-446-55; R-726-59; R-776-59; R-841-60.

3. Bressler and Marcuvitz, Polytechnic Institute of Brooklyn, MRI, R-495-59; R-565-57.

- - - - -

5. The Long Antenna, S. Prasad, K. Iizuka, and R. W. P. King. Contract Nonr-1866(32).

Dipole Antennas Driven by a Two-Wire Line

Studies were made of dipole antennas driven by a two-wire line of both short length ($\beta h > 0.3$) and of long length ($\beta h < 63.1$). The measured values of the driving-point admittance are in good agreement with the King-Middleton second-order theory for the shorter lengths of antennas and with Wu's theory for the longer lengths, if the newly proposed end correction is taken into account. The results are illustrated in Fig. 4 .

The extrapolation to infinite length of the measured driving-point admittance of very long antennas is in good agreement with the theoretical values reported by Papas, and by King and Schmitt.

The terminal-zone effects on a dipole antenna driven by a two-wire transmission line have been re-examined. A series inductive correction $j\omega L_g$ together with other terminal-zone corrections is found necessary to reduce the measured apparent admittance of the antenna terminating the two-wire line to the ideal admittance of the dipole antenna when driven by a delta-function generator.

It was found that an unbalanced component of current on the line significantly influences the measured distributions of current along antennas of shorter lengths. A quantitative study was made by decomposing the currents into symmetric and anti-symmetric parts.

Papers published during the year on this subject:

1. K. Iizuka and R. W. P. King, "Terminal Zone Correction on the Admittance of the Dipole Antenna Driven by a Two-Wire Line, " J. of Research of N.B.S., November, 1962.

2. K. Iizuka and R. W. P. King, "The Effect of an Unbalance on the Current in a Dipole Antenna. " Accepted by Trans. PGAP of IRE.

3. K. Iizuka, R. W. P. King, and S. Prasad, "The Admittance of Very Long Cylindrical Antennas. " Accepted by IIE (London).

Technical reports issued on this subject during the year:

1. K. Iizuka, R. W. P. King, and S. Prasad, "The Long Cylindrical Antenna; Current and Admittance, " Cruft Lab. Tech. Report No. 351. Two papers based on this report were accepted by Trans. PGAP of IRE, and also by IIE (London).

2. K. Iizuka and R. W. P. King, "Terminal-Zone Corrections on the Admittance of the Dipole Antenna, " Cruft Lab. Tech. Report No. 352. A paper based on this report was published by the J. of Research of N.B.S.

- - - - -

6. Theory of the Dipole Antenna, D. Gooch, R. W. P. King, and T. T. Wu. Contract Nonr-1866(32), the Sandia Corporation, the Alfred P. Sloan Foundation, and National Science Foundation Grant 9721.

Extensive computations of the impedance of electrically long, center-driven dipoles have been made from the Wu theory. Technical Report No. 353, "Impedances and Admittances of Long Antennas in Air and in Dissipative Media with Tables of Functions $f(p) \pm ig(p) = \sqrt{1 \pm ip}$, " by D. Gooch, C. W. Harrison, Jr., [*] R. W. P. King, and T. T. Wu will be issued soon. The electrical half-length ranges from 1 to 100 for dipoles in air and from 1 to 19.7 for dipoles in a dissipative medium. Three ratios of radius of the antenna to wavelength in air have been used.

- - - - - - - -

[*]Sandia Corporation, Albuquerque, New Mexico.
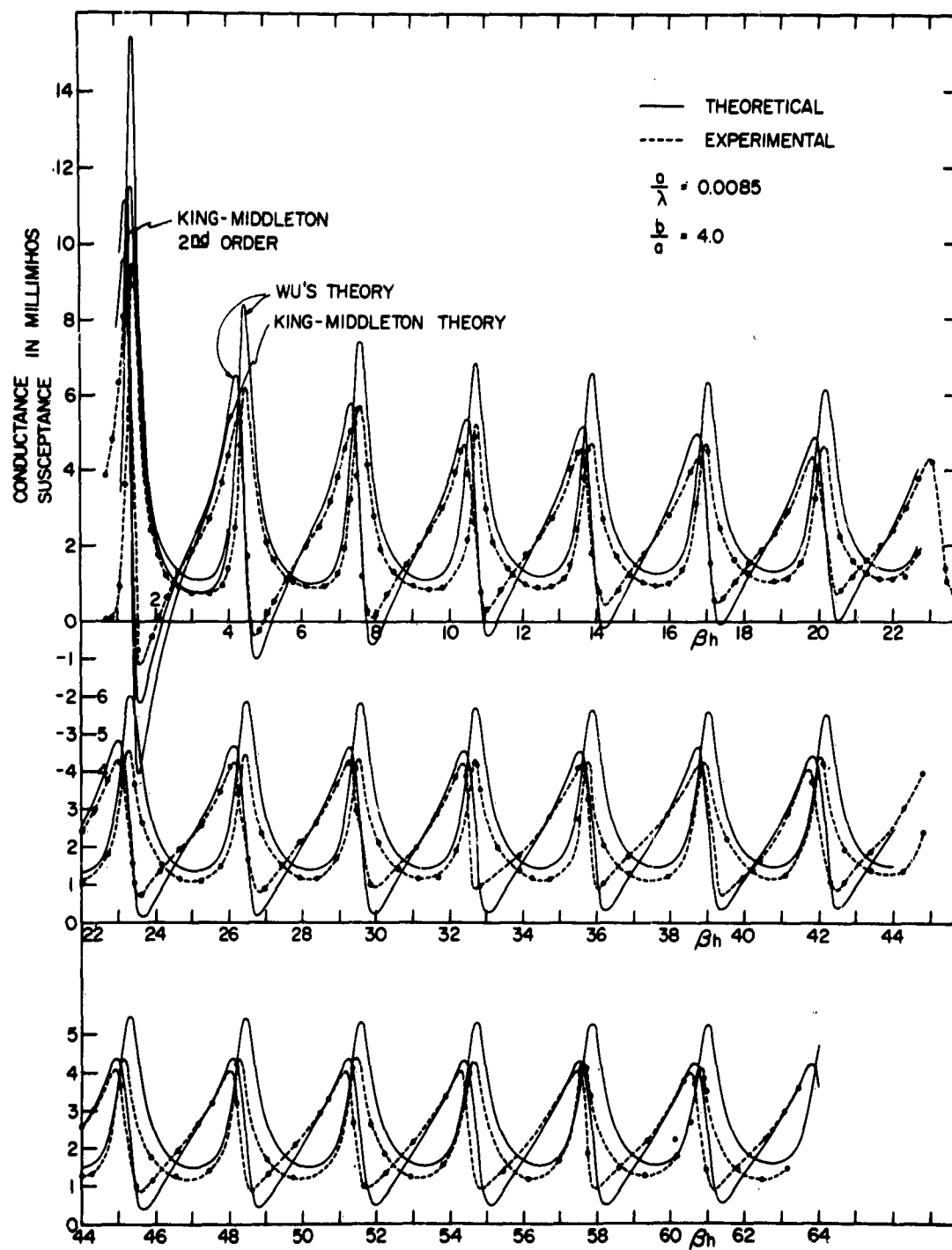
FIG. 4 DRIVING-POINT ADMITTANCE OF LINEAR CYLINDRICAL ANTENNA

It has been shown that the apparent terminal admittance of a linear antenna driven from a coaxial line can be additively separated into two parts when the transverse dimensions are small compared with the wavelength: one depending only on the wavelength and the dimensions of the antenna, and the other which may be interpreted as a capacitance that depends only on the radii of the coaxial line. Two technical reports have been published: No. 357, "Input Admittance of Linear Antennas Driven from a Coaxial Line, " and No. 362, "Input Admittance of Infinitely Long Dipole Antennas Driven from Coaxial Lines, " by Tai Tsun Wu.

- - - - -

8. Theory of the Thin Circular Loop Antenna, T. T. Wu, Alfred P. Sloan Foundation and National Science Foundation Grant 9721.

The current distribution on a thin circular loop transmitting antenna driven by a delta-function generator has been determined approximately by Fourier series expansion. A difficulty encountered in previous analysis was shown to be due to an inadequate approximation. Technical Report No. 361, "Theory of the Thin Circular Loop Antenna, " was issued.

- - - - -

9. Transient Characteristics of Antennas

A. Transient Response of a Dipole Antenna, H. J. Schmitt, R. W. P. King, and T. T. Wu. Contract Nonr-1866(32).

A paper entitled, "The Transient Response of Linear Antennas and Loops, " by R. W. P. King and H. J. Schmitt was presented at the Spring Meeting of URSI in Washington. It is scheduled for publication in a forthcoming issue of Transactions of IRE, PGAP. In it the transient response of straight wires and circular loops is studied experimentally and theoretically. It is shown that the initial response of a sufficiently short pulse is that of an infinitely long antenna at a frequency near the upper limit of frequencies contained in the pulse.

Technical Report No. 370, "Transient Response of Linear Antennas Driven from a Coaxial Line, " by T. T. Wu and R. W. P. King has been

completed. In it the initial transient response of straight wires connected to
coaxial lines is studied theoretically for the case when the pulse is applied to the
coaxial line. The wave form of the returned pulse is found for zero rise time
and for finite rise time that may be adjusted to fit experimental conditions.
Numerical results are obtained for several special cases, including one that
approximates experimental results reported by King and Schmitt. The agree-
ment is good.

B. Transient Characteristics of Circular Loop Antennas, B. Rama Rao,
     and H. J. Schmitt. Contract Nonr-1866(32).

This project is primarily directed towards a theoretical and experi-
mental study of the transient response characteristics of circular loop antennas
when subjected to a step-function excitation.

Further experimental work on this project has not been possible because
of construction work and repairs to the ground plane. Work will be resumed as
soon as this is completed.

- - - - -

10. A Study of Curtain Arrays of Dipole Antennas, S. S. Sandler and R. W. P.
     King. Contract AF19(604)-4118.

The research reported in the last yearly report on curtain arrays with
elements of equal length has been published as Cruft Laboratory Scientific
Report No. 12(Series 2). Portions of this work were presented at the National
Electronics Conference in October 1961, at the Boston Section IRE, PGAP, in
April 1962, and at the URSI Convention in Copenhagen in June 1962.

The quasi-zeroth-order analysis for curtain arrays was extended to
arrays with elements of unequal length. This extension follows from the modifi-
cation of the representations for the coupling terms which appear in the integral
equation. Two separate cases were considered: all elements driven by slice
generators and arrays with at least one parasitic element. Numerical calcu-
lations of the two-element parasitic couplet confirm the well-known phenomenon
that the main radiation beam may be directed by adjusting the length of the
parasitic element. The yagi array was also investigated and numerical results

were derived for a three-element array.   The above work is described in Cruft
Laboratory Scientific Report No. 12(Series 2). At the URSI Spring Meeting in
Washington, a paper was given which covered the arrays with elements of
unequal length.

The IBM 7090 program for curtain arrays written by B. Sandler is now
investigating curtain arrays for a wide range of spacings, driving conditions,
element lengths, and overall size.   This work should be completed in the near
future.

- - - - -

11. The Biconical Antenna in a Radially Stratified Medium, J. Fikioris.
     Contract Nonr-1866(32).

The electromagnetic field in the presence of an inhomogeneous and
dissipative medium has attracted considerable attention.   In the general case,
the medium is characterized by a dielectric constant ϵ and conductivity σ that
vary with the coordinates x , y , z.   Examples: inhomogeneous plasma, under-
water communication, propagation of E. M. into the earth, E. M. lenses, and
antennas used as probes into such media to measure their properties.

The present research is restricted to radially stratified media with
$\epsilon = \epsilon_{(r)}$, $\sigma = \sigma_{(r)}$ where r is the radial distance in spherical coordinates.
Many physical problems can be described by this model; they can be found in
the literature.   The list of references is lengthy and will not be given.   In
general, the references deal with idealized cases where the solution of the equa-
tions can be expressed in terms of well-known functions.   This research is
concerned with more realistic cases.

In spherical coordinates, Maxwell's equations are still separable, if
the complex dielectric constant ($\xi = \epsilon - j\frac{\sigma}{\omega} = \epsilon_0 f_{(r)}$) depends only on r .   The
angular equation is not affected; it remains the Legendre differential equation of
the homogeneous case.   However, the radial equation is no longer the spherical
Bessel equation of the homogeneous case.   Its coefficients depend on the "strati-
fication function" $f_{(r)}$, and contain additional singularities in the complex r
plane.   The biconical antenna is the most general problem that can be encounter-
ed; it involves the problem of the matching of the E. M. fields and requires the

complete solution of the radial equation from $r = 0$ to ∞. More specifically, series solutions $R_{1(x)}$, $R_{2(x)}$ around $x = 0$ and asymptotic solutions $R_{3(x)}$, $R_{4(x)}$ around $x = \infty$ of the second-order of differential equations are found first. For computational purposes and for reasons of matching linear connecting formulas between the two sets of solutions (around $x = 0$ and $x = \infty$) of the form:

$$R_{1(x)} = CR_{3(x)} + DR_{4(x)} \tag{1}$$

$$R_{2(x)} = GR_{3(x)} + HR_{4(x)} \tag{2}$$

must be determined. They provide the analytic continuation of $R_{3(x)}$, $R_{4(x)}$ in the vicinity of $x = 0$, and the asymptotic expansions of $R_{1(x)}$, $R_{2(x)}$ for large x. The determination of the coefficients C, D, G, H thus becomes the central problem of the analysis. It requires the solution of the associated linear difference equation as explained in reference 1. The author generalized Ford's method [1], and was able to provide explicit formulas for the evaluation of these coefficients. He has also extended the analysis to the special, but important, case of integral order (i.e., for integral values of the separation constant), when the second independent solution $R_{2(x)}$ becomes logarithmic at $x = 0$. Explicit formulas for the coefficients G and H of Eq. 2 have been obtained in this case, also. The mathematical interest of the analysis regarding the solution of the wave equation and the contribution to the theory of asymptotic expansions must be noted. The results are used to obtain the behavior of a biconical antenna in a radially stratified medium, but their applicability to a much wider class of problems should be pointed out.

For the stratification function $f_{(r)}$ the following variation was considered:

$$f_{(r)} = \frac{r + a}{r + b} = 1 + \frac{c}{r + b} \; ; \; (c = a - b) \tag{3}$$

where a, b are constant parameters, complex in general. It leads to a radial differential equation for TM waves of the form:

$$R''_{(x)} + \frac{c}{(x + a)(x + b)} R'_{(x)} + \left[1 + \frac{c}{x + b} - \frac{v(v + 1)}{x^2} \right] R_{(x)} = 0 \tag{4}$$

where v is the separation constant.

The corresponding equations for TE and TEM spherical waves are simpler. Even the above rather simple dependence introduces, as it now becomes obvious, two new finite singularities into the equation--at $x = a$, $x = b$-- beyond the singularities of the Bessel equation at $x = 0$ and $x = \infty$. A complete explicit solution was obtained in this case. It has also been proved that the analysis can be extended readily to more general types of $f_{(r)}$.

An IBM 7090 computer is being used to obtain numerical results on the behavior of a biconical antenna in certain cases. Dissipative media (where either a or b , or both, become complex) are going to be examined, too. Numerical results obtained up to now have completely verified the theoretical part of the research.

Referring to Eqs. 1 and 2, values for $R_{1(x)}$, $R_{2(x)}$ were computed with the use of convergent series up to a certain value of x . Next, values of $R_{3(x)}$, $R_{4(x)}$ were computed with the use of asymptotic series, and the coefficients C , D , G , H were evaluated according to the theory. For values of r up to 25, an overlapping region exists between the two expressions on both sides of Eqs. 1 and 2 . In the middle of the overlapping region agreement of 4 or 5 significant figures in the values of the functions was obtained.

References

1. W. B. Ford, The Asymptotic Development of Functions Defined by Maclaurin Series, Chelsea Publishing Co. , New York, N. Y. , 1960.

2. L. M. Milne-Thomson, The Calculus of Finite Differences, Macmillan and Co. , Ltd. , London, 1951.

3. N. E. Norlund, Leçons sur les Équations Linéaires aux Différences Finies, Gauthier-Villars et Cie. , Paris, 1929.

4. C. T. Tai, "The Electromagnetic Theory of the Spherical Luneberg Lens, " Appl. Scientific Research, Section B, Vol. II, 1958, pp. 113-130.

- - - - -

12. A Study of Circular Antenna Arrays, R. B. Mack. Contract Nonr-1866(32).

A. Object.

The object of this research is to compare measured and theoretical values of self and mutual admittances, the currents along the radiating elements, and simple radiation patterns of circular dipole arrays in order to establish the limits of validity of the theories describing performance of such arrays.

B. Experimental Equipment.

The major effect has been directed toward obtaining measured values of the required quantities for various ranges of parameters. This first required the design, fabrication, and assembly of an experimental equipment which could be used to measure with sufficient accuracy the desired quantities: the self and mutual admittances, the currents along the radiating elements, and the radiation patterns. Previous experimental setups were capable of measuring only self and mutual admittances, current distributions, and the radiation field in the forward and backward direction.

In the experimental setup finally used, the radiating elements are formed by extending the coaxial line inner conductor above a 24' x 48' aluminum ground plane. The outer radius of the coaxial line inner conductor was 1/8" , the inner radius of the outer conductor was 3/8" , and the coaxial lines were filled with HD-2 polyfoam. A small current loop probe can be moved along a 1/16" slot in the inner conductor to measure current along the antenna and standing wave ratios in the coaxial line. The assembly of coaxial lines fitted into a cradle whose aluminum top plate replaced one of the aluminum plates in the ground plane. This cradle could be rotated through 360° to permit measurement of radiation patterns. A corner reflector antenna was mounted on the ground plane sufficiently far away from the rotatable cradle to be in the far zone of any of the arrays used.

Antenna lengths of h/λ = 1/4 , 3/8 , 1/2 , 5/8 , 3/4 were used for the measurements. Here h is the antenna half-length and λ is the wavelength. Measurements of self and mutual admittances were made for arrays of 2 , 3 , 4 , 5 antennas placed at the corners of equilateral polygons of side d/λ where

d/λ was varied from $1/8$ to 1 . The current distributions were measured for various driving conditions with $d/\lambda = 1/8$, $3/16$, $1/4$, $1/2$, 1 , and for arrays of 2 , 3 , 4 , 5 elements. Radiation patterns were measured for $h/\lambda =$ $1/4$, $3/8$, $1/2$ for various combinations of driving conditions, d/λ , and a number of antennas.

C. Theoretical Results.

Extensive computations were made using the IBM machines at the Computation Center, Massachusetts Institute of Technology. These calculations were based on the King quasi-zeroth-order and quasi-first-order theory. A table of the complete range of parameters for which computations have been made, is given in Annual Progress Report No. 60, page 71.

D. Sample Results.

The self and mutual admittances of two identical antennas with $h/\lambda = 1/4$ (half-wave dipoles) are shown in Fig. 5a, and with $h/\lambda = 1/2$ (full-wave dipoles) are shown in Fig. 5b . In Fig. 5a the King-Middleton approximate second-order theory is in somewhat better agreement with the experimental values than the quasi-zeroth-order theory. This is particularly important for G_{11} where the quasi-zeroth-order gives values too high by about 1.250 millimhos. In Fig. 5b where $h/\lambda = 1/2$ the situation is quite different. Here the quasi-zeroth-order theory is in excellent agreement with experimental results, whereas the approximate second-order theory agrees very poorly with experimental values. This is to be expected, since the approximate second-order assumes only a $\sin \beta (h - |z|)$ current and the quasi-zeroth-order assumes a combination of this and a shifted cosine current, $\cos \beta z - \cos \beta h$. When $h/\lambda = 1/4$ the sine current is a good approximation to the total current, but when $h/\lambda = 1/2$ the actual current includes a significant component of the shifted cosine current.

The particular advantages demonstrated here of the quasi-zeroth-order theory are that it gives a good representation of both single and coupled antennas for lengths up to about $h/\lambda \doteq 0.6$ and can be used to compute improved radiation patterns without resorting to numerical integration techniques.

Examples of the horizontal plane radiation patterns resulting from one driven and one unloaded parasitic antenna separated by $\lambda/8$ are shown in Fig. 6a for $h/\lambda = 1/4$, and in Fig. 6b for $h/\lambda = 1/2$. In Fig. 6a the quasi-zeroth-order theory gives slightly better agreement with experimental results than the zeroth-order theory. When $h/\lambda = 1/2$, Fig. 6b, the zeroth-order theory is not much help, but the quasi-zeroth-order is in good agreement with the experimental values.

E. Status.

The measurements have been completed and most of the data have been reduced to a form suitable for comparison and presentation. The results are being assembled into a series of technical reports.

- - - - -

13. Scattering of Electromagnetic Waves from Acoustically Excited Plasmas, W. A. Saxton.   Contract Nonr-1866(26).

It is well known that the transmission and reflection of microwave energy in an ionized gas is a function of its electron density; propagation through a quiet plasma is practically impossible at microwave frequencies below the plasma frequency. However, Drummond [1] has theorized that propagation windows will result if the plasma is disturbed either by harmonic acoustic waves or other externally applied forces, and transmission below the plasma frequency can occur. It is also expected that interesting effects will be found when a plasma with plasma frequency close to the microwave frequency is excited by acoustic waves. This provides the motivation for an experimental study of the electromagnetic wave scattering properties of acoustically excited plasmas.

Early work was primarily concerned with the realization of laboratory plasmas with plasma densities within a range which would enable practical observations of effects using waveguide or free-space measuring techniques. Plasmas now being used include mercury arcs, and both hot and cold gas discharges. While presently striving to incorporate sound transducers into glass discharge tubes for the subsequent experiments, simultaneous investigations of the low frequency fluctuations in the discharges are being made. Crawford and
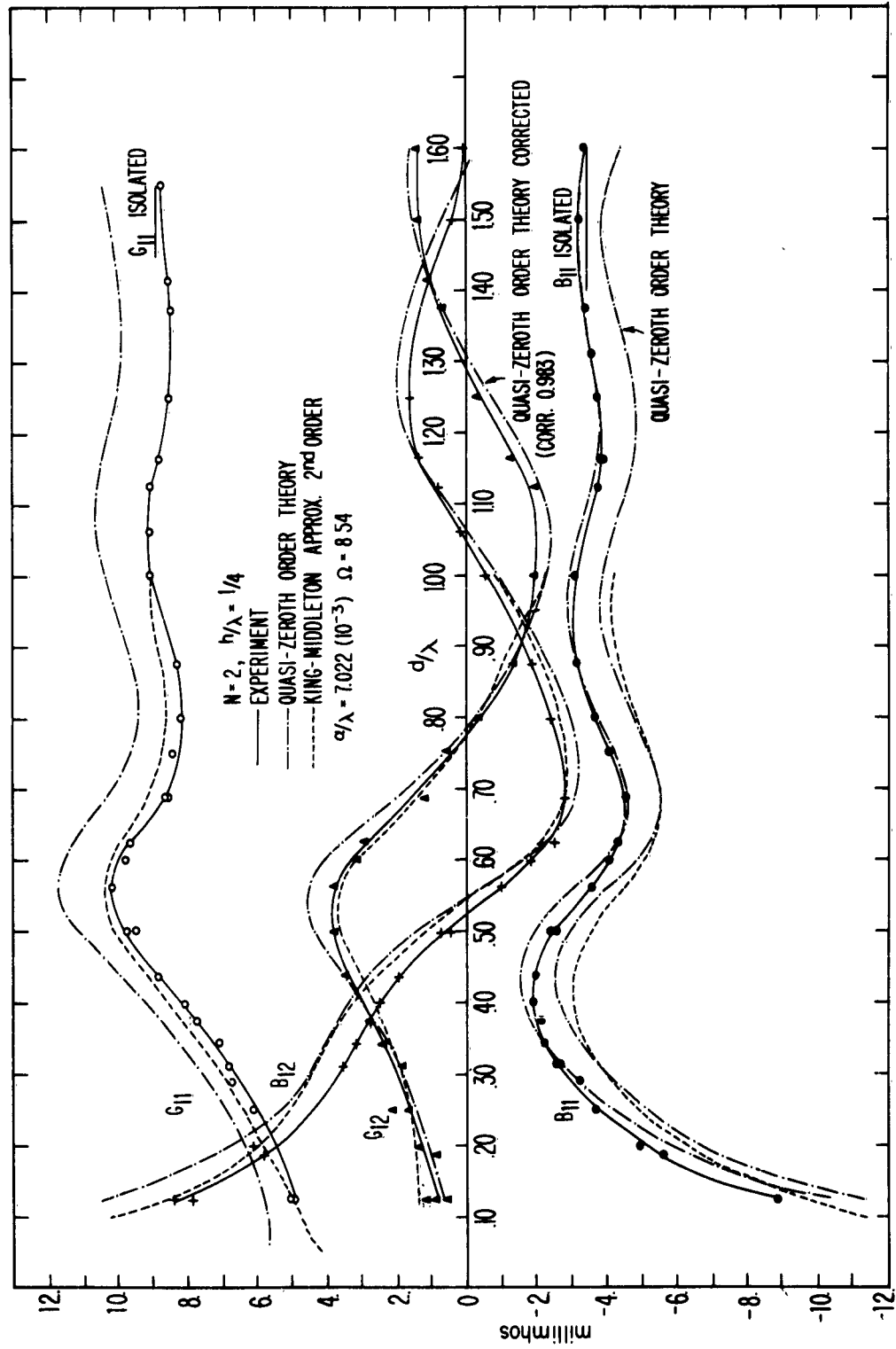
FIG. 5a. SELF AND MUTUAL ADMITTANCES OF TWO IDENTICAL HALF-WAVE DIPOLES
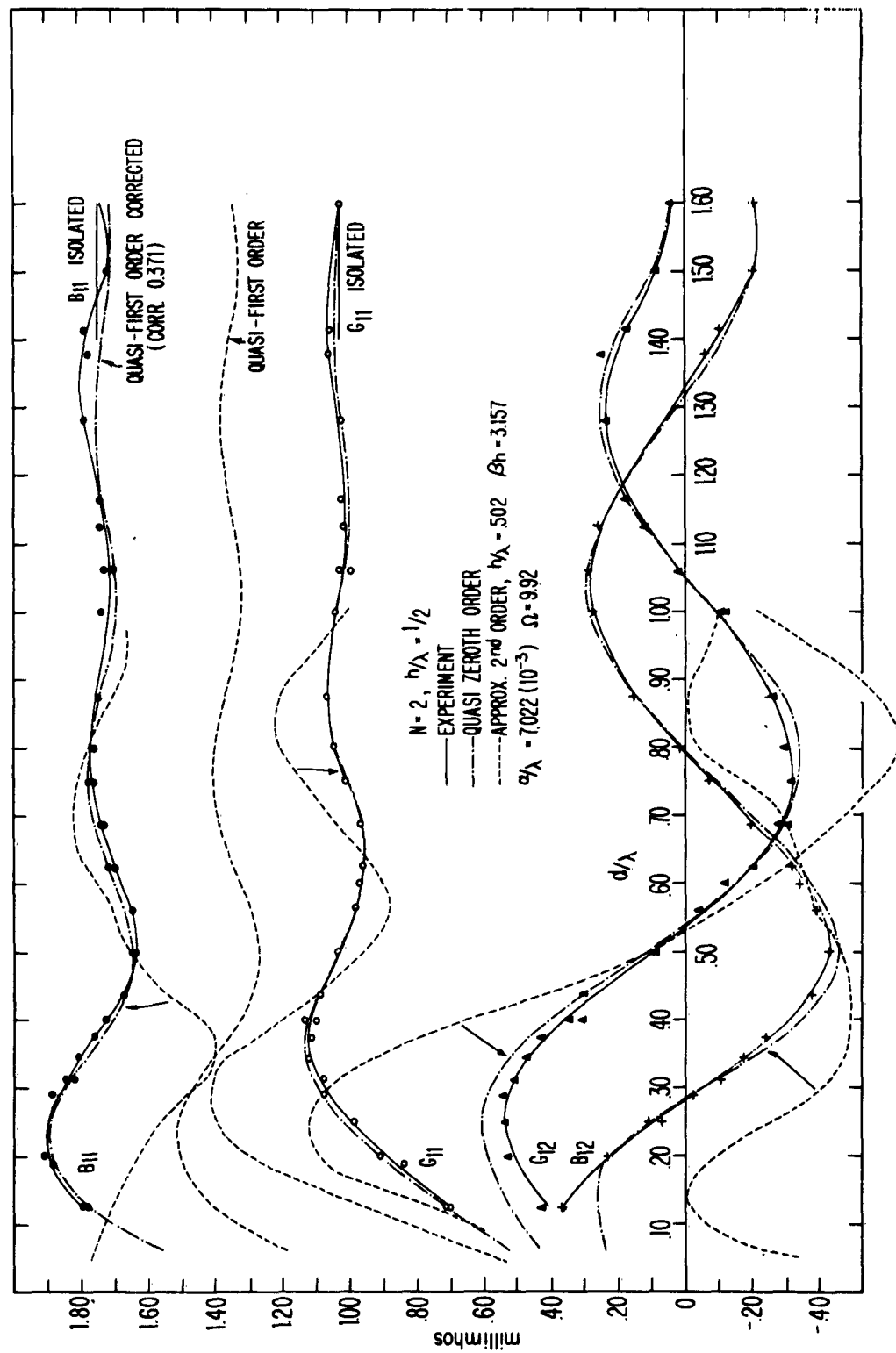
FIG 5b SELF AND MUTUAL ADMITTANCES OF TWO IDENTICAL
FULL-WAVE DIPOLES
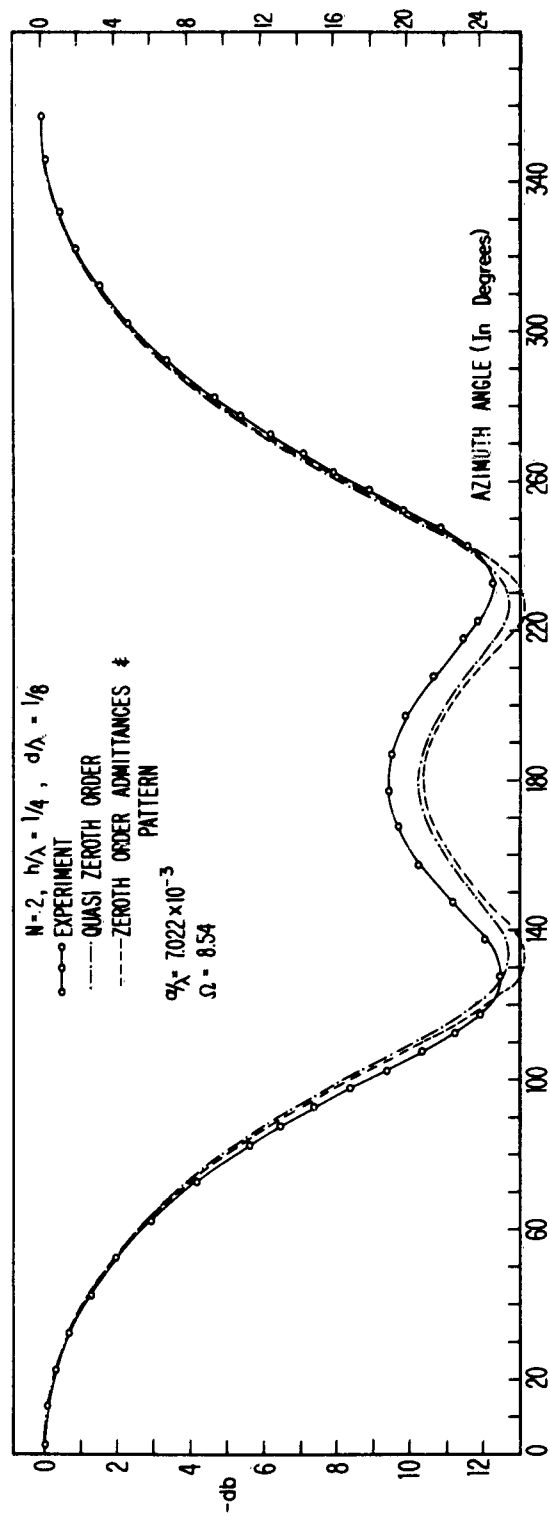
FIG. 6a RADIATION PATTERN, ONE DRIVEN AND ONE PARASITIC ANTENNA

$d/ = 1/8$, $h/ = 1/4$

N = 2, $h/\lambda = 1/4$, $d/\lambda = 1/8$

—○— EXPERIMENT
—·—· QUASI ZEROTH ORDER
—·—·— ZEROTH ORDER ADMITTANCES & PATTERN

$a/\lambda = 7.022 \times 10^{-3}$
$\Omega = 8.54$

AZIMUTH ANGLE (In Degrees)
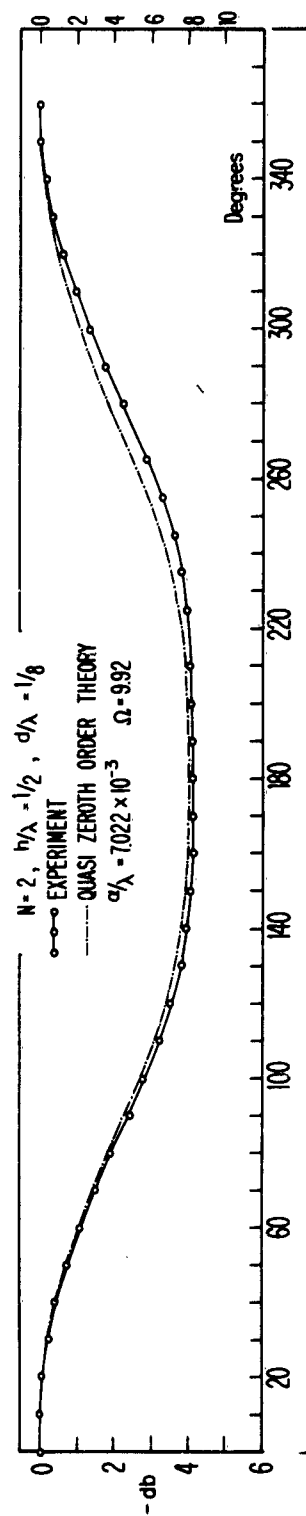
FIG. 6b RADIATION PATTERN, ONE DRIVEN AND ONE PARASITIC ANTENNA

$d/ = 1/8$, $h/ = 1/2$

N = 2, $h/\lambda = 1/2$, $d/\lambda = 1/8$

—○— EXPERIMENT
—·—· QUASI ZEROTH ORDER THEORY

$a/\lambda = 7.022 \times 10^{-3}$ $\Omega = 9.92$

Degrees

and Kino [2] have reviewed the noise problem in plasma, and it is not yet known whether these naturally occurring disturbances will materially affect the externally applied acoustic waves. From all indications it appears that acoustic frequencies can be chosen where any interactions due to these effects can be minimized [3].

Present plans call for the insertion of properly excited plasmas into large waveguides with low cut-off frequencies, arms of very sensitive waveguide bridges, and between radiating and receiving horns in free space. Each of these possibilities has advantages depending upon the plasma densities involved.

References

1. J. E. Drummond, "High Frequency Propagation Across an Ion Plasma Wave." Paper presented at the Fifth International Conference on Ionization Phenomena in Gases, Munich, 1961.

2. F. W. Crawford and G. S. Kino, Proc. IRE, December, 1961, pp. 1767-1788.

3. G. M. Sessler and M. R. Schroeder, "Interaction of Sound Waves with a Gas Discharge." Paper to be given in August, 1962, at the Fourth International Congress on Acoustics.

- - - - -

14. The Scattering of Waves by Obstacles, H. S. Tuan, S. R. Seshadri, and T. T. Wu. National Science Foundation Grant No. 9721.

The investigation of the problem of diffraction by a smooth, convex, three-dimensional obstacle possessing an axis of symmetry was undertaken. The incident wave function is assumed to be in the direction of the axis of the obstacle. Using the method previously developed for the case of a convex cylinder, the first two terms in the asymptotic series for the field in the shadow region have been found. Insofar as the determination of the field in the shadow region is concerned, the rotationally symmetric convex body differs from that of a convex cylinder in one important respect. The axis of rotation is caustic and the determination of the field near the caustic requires separate treatment.

The first two terms in the series for the field in the shadow region near the axial caustic have also been found. In this treatment the boundary condition used is that the wave function vanishes on the surface of the obstacle.

Diffraction of a plane electromagnetic wave by a perfectly conducting sphere was examined next. The aim, as before, was to find the first two terms in the asymptotic series for the field in the shadow region including the region near the axial caustic. The vector nature of the problem has increased the complexity of the calculations, but the principle involved is the same as that used in the scalar case. The first two terms in the asymptotic series for the field in the shadow region have been found for both the region near the axial caustic and the region away from the caustic. The extension of this procedure to the case of a smooth, convex, three-dimensional obstacle possessing an axis of symmetry with a plane electromagnetic wave incident in the direction of the axis of the obstacle is simple. In this case, also, the leading term in the series for the field in the shadow region has been found.

The scattering of a plane electromagnetic wave by a finite cone was investigated for the case of nose-on incidence. The main purpose of this research was restricted to studying the possibility of lowering the radar scattering cross section of a finite cone for nose-on incidence by controlling the shape of the aft-end. A number of qualitative prescriptions for minimizing the back-scattering cross section have been given previously by other investigators. In the present study, effort was made to obtain quantitative results which will enable more precise statements to be made on the problem of reduction of the cross section. No significant progress has been made in this investigation. For the investigation of this subject additional support was received from the Missiles and Space Vehicles Department, General Electric Company, Philadelphia.

During the past year, two scattering problems involving unidirectionally conducting screens were investigated and the results of those studies have since been published in the following two papers: (1) "Scattering by a Narrow Unidirectionally Conducting Infinite Strip, " by S. R. Sheshadri, Can. J. Phys., 38, 1623-1631, 1960, and (2) "Diffraction of a Plane Wave by an Infinite Slit in a Unidirectionally Conducting Screen, " by S. R. Seshadri, Trans. IRE, PGAP, AP-9, 199-207, 1961. In the course of the above investigation, it was noticed that

surface-wave terms were present in the expression for the scattered field. It was, therefore, of interest to study the problem of excitation of surface waves on a unidirectionally conducting screen. The excitation of surface waves by a line source on a unidirectionally conducting screen was investigated. In particular, topics such as the optimum position of the line source which maximizes the efficiency of excitation and the purity of the surface waves near the unidirectionally conducting screen were studied. The results of this investigation have been published in Cruft Lab. Technical Report No. 344, "Excitation of Surface Waves on a Unidirectionally Conducting Screen," by S. R. Seshadri. This report was presented at the 1962 Spring URSI Meeting in Washington, D. C. This paper has been accepted for publication in the IRE Transactions on Microwave Theory and Techniques.

As a continuation of the above work, the problem of scattering of surface waves on a unidirectionally conducting screen by discontinuities was investigated. The following types of discontinuities were considered: (1) a semi-infinite unidirectionally conducting screen terminated in open space, (2) a semi-infinite unidirectionally conducting screen joined to a perfectly conducting semi-infinite screen, and (3) two semi-infinite unidirectionally conducting screens joined to one another along a straight line. All the three cases have been formulated in terms of a one-dimensional Wiener-Hopf integral equation. The solution has been obtained in each case and the reflection and transmission coefficients have been evaluated. Technical Report No. 349, "Scattering by Discontinuities of Surface Waves on a Unidirectionlly Conducting Screen," by S. R. Seshadri has been issued, and covers the work done on this subject. This report is also to be published shortly in the IRE Transactions on Microwave Theory and Techniques.

Another problem which was investigated was the diffraction of a normally incident plane electromagnetic wave, by a circular aperture in an infinite, unidirectionally conducting screen. This problem is formulated in terms of an integral equation for the current on the shadow side of the screen. The integration with respect to the angle variable is carried out by the method of stationary phase, resulting in a one-dimensional integral equation for the unknown function. By employing the Wiener-Hopf technique and an iterative procedure,

the first two terms in the asymptotic series solution in inverse powers of the wave number are obtained. In particular, the first correction term to the geometrical optics value of the transmission cross section is evaluated. A new feature of this problem is that a set of rays in the sense of Keller's geometrical theory of diffraction emanates from the regions of the aperture rim to which the current on the screen is nearly tangential and proceeds in all directions. For the case of normal incidence, these rays do not contribute to the transmission cross section up to the order $(ka)^{-3/2}$, where k is the wave number and a is the radius of the aperture. Cruft Lab. Technical Report No. 360, "Diffraction by a Circular Aperture in a Unidirectionally Conducting Screen, " by S. R. Seshadri and T. T. Wu has been issued covering the work done so far in this topic. It has been accepted for publication in the IRE Transactions on Antennas and Propagation. The contribution that might arise from the new kind of rays still remains to be evaluated in order to complete the calculation of the higher order terms in the asymptotic series for the transmission cross section.

The field due to a line source of magnetic current situated in a lossless plasma region above a perfectly conducting screen was investigated for the case in which a uniform static magnetic field is impressed throughout the plasma region parallel to the direction of the line source. A very simple model is assumed for the plasma and as a consequence it can be characterized by a dielectric medium possessing a tensor dielectric constant. It is found that under certain conditions surface waves are excited on the screen. The dependence of the efficiency of excitation of surface waves on the distance d of the line source from the screen was examined. The asymptotic series for the radiation field is derived, and its leading term is shown to vanish for a particular choice of d. Under these conditions a strong surface-wave field is maintained near the guiding surface. This work is written in Cruft Lab. Technical Report No. 366, "Excitation of Surface Waves on a Perfectly Conducting Screen Covered with Anisotropic Plasma, " by S. R. Seshadri. This report has been accepted for publication in IRE Transactions on Microwave Theory and Techniques.

- - - - -

16. The Fluid Electrodynamics of Poorly Conducting Liquids, W. F. Pickard.
National Science Foundation Grants 12164 and 21869.

Again this year it is possible to report considerable progress in the
understanding of electrical force effects in dielectric liquids.

The investigation of the Sumoto effect (i.e., a polarity dependent rising
of a dielectric liquid along electrodes which have been dipped into it) has been
concluded with a paper [J. Appl. Phys. 33, 941-942 (1962)] discussing the
physical mechanisms underlying this phenomenon. It was shown there that this
effect is due to an anomalous potential drop near an electrode and by ion-drag
forces in the sheath of liquid about the electrode. The decay of the rise with
increasing applied frequency was explained by the finite time required to form
the electrode space charge characteristic of both the anomalous potential drop
and the ion-drag effects. Finally, it was shown that by electrical measurements
the chemical purity of the liquid changes while the Sumoto effect is in progress;
unfortunately, the impurity concentration always remained below levels
measurable by chemical means.

Co-field and cross-field pumping of dielectric liquids were studied ex-
tensively. The results of the pumping investigations of the past several years
have been summarized in Cruft Lab. Technical Report No. 350 [Harvard Univer-
sity, December 1961]. Cross-field pumping was shown to be a result of the
Sumoto effect at air-liquid interfaces and co-field pumping in the fringing fields
of the electrodes. The data from the co-field pumping experiments were shown
to be consistent with a model based on a non-space-charge-limited emission of
ions from the electrodes; this model was independently supported by data obtained
by photomicrographic studies of the electrodes and qualitative microanalyses of
the chemical constitution of the electrode surfaces. The emission theory of co-
field pumping was extended to derive various new results for non-space-charge-
limited emission into fluids flowing with arbitrary non-relativistic velocities:the
physical limits of the theory were examined in detail. Finally, the data was
gathered to illustrate the behavior of the pumping with variations of the voltage,
liquid flowrate, electrode aging, electrode spacing and orientation, and liquid
temperature. The results, too lengthy to be detailed here, showed that the

chief problem confronting researchers in this field is the gaining of an under-
standing of the nature of the ion creation and annihilation processes at the elec-
trode surfaces and within the liquid. No further work on pumping is currently
contemplated.

The previously reported work [Annual Progress Report No. 52, July, 1959]
on the electrophoresis of a spherical particle was published [Kolloid-Z. 179,
117-130 (1961)].

Experiments performed here on the rising of dielectric liquids between
the plates of a condenser show that the magnitude of the rise is not in agreement
with the classical theory, that the height of rise varies strangely in the applied
frequency, and that, therefore, the method of Greinacher [Helv. Phys. Acta 21,
261-272 (1948)] for measuring permittivity is open to serious question. These
effects are thought to be related to space-charge formation at the electrodes,
and some effort will be expended in the coming year to examine this hypothesis.

The electrodeless measurements of conductivity described last year have
been discontinued temporarily. They will be resumed.

Finally, it has been recently reported [P. K. Katti and M. M. Chaudhri,
Nature (London) 190, 80 (1961)] that the boiling point of a liquid dielectric is
altered by the application of high electric fields to the liquid. This alteration
is much larger than the classical theory [R. K. Lyon, Nature (London)192, 1285
-1286 (1961) predicts. Since most of the necessary apparatus is at hand, it is
planned to investigate the change of boiling point with both the applied voltage
and the applied frequency.

- - - - -

17. An Experimental Study of the Properties of a Dipole Antenna When Immersed
in a Conducting Dielectric, K. Iizuka. Contracts AF19(604)-7262, Nonr-1866(32),
and National Science Foundation Grant 20225.

Studies on the Properties of the Antennas in a Conducting Medium

Measurements have been made of the driving-point admittance and of the
amplitude phase distributions of the current relative to the phase at the driving-
point for both bare and insulated dipole antennas when immersed in homogeneous

and inhomogeneous conducting media. In general, the experimental results are in good agreement with available theories by King-Harrison and by Wu. The results of these experiments indicate that either an antenna of a short electrical length or a half-wave dipole antenna can be used as a probe to measure the dielectric constant and conductivity of the medium in which it is immersed. A half-wave dipole antenna could well be used to detect an inhomogeneity in an extended medium.

Comparisons were made of the characteristics of the insulated and uninsulated antennas in dissipative media.

The driving-point admittances of the insulated and uninsulated antennas when immersed in a conducting medium are compared in Figs. 7a to 7j as functions of βh. The experimental results would be useful in designing the optimum diameter of the insulator and the length of the antenna for such antennas as those buried under the runway of the landing strip for aircraft, probe antennas for geophysical exploration, submerged submarine antennas, missile antennas in plasmas, or buried antennas for anti-air-raid survival telecommunications.

Papers and scientific reports published on this subject during the year were:

1. "Dipole Antennas in Conducting Media," IRE meeting sponsored by the Boston Section, November 29, 1961(Boston).

2. K. Iizuka and R. W. P. King, "Apparatus for the Study of the Properties of Media, " Cruft Lab. Scientific Report No. 1 (Contract AF19(604)-7262). A paper based partially on this report is published in the IRE Transaction PGAP of July 1962.

3. K. Iizuka and R. W. P. King, "An Experimental Study of the Properties of Antennas Immersed in Conducting Media, " Cruft Lab. Scientific Report No. 2 (Contract AF19(604)-7262). Two papers based on this report are to be published in the IRE Transaction PGAP. The paper scheduled for the July issue will be titled:"The Dipole Antenna Immersed in a Homogeneous Conducting Medium, " and that for November:"The Dipole Antenna as a Probe for Determining the Electrical Properties of a Stratified Medium. "

4. K. Iizuka, "An Experimental Study of the Insulated Dipole Antenna Immersed in a Conducting Medium, " Cruft Lab. Scientific Report No. 3 (also published --and listed--under Contract AF19(604)-7262). A paper based on this report was presented at the URSI Symposium on Electromagnetic Theory and Antennas in Copenhagen in June 1962, and has been submitted for publication in the Symposium Proceedings.

- - - - -

18   Theory of Antennás Immersed in a Conducting Dielectric, R. W. P. King
       and C. L. Chen. National Science Foundation Grant No. 20225.

The input admittance of a small thin-wire circular loop antenna, driven by a slice generator, immersed in a dissipative medium was considered. It was found that Storer's expression for the input admittance of a circular loop antenna in a lossless medium can be carried over readily by replacing ζ_0 by complex ζ, and k_0 by k.

The numerical values of the normalized input conductance and normalized input susceptance of a small loop antenna $\beta b \lessgtr 0.3$, $\Omega = 10$, immersed in a medium of different degrees of dissipation were calculated. It is to be noted that the input susceptance is practically independent of k while the input conductance changes as much as 17 times in this special case.

Cruft Lab. Technical Report No. 369, "The Small Loop Antenna Immersed in a Dissipative Medium, " by C. L. Chen is to be published.

- - - - -

19. Theory of Dipoles Immersed in a Semi-Infinite Dissipative Medium, K. Sivaprasad. Contract Nonr-1866(32) and National Science Foundation Grant No. 20225.

The investigation of the radiation fields of dipoles immersed in a semi-infinite medium is being continued. Solutions valid for large distances both in air and conducting medium were obtained by a suitable modification of a method suggested by Lighthill for the asymptotic evaluation of Fourier integrals. The advantages of this method are its simplicity and ease of application. The results

FIG. 7(a) MEASURED ADMITTANCE IN THE
SOLUTION WITH $\epsilon_r = 78$, $\frac{\sigma}{\omega\epsilon_r\epsilon_0} = 0.036$

FIG. 7 (c) MEASURED ADMITTANCE IN THE
SOLUTION WITH $\epsilon_r = 78$, $\frac{\sigma}{\omega\epsilon_r\epsilon_0} = 0.18$

FIG. 7 (b) MEASURED ADMITTANCE IN THE
SOLUTION WITH $\epsilon_r = 78$, $\frac{\sigma}{\omega\epsilon_r\epsilon_0} = 0.088$

FIG. 7 (d) MEASURED ADMITTANCE IN THE
SOLUTION WITH $\epsilon_r = 78$, $\frac{\sigma}{\omega\epsilon_r\epsilon_0} = 0.35$
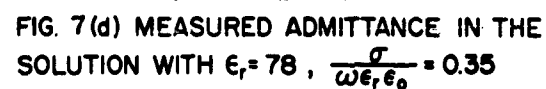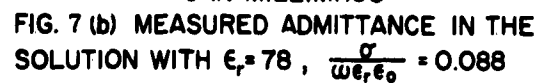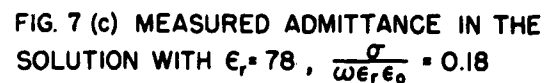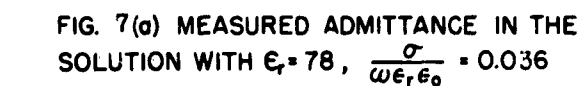
- - -•- -•- - $D/2a = 1$ ———•———•——— $D/2a = 6$
———▲———▲——— $D/2a = 1.25$ ———o———o——— $D/2a = 12$
———✕———✕——— $D/2a = 4$

FIGS. 7a-7d MEASURED ADMITTANCE

FIG. 7 (e) MEASURED ADMITTANCE IN THE SOLUTION WITH $\epsilon_r = 78$, $\dfrac{\sigma}{\omega \epsilon_r \epsilon_0} = 0.53$

FIG. 7 (h) MEASURED ADMITTANCE IN THE SOLUTION WITH $\epsilon_r = 72$, $\dfrac{\sigma}{\omega \epsilon_r \epsilon_0} = 4.4$

FIG. 7 (f) MEASURED ADMITTANCE IN THE SOLUTION WITH $\epsilon_r = 77$, $\dfrac{\sigma}{\omega \epsilon_r \epsilon_0} = 1.06$

FIG. 7 (i) MEASURED ADMITTANCE IN THE SOLUTION WITH $\epsilon_r = 70$, $\dfrac{\sigma}{\omega \epsilon_r \epsilon_0} = 6.2$

FIG. 7 (g) MEASURED ADMITTANCE IN THE SOLUTION WITH $\epsilon_r = 74$, $\dfrac{\sigma}{\omega \epsilon_r \epsilon_0} = 2.64$

FIG. 7 (j) MEASURED ADMITTANCE IN THE SOLUTION WITH $\epsilon_r = 69$, $\dfrac{\sigma}{\omega \epsilon_r \epsilon_0} = 8.8$

—•—•—•— D/2a = 1   —•—•— D/2a = 6
—▲—▲— D/2a = 1.25   —•—•— D/2a = 12
—⊁—⊁— D/2a = 4
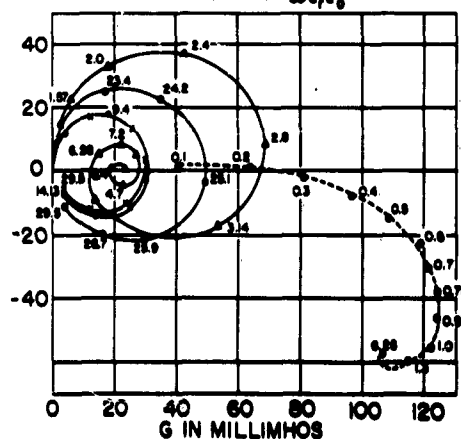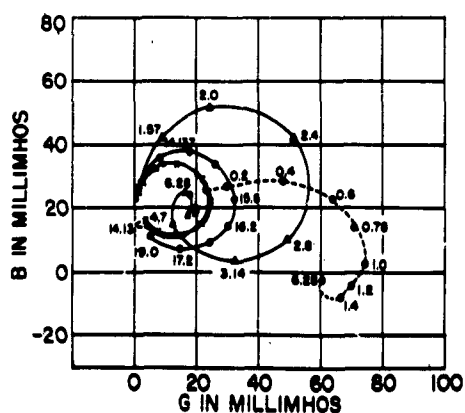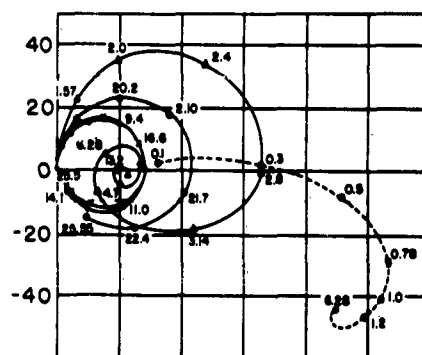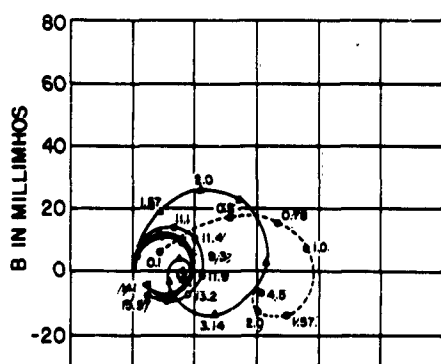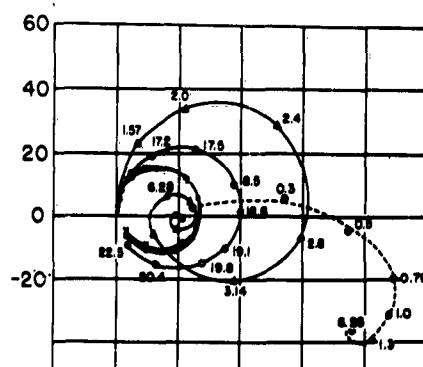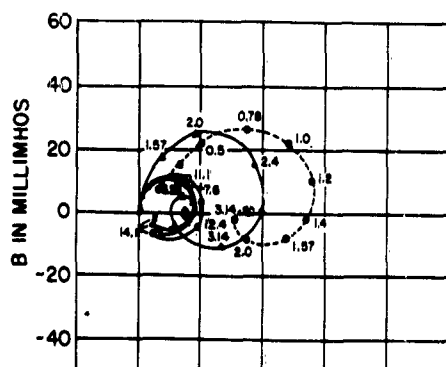
FIGS. 7e-7j MEASURED ADMITTANCE

obtained agree closely with those of Baños and Wesley, who used a modified
saddle-point technique to evaluate the integrals. These results have been published
as a technical report (Cruft Lab. Technical Report No. 354). By a suitable ex-
tension of this method, new results are being evaluated which correspond to those
published earlier by Stein (Cruft Lab. Technical Report No. 226). The low fre-
quency solution is also being investigated.

For practical applications, e. g., communication between submarines,
one would like to have most of the radiated energy in a desired direction. So the
solutions of a single horizontal dipole are being used to study the electric field of
an array of dipoles. The strengths, phase differences, and separations of the
sources are being varied to determine whether a narrowly directed beam can be
obtained. The results of the study will be published shortly in a report.

- - - - -

20. Theory of the Strip Antenna, J. Myers. Supported in part by the Raytheon
    Company and Contract Nonr-1866(32).

The scattering of a plane wave by a strip was studied in a way which leads
to qualitatively new data for the field pattern and which makes feasible the com-
putation of many numerical results. A perfectly conducting strip is considered
to be in an electromagnetic field governed by the two-dimensional Helmholtz
equation, with an illuminating plane wave incident along an arbitrary direction
in the plane transverse to the strip. Both electric and magnetic polarizations
(i. e., Dirichlet and Neumann boundary conditions) were considered.

The strip as a scatterer may be characterized by the fact that its
scattered field possesses a plane of symmetry independent of the direction of the
incident wave. It was shown that this symmetry is reflected in the functional
nature of the field pattern. This field pattern appears to be a non-trivial function
of the two variables:"angle of incidence" and "angle of observation." It was shown
that for the strip this function of two variables may be expressed algebraically in
functions of only one angle. Such a form is seen to be characteristic of the strip,
and closely related to the simplest form which would permit the maintenance of a
plane of symmetry independent of the angle of incidence. This property of the
strip has the consequence that a table of two functions of one variable permits the

construction of the field pattern, and the experimental consequence that if the field pattern is measured for one angle of incidence, then the field pattern at an arbitrary angle of incidence may be constructed from the data of the measurement at the one angle.

Once it was shown that there exist functions of one variable from which the field pattern may be constructed, it is of interest to find these functions explicitly. . A method due to G. E. Latta[1] was employed to show that the Fourier transforms of the one-variable functions satisfy a second-order system of ordinary differential equations and then it was shown that the functions themselves satisfy a similar set of equations. Latta's method fails to provide a means of finding coefficients which appear in the differential equations. When the coefficients were viewed as functions of the frequency parameter it was found possible to express them as solutions of a differential equation in the frequency parameter, and so complete the theoretical solution to the problem.

In the course of differentiating with respect to the frequency parameter to find Latta's coefficients, it was shown that the current and field pattern of the strip may be formulated as solutions to ordinary differential equations with the frequency parameter as the variable. Thus, for example, the current at the center of the strip may be found as a function of frequency.

The strip problem has already been solved by expansion in Mathieu functions, as discussed by Morse and Rubenstein [2], and by the integral representation of Kleinman and Timman [3]. Neither of these methods, however, led to the decomposition of the field pattern into functions of one angle. Further, the new method, by expressing the desired quantities as solutions to ordinary differential equations, makes the finding of the field patterns and related quantities numerically much more efficient than either of the already known methods.

The problem of two parallel strips has been formulated, and it was shown that the field pattern for two strips is also expressible in functions of one angle, but that twice as many functions are required as in the case for one strip. If the strips are not only parallel, but lie in the same plane, it appears that the new technique may be extended to give an explicit solution. For the co-planar case, as for the single strip, Babinet's principle may be applied to interpret the strip

solutions as applying to the dual split problem. This is not the case if the two strips are not co-planar, as may be shown from symmetry considerations.

A solution was obtained for the limiting case of a fat cylindrical antenna, the radius of which was allowed to increase without bound. It was found impossible to extend the method to handle an antenna of finite radius. However, the scattering by a very thin cylindrical rod is often treated approximately by ignoring the azimuthal variation of the current and the scattered field. To this approximation, the thin rod has a symmetry plane (in fact a family of them) independent of the angle of incidence, and the current is determined by a one-dimensional integral equation with a difference kernel; the same is true of the current in the strip. It may be shown that the field-pattern decomposition, which holds exactly for the strip, holds to this approximation for a thin rod.

Numerical results were found for the one-angle functions from which the field pattern of the strip may be constructed. The scattering cross section and back-scattering cross section were tabulated as functions of the angle of incidence for several values of the frequency parameter, and the radiation pattern was tabulated as a function of the angle of observation for a selection of frequencies and angles of incidence. The field pattern was tabulated for two sample cases. For normal incidence, the scattering cross section, back-scattering cross section, and current at the center of the strip were tabulated as functions of frequency. Again, for normal incidence, the near fields were tabulated for three values of frequency.

In summary, it has been shown that the field pattern of the strip has a structure which is simpler than was realized, and that functions of one angle suffice to express its properties. These functions were found through an extension of the method of G. E. Latta, which extension consists of the finding of certain coefficients appearing in his equations. Some of the extensions and ramifications of the strip problem were examined, and numerical results were obtained.

References

1. G. E. Latta, "The Solution of a Class of Integral Equation, " J. Rational Mech. and Analysis, 5 , 821-833 (1956).

2. P.M. Morse and P. J. Rubenstein, "The Diffraction of Waves by Ribbons and Slits," Phys. Rev., $\underline{54}$, 895-898 (1938).

3. R. E. Kleinman and R. Timman, "Integral Representations of Solutions of the Helmholtz Equation with Application to Diffraction by a Strip," University of Michigan, E. E. Dept., Radiation Laboratory Rep. No. 3648-3-T, Ann Arbor, Michigan (1961).

- - - - -

23. Perturbation Theory of Pion-Pion Interaction, T. T. Wu. Alfred P. Sloan Foundation and National Science Foundation Grant 9721.

The problem of the pion-pion scattering was studied on the basis of the model of a four-particle direct interaction without derivative coupling. Renormalization was carried out for this model with a detailed analysis of overlap insertions, and relations were obtained among the various renormalized quantities related to pion-pion interaction. Two technical reports were issued: Cruft Laboratory Technical Report No. 346, "Perturbation Theory of Pion-Pion Interaction I: Renormalization," and No. 348, "Perturbation Theory of Pion-Pion Interaction II: Two-Pion Approximation." A paper based on I appeared in the Physical Review, Vol. 125, No. 4, February 15, 1962, and one based on II has also been accepted for publication in the Physical Review.

- - - - -

25. New Probe Techniques in the Measurement of Electromagnetic Fields, K. Iizuka. Contract Nonr-1866(32) and National Science Foundation Grant-20225.

Efforts have been made to reduce the effect of the lead wires which connect the probe and the detecting system in the measurement of the electromagnetic field intensity. A photo probe which consists of a small dipole that is center-headed with a photocell was used as a reradiating or scattering antenna. Thus, the lead wire to the probe was completely eliminated, yet the scattered signal could be modulated by illuminating the photocell load by a beam of chopped light (see Fig. 8). The same principle has also been applied to measure the distribution of current along an antenna of an arbitrary shape with a shielded-loop probe that is loaded with a photocell.
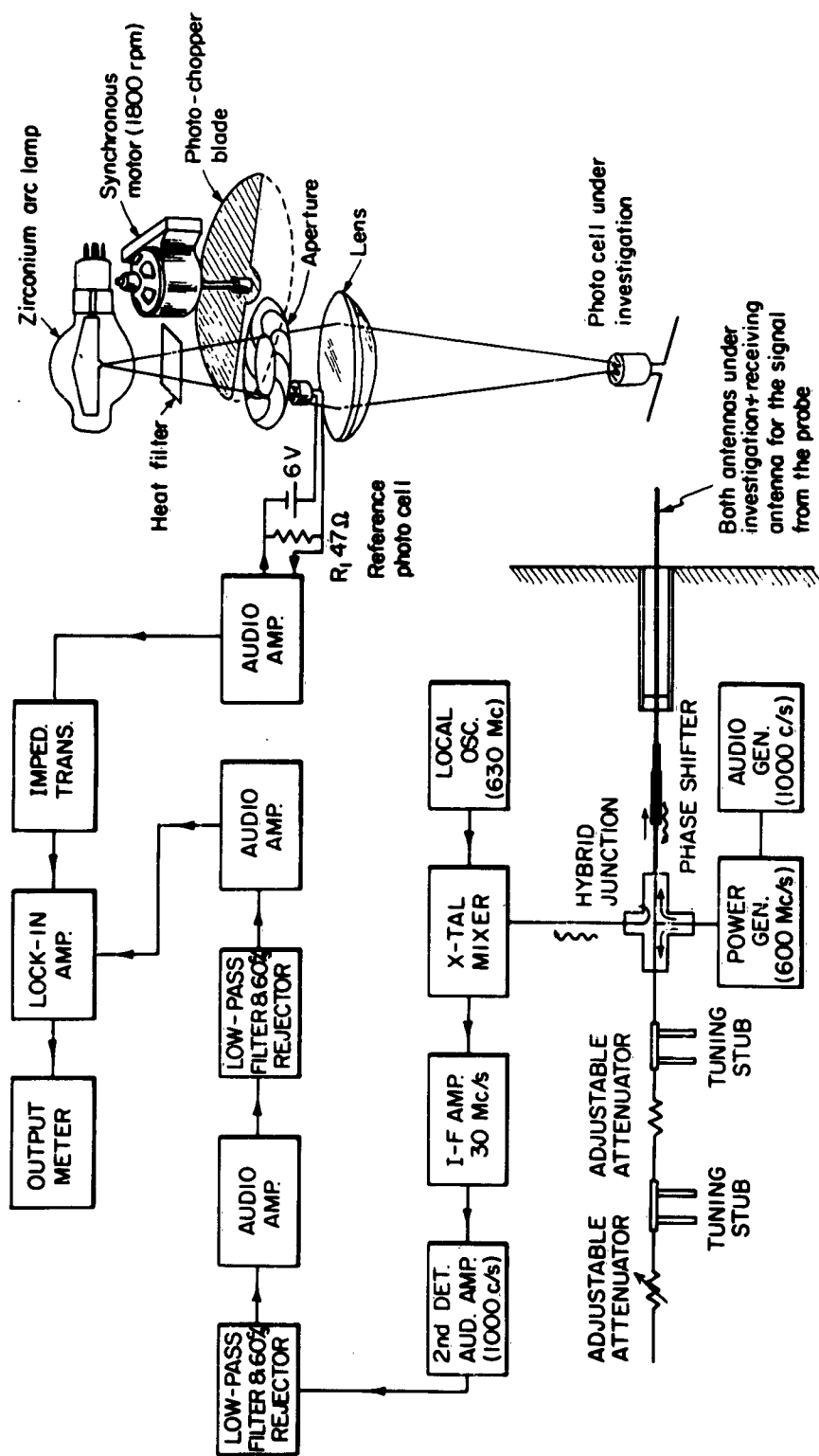
FIG. 8 BLOCK DIAGRAM OF EXPERIMENTAL EQUIPMENT FOR MEASURING
ELECTROMAGNETIC FIELD BY PHOTO PROBE

Both measured patterns of a known field and the distribution of a known current along an antenna proved the usefulness of this new method.

In connection with a photocell probe, a new technique has been developed to measure a time-dependent load impedance. It was used to measure the instantaneous impedance of a photocell during the rise and decay times.

A principle similar to that used in the photocell probe can be applied to the measurement of field intensity by means of a coil spring which was arranged to modulate the scattered signal.

A small FM transmitter was constructed to measure the near-zone field of an antenna immersed in a conducting medium.

Papers and technical reports on this subject published during the year:

1. K. Iizuka, "A Method of Measuring the Time-Dependent Impedance of the Load, " Cruft Lab. Technical Report No. 364. A paper accepted by the Microwave Journal. is based on this report.

2. K. Iizuka, "A New Technique for Measuring an Electromagnetic Field by a Coil Spring, " Cruft Lab. Technical Report No. 365. A paper based on this report was submitted to the Review of Scientific Instruments, and was also presented at the Spring URSI-IRE meeting on May 2, 1962, in Washington, D. C.

- - - -

26. Slot Transmission Lines and Radiators in Non-Planar Structures, R. Burton. Contract Nonr-1866(32).

An experimental study of arrays of slots in a ground screen that may be curved or otherwise made to depart from planar form is in progress.

- - - - -

27. The Computation of Surface Profiles in Hydraulics, W. F. Pickard. National Science Foundation Grant-21869.

It can be shown that the computation of water surface profiles, either upstream or downstream from a dam or other similar obstacle, is reducible, in the case of a uniform channel to the evaluation of the three integrals:

$$\mathfrak{B}_\gamma^{(1)}(z) = \int \frac{z^{\gamma-1}}{1-z} \, dz \qquad\qquad 0 < z < 1$$

$$\mathfrak{B}_\gamma^{(2)}(z) = \int z^{\gamma-1} \, dz \qquad\qquad 0 < z < \infty$$

$$\mathfrak{B}_\gamma^{(3)}(z) = \int \frac{z^{\gamma-1}}{1+z} \, dz \qquad\qquad 0 < z < 1$$

where $\left\{ \begin{array}{l} -1/2 \leq \gamma < 0 \\ 0 < \gamma \leq 3/2 \end{array} \right\}$ for integrals of the first and third kinds and $\left\{ 0 < \gamma < 7 \right\}$

for integrals of the second kind.

The integration for $\mathfrak{B}_\gamma^{(2)}$ is trivial. That for $\mathfrak{B}_\gamma^{(1)}$ or $\mathfrak{B}_\gamma^{(3)}$ is extremely difficult, but can be reduced to the problem of evaluating an integral of the form

$$\int_0^z \lambda^{\gamma-1} \, Li_2(\pm\lambda) \, d\lambda$$

where Li_2 is the dilogarithm function. The evaluation of the latter integral is conveniently effected by expanding Li_2 in an economized power series, the truncation error of which has been distributed "appropriately." By "appropriately" one means merely that the properties of the $\mathfrak{B}_\gamma(z)$ are such that a truncation error will be less noticeable for some z than for others and that it is desirable to push the truncation error into insensitive z-ranges. To accomplish this, a method of Spitzbart and Macon [Proc. Am. Math. Soc. 9, 243-249 (1958)] has been utilized and an iterative approximating technique evolved using it.

The problem has now reached the stage of programming for an IBM 7090. A special purpose logarithm routine, exponential, and power-taking subroutine has been written and debugged. A dilogarithm routine has been written and is in the final stages of debugging. The approximating routine is currently being coded.

The completion of the calculations for the polynomial approximation of Li_2 will enable one to calculate the backwater functions using only logarithms and powers. It is planned to construct a 7090 program based upon this.

- - - - -

28. Electromagnetic Wave Propagation in Dispersive Media, H J. Schmitt.
    Contract Nonr-1866(26).

        A new research project on the experimental measurement and theoret-
ical investigation of the propagation of complex electromagnetic signals in dis-
persive media has been started. Specifically, the study includes a continuation
and completion of the research on the propagation of extremely short pulses in
perfectly conducting hollow waveguides. Emphasis is laid on the analogy with the
dispersion in an ionized gas and the possible use of transient oscillations for
diagnostic purposes.

        For the experimental phase of this project a big waveguide with inside
dimensions of 8' x 4' x 40' is available. The cut-off frequency for the dom-
inant mode is about 60 Mc/sec. The driving antenna consists of a half-loop at one
end of the guide. A linear dipole which can be moved in a longitudinal direction
is used as the pick-up device. For transient observation the signal is led directly
to a high-speed oscilloscope. Preliminary measurements involving the excitation
of the waveguide with short, direct-current pulses with variable duration in the
nano-second range indicate that the pulse is dispersed into a damped wavetrain
with nearly sinusoidal oscillations. The periodicity of the oscillations approaches
for large times. that which corresponds to the cut-off frequency of the guide, i. e.,
about 60 Mc/sec. This behavior is expected from theory. Various lengths have
been used for the pick-up probe to determine the effect of the characteristics of
the receiving antenna on the shape of the measured transient response. Further
measurements will be carried out to determine the effect of the driving antenna.

        A number of coaxial gas-discharge tubes have been constructed for the
experimental observation of pulse dispersion in plasma media.

                        - - - - -

29. Fresnel Gain of Aperture Antennas, T. Soejima. Contract AF(604)-4118.

        When a transmitting aperture A_o and a receiving aperture B_o are
coupled in the Fraunhofer region, the ratio of received to transmitted power is
given by the Friis formula. It is well known that the Fraunhofer gains G_{ao} and
G_{bo} of A_o and B_o are constant and are determined independently.

The product of the gains $G_a G_b$ in the Fresnel region is determined as an integral over both apertures, assuming the gains G_a and G_b for A_o and B_o. It is pointed out that $G_a G_b$ cannot generally be separated into the individual factors, but a formula similar to that of Friis still holds in the Fresnel region. It is proposed to define the "gain product reduction factor," $Y_a Y_b$, as the ratio of $G_a G_b$ to $G_{ao} G_{bo}$. The individual gain G_a or G_b may be determined only when A_o and B_o are identical and the illuminations of both apertures are the same. Then, "the gain reduction factor," Y, is defined as the ratio of G_a to G_{ao}.

Assuming uniform amplitude and phase of illumination over A_o and B_o, $Y_a Y_b$ and Y are determined for circular and rectangular apertures. For circular apertures, the same factors are determined for a set of illuminations which approximate commonly used tapers.

In the Fraunhofer region, the best gain will be obtained from an aperture antenna when the phase of illumination is constant over the aperture. Because the field point is far enough away from the aperture, the path length from the aperture points to the field point will be approximately equal, resulting in an optimum additive effect. When the field point lies in the Fresnel region, the path differences from the points in the aperture to the field point must be compensated in some way in order to get an optimum additive effect in the radiation field. Assuming the phase front of the illumination on A_o is a zone of the sphere centered on B_o and the phase front of the illumination on B_o is a zone of the sphere centered on A_o, the effect of defocusing the primary feed in lenses and dishes on the Fresnel gain is discussed. Such an illumination can be realized practically in lenses or dishes by slightly defocusing the phase center of the primary feed along the lens or reflector axis. The variation of Y with δ (= aperture area / λd) shows clearly the effect of defocusing.

- - - - -

APR64

VII. REPORTS PUBLISHED SINCE JULY 1, 1961[*]

Contract Nonr-1866(16)/NR-372-012

TR315 Nuclear Magnetic Resonance in Antiferromagnetic MnF_2 under Hydrostatic Pressure, G. B. Benedek and T. Kushida.

TR316 The Temperature of Shock Wave in Solids, G. B. Benedek.

TR345 Matched Filters and Intersymbol Interference, D. W. Tufts.

TR347 On Computing Minima by the Penalty Function Approach, Y. C. Ho

TR355 Certain Results in Pulse Transmission, D. W. Tufts.

TR356 Comparison of Different Modes of Representation of Multivariable Systems, K. S. Narendra and L. E. McBride, Jr.

TR358 Interactions between Light Waves in a Nonlinear Dielectric, J. A. Armstrong, N. Bloembergen, J. Ducuing, and P. S. Pershan. Supported in part by ARPA Contract SD-88.

TR359 A Self-Organizing Control System Based on Correlation Techniques and Selective Reinforcement, D. N. Streeter and K. S. Narendra.

TR367 Light Waves at the Boundary of Nonlinear Media, N. Bloembergen and P. S. Pershan. Supported in part by ARPA Contract SD-88.

TR368 Optimal Control Problems with Input and Output Constraints, Y. C. Ho.

TR371 Relaxation Time Measurements in Ruby by a DC Magnetization Technique, S. Y. Feng.

Contract Nonr-1866(17)/NR-372-011 (Final Report)

TR326 Radio-Wave Propagation, H. R. Mimno.

Contract Nonr-1866(26)/NR-371-015[**]

TR317 Electromagnetic Reflection from Sound Waves, H. J. Schmitt and T. T. Wu. Supported in part by Contract NSF-G9721.

- - - - - - -

[*] Abbreviations used in this section: TR for technical report, and SR for scientific report. The letters NSF indicate the National Science Foundation, and ARPA, the Advanced Research Projects Agency.

[**] Research by Prof. Wu under these contracts was also supported in part by the Alfred P. Sloan Foundation.

-127-

Contract Nonr-1866(26)/NR-371-015 (continued)

TR324   Diffraction of Electromagnetic Waves by Sound Waves, H. J. Schmitt.

TR363   Electromagnetic Reflection from Sound Waves, II, H. J. Schmitt and
         T. T. Wu. Supported in part by Contract NSF-G9721.

Contract Nonr-1866(32)/NR-371-016

TR318   Theory of the Dipole and the Two-Wire Transmission Line, T. T. Wu.
         Supported in part by Contract NSF-G9721.

TR319   Transient Response of a Dipole Antenna, T. T. Wu. Supported in
         part by Contract NSF-G9721.

TR320   Some Non-Equilibrium Properties of a Bose System of Hard Spheres
         at Extremely Low Temperatures, T. T. Wu. Supported in part by
         Contract NSF-G9721.

TR321   Exchange Terms in Sawada Approximation (A Preliminary Discussion),
         T. T. Wu. Supported in part by Contract NSF-G9721.

TR344   Excitation of Surface Waves on a Unidirectionally Conducting Screen,
         S. R. Seshadri. Supported in part by Contract NSF-G9721.

TR346   Perturbation Theory of Pion-Pion Interaction I: Renormalization,
         T. T. Wu. Supported in part by Contract NSF-G9721.

TR348   Perturbation Theory of Pion-Pion Interaction II: Two-Pion Approxi-
         mation, T. T. Wu. Supported in part by Contract NSF-G9721.

TR349   Scattering by Discontinuities of Surface Waves on a Unidirectionally
         Conducting Screen, S. R. Seshadri. Supported in part by Contract
         NSF-G9721.

TR350   The Electrical Pumping of Dielectric Liquids, W. F. Pickard.
         Supported in part by Contract NSF-G21869.

TR351   The Long Cylindrical Antenna: Current and Admittance, K. Iizuka,
         R. W. P. King, and S. Prasad. Supported in part by Contract
         NSF-G20225.

TR352   Terminal-Zone Corrections for a Dipole Driven by a Two-Wire Line,
         K. Iizuka and R. W. P. King. Supported in part by Contract
         NSF-G20225.

Contract Nonr-1866(32)/NR-371-016 (continued)

TR353   Impedances and Admittances of Long Antennas in Air and in Dissipa-
         tive Media with Tables of the Functions $f(p) \pm i\,g(p) = \sqrt{1 + ip}$, D. W.
         Gooch, C. W. Harrison, Jr., R. W. P. King, and T. T. Wu.
         Supported in part by Contract NSF-G9721.

TR354   An Asymptotic Solution of Dipoles in a Conducting Medium, K.
         Sivaprasad. Supported in part by Contract NSF-G20225.

TR357   Input Admittance of Linear Antennas Driven from a Coaxial Line,
         T. T. Wu. Supported in part by Contract NSF-G9721.

TR360   Diffraction by a Circular Aperture in a Unidirectionally Conducting
         Screen, S. R. Seshadri and T. T. Wu. Supported in part by Contract
         NSF-G9721.

TR361   Theory of the Thin Circular Loop Antenna, T. T. Wu. Supported
         in part by Contract NSF-G9721.

TR362   Input Admittance of Infinitely Long Dipole Antennas Driven from
         Coaxial Lines, T. T. Wu. Supported in part by Contract NSF-G9721.

TR364   A Method of Measuring the Time-Dependent Impedance of the Load,
         K. Iizuka. Supported in part by Contract NSF-G20225.

TR365   A New Technique for Measuring an Electromagnetic Field by a Coil
         Spring, K. Iizuka. Supported in part by Contract NSF-G20225.

TR366   Excitation of Surface Waves on a Perfectly Conducting Screen Covered
         with Anisotropic Plasma, S. R. Seshadri. Supported in part by
         Contract NSF-G9721.

TR369   The Small Loop Antenna Immersed in a Dissipative Medium, C. L. Chen.

TR370   Transient Response of Linear Antennas Driven from a Coaxial Line
         T. T. Wu and R. W. P. King. Supported in part by Contract NSF-
         G9721.

Contract AF19(604)-4118

Series 2

SR10   Linear Arrays: Currents, Impedances, and Fields, II, R. W. P.
         King and S. S. Sandler.

SR11   Plane Waves on a Periodic Structure of Circular Disks and their
         Application to Surface-Wave Antennas, J. Shefer.

Contract AF19(604)-4118 (continued)

SR12   Linear Arrays: Currents, Impedances, and Fields, III, R. W. P.
        King and S. S. Sandler.

SR13   Fresnel Gain of Aperture Antenna, T. Soejima.

SR14   Periodic Cylinder Arrays as Transmission Lines, J. Shefer

Contract AF19(604)-7262

SR2   An Experimental Study of the Properties of Antennas Immersed in
        Conducting Media, K. Iizuka and R. W. P. King.

SR3   An Experimental Study of the Insulated Dipole Antenna Immersed in
        a Conducting Medium, K. Iizuka.

VIII. ABSTRACTS OF TECHNICAL AND SCIENTIFIC REPORTS

ISSUED SINCE JULY 1, 1961

Contract Nonr-1866(16) / NR-372-012

TR315

Nuclear Magnetic Resonance in Antiferromagnetic $Mn F_2$ under Hydrostatic Pressure

G. B. Benedek and T. Kushida

The nuclear magnetic resonance frequency of the F^{19} nucleus in antiferromagnetic $Mn F_2$, in zero external field, has been measured as a function of pressure at $4.2^{\circ} K$, $20.4^{\circ} K$, and $35.7^{\circ} K$ using a new type v. h. f. variable frequency spectrometer. From these measurements we have deduced the pressure dependence of the hyperfine coupling constant (A) between the manganese electrons and the fluorine nucleus, and the pressure dependence of the Néel temperature. This deduction gives $(1/A)$ $(dA/dP) = + (1.9 + 0.1)$ x 10^{-6} / (kg/cm^2) and $(1/T_N)$ $(dT_N/dP) = + (4.4 \pm 0.3)$ x $10^{-6}/(kg/cm^2)$. We have also measured the compressibility of $Mn F_2$. The magnitude and pressure dependence of A is explained using the theories of A. Mukherji and T. P. Das, and W. Marshall and R. N. Stuart, which permit a calculation of the dependence of A on the interatomic distances, starting from the Hartree-Fock self-consistent field wave functions for Mn^{2+} and F^- with the Mn^{2+} wave functions properly adjusted to bring it into agreement with neutron scattering form factor measurements. The theory is in very good agreement with the experimental results.

- - - - -

TR316

The Temperature of Shock Waves in Solids

G. B. Benedek

A theory is presented which enables a relatively simple calculation of the temperature rise in a solid undergoing shock-wave compression. The method first makes use of a previous determination of the volume dependence of the cohesive energy to obtain the increase in vibrational energy on shock compression. The increase in vibrational energy is then analyzed using the Debye model to obtain the associated rise in temperature. Explicit calculations have been carried out for aluminum, providing results which are in good agreement with the thermodynamic calculations which have previously been made by the Los Alamos Group.

- - - - -

Matched Filters and Intersymbol Interference

D. W. Tufts

     The purpose of this report is to shape a new tool for the design of synchronous, pulse-transmission links.   This is accomplished by combining the viewpoints which led to the formulation of two tools of proven worth in communication theory--the matched filter [1, 2] and Nyquist's methods for pulse shaping and transmission line equalization [3, 4].

     Our model for a synchronous, pulse-transmission link is depicted in Fig. 1.

<table>
<tr><td>$\{a_n\}$</td><td>→</td><td>pulse modulator</td><td>→</td><td>$\displaystyle\sum_{n=1}^{N} a_n s(t - nT)$</td><td>→</td><td>transmission filter , h(t), H(f)</td></tr>
<tr><td>transmitted message sequence</td><td></td><td>transmitter</td><td></td><td>transmitted pulse sequence</td><td></td><td>transmission medium</td></tr>
</table>

noise generator

n(t)

$\boxed{+}$ → n(t) + $\displaystyle\sum_{k=1}^{N} a_k r(t - kT)$ → $\boxed{\text{message detector}}$ → $\{b_n\}$

transmission medium   received waveform   receiver   received message sequence

FIGURE 1 - Synchronous Pulse Link Model
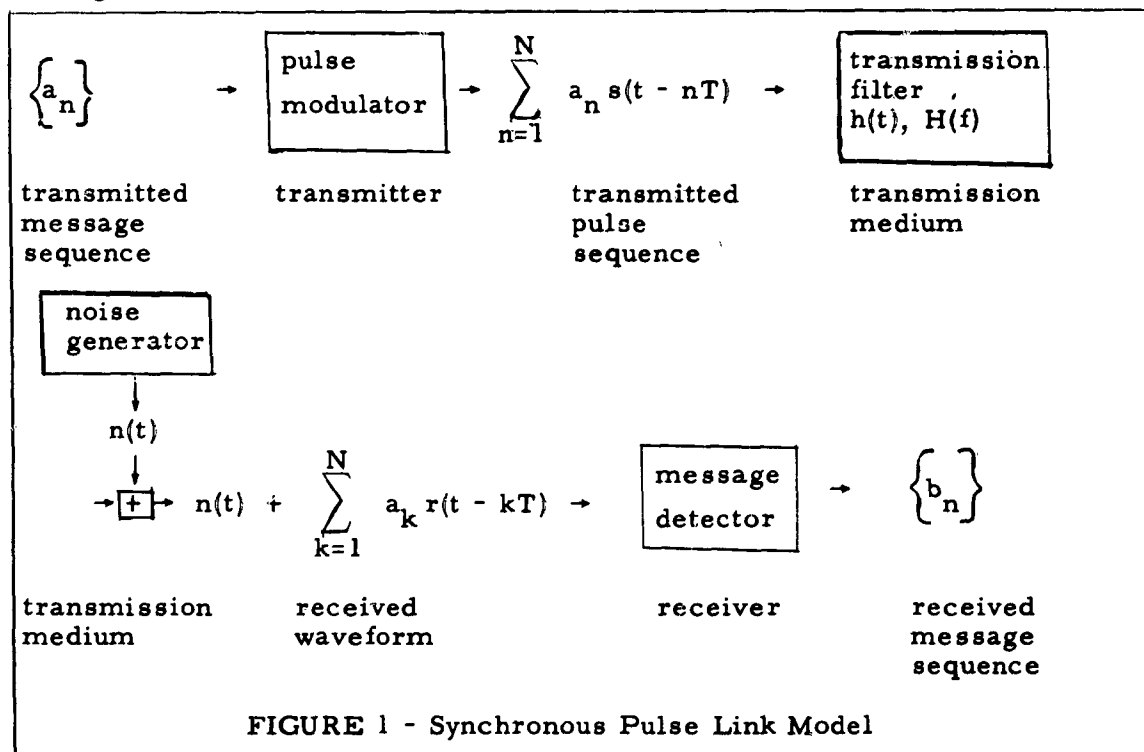
In this model the message is a finite sequence of N real numbers, $\{a_n\}$, n = 1, 2, ..., N . This message sequence is used to amplitude modulate a sequence of N identically shaped pulses in such a way that the transmitted pulse train can be represented by the series $\displaystyle\sum_{n=1}^{N} a_n s(t - nT)$, where s(t) is a time function with Fourier transform S(f). The transmission medium is represented by a filter followed by an additive noise generator. The

transmission filter is linear, time invariant, and has an impulse response $h(t)$ and a frequency transfer function $H(f)$. The additive noise has auto-correlation $\phi(\tau)$ and power density spectrum $\Phi(f)$. The message detector forms an estimate, $\{b_n\}$, $n = 1, 2, \ldots, N$, of the transmitted message sequence by performing N weighted integrations of the received waveform. Specifically, for $n = 1, 2, \ldots, N$

$$b_n = \int_{-\infty}^{\infty} w(t - nT - \delta) \cdot \left[n(t) + \sum_{k=1}^{N} a_k r(t - kT) \right] dt \qquad (1)$$

where $w(t)$ is a weighting function that we wish to determine and δ is a delay parameter that can be chosen by the system designer.

In order to define the term intersymbol interference in the context of our model, we first make the following definitions. For $n = 1, 2, \ldots, N$ let

$$b_n = c_n + d_n \qquad (2)$$

where

$$c_n = \int_{-\infty}^{\infty} w(t - nT - \delta) n(t) dt \qquad (3)$$

and

$$d_n = \int_{-\infty}^{\infty} w(t - nT - \delta) \sum_{k=1}^{N} a_k r(t - kT) dt \qquad . \qquad (4)$$

The intersymbol interference of the nth message element, I_n, for $n = 1, 2, \ldots, N$, is defined by the formula

$$I_n = a_n - d_n \qquad (5)$$

and we call c_n the noise interference of the nth message element.

Our new tool is a method for choosing the weighting function $w(t)$ in such a way that the mean square value of c_n is as small as possible, subject to the constraints that

$$I_n = 0 \text{ for } n = 1, 2, \ldots N \qquad . \qquad (6)$$

This tool is embodied in the following formula for $W*(f)$, the complex conjugate of the Fourier transform of $w(t)$:

$$W*(f) = \frac{S*(f) H*(f) e^{-j2\pi \delta f}}{\mu + \Phi(f)} \sum_{m = -(N-1)}^{N-1} \lambda_m e^{-j2\pi mTf} \qquad (7)$$

where S*(f) is the complex conjugate of the Fourier transform of s(t) ;
μ is a LaGrange multiplier that is used to constrain W(f) to be square
integrable; and $\{\lambda_m\}$, m = 0 , $\pm$ 1, $\pm$ 2 ,..., $\pm$ (N - 1) is a set of LaGrange
multipliers that are chosen to satisfy the constraints of Eq. 6. The crux of
this work is that such a set of λ's is obtainable and unique, if the inequality

$$\frac{|S(f)H(f)|^2}{\mu + \Phi(f)\,|\,H(f)\,|^2} > 0 \tag{8}$$

is satisfied over some frequency interval, no matter how small.

Our results lead to a new method of signaling faster than the Nyquist
rate of 2B independent symbols per second through a bandwidth of B cycles
per second. However, our aim is an improvement in digital pulse trans-
mission at present rates, not an increase in rate.

References

1. J. Van Vleck and D. Middleton, "A Theoretical Comparison of the Visual,
   Aural, and Meter Reception of Pulsed Signals in the Presence of Noise, "
   J. Appl. Phys.,17, 940-971 (November, 1946).

2. G. L. Turin, "An Introduction to Matched Filters, " IRE Transaction on
   Information Theory, vol. IT-6, pp. 311-329 (June, 1960).

3. H. Nyquist, "Certain Topics in Telegraph Transmission Theory, " Trans.
   AIEE, 47, 617-644 (April, 1928).

4. J. M. Wier, "Digital Data Communication Techniques, " Proc. IRE, 49,
   197 (January, 1961).

- - - - -

TR347

On Computing Minima by the Penalty Function Approach

Y. C. Ho

This report examines the computational problem associated with the
use of the penalty function method in solving optimization problems. It is
concluded that the penalty function is useful for constraints of the equality
type. However, for inequality constraints, it may present serious numerical
difficulties.

- - - - -

TR355

Certain Results in Pulse Transmission Theory

D. W. Tufts

This report discusses some results that pertain to the problem of controlling intersymbol interference and additive noise interference in a certain type of pulse transmission system. In this type of system, an amplitude-modulated, periodic pulse train is the input to a noisy, linear, and time-invariant transmission medium. At the receiver, the amplitude of each transmitted pulse is estimated by performing a weighted integration of the received waveform. A pulse code modulation link is a special case of such a system.

Considering interference to be the mean square difference between a transmitted pulse amplitude and the receiver's estimate of this amplitude, we derive an expression for the minimum interference that is possible in the case of transmitted pulses of finite energy. We also present an explicit method for specifying a transmitted pulse shape and a receiver weighting function which permit the minimum interference to be attained.

The ways in which the minimum interference and the optimum pulse shapes are affected by

1) the transmitted data rate,

2) the frequency response of the transmission medium,

3) the noise power density,

4) time jitter in the synchronization between the received pulse train and the receiver weighting function, and

5) the transmitted pulse energy

are explored and compared with previous results.

The inequality

$$\left(\frac{N(f)}{\lambda}\right)^{1/2} \frac{1}{M(f)\,|H(f)|} \leq |P(f)| \qquad (a)$$

plays a critical role in our investigation. In this inequality $N(f)$ is the noise power density spectrum; $M(f)$ is the power density spectrum of the discrete message sequence; $H(f)$ is the frequency transfer function of the transmission medium; $P(f)$ is the characteristic function of the time jitter probability distribution; and λ is a message of the allowable transmitted pulse energy. The significance of Eq. a is that the optimized transmitter will put out power only at frequencies for which Eq. a is satisfied. Physically speaking, at frequencies for which Eq. a is not satisfied either the noise power is too great, the available signal power (as measured by $\lambda^{1/2}\cdot M(f)$ is too small, or the transmission medium has too much loss).

- - - - -

TR356

Comparison of Different Modes of Representation of Multivariable Systems

K. S. Narendra and L. E. McBride, Jr.

A multivariable system may be conveniently represented either by a matrix of transfer functions or by a set of first-order differential equations. The mode of representation depends on the nature of the problem and the constraints involved. The report deals with the relative merits of several methods as well as their inherent limitations. Concepts such as "controllability, observability, structure, " and "interaction" which are peculiar to multivariable systems are examined to form a basis for the comparison.

- - - - -

TR358

Interactions Between Light Waves in a Nonlinear Dielectric

J. A. Armstrong, N. Bloembergen, J. Ducuing, and P. S. Pershan

The induced nonlinear electric dipole and higher moments in an atomic system, irradiated simultaneously by two or three light waves, are calculated by quantum mechanical perturbation theory. Terms quadratic and cubic in the field amplitudes are included. An important permutation symmetry relation for the nonlinear polarizability is derived and its frequency dependence is discussed. The nonlinear microscopic properties are related to an effective macroscopic nonlinear polarization, which may be incorporated into Maxwell's equations for an infinite, homogeneous, anisotropic, nonlinear dielectric medium. Energy and power relationships are derived for the nonlinear dielectric which correspond to the Manley-Rowe relations in the theory of parametric amplifiers. Explicit solutions are obtained for the coupled amplitude equations, which describe the interaction between a plane light wave and its second harmonic or the interaction between three plane electromagnetic waves which satisfy the energy relationship $\omega_3 = \omega_1 + \omega_2$ and the approximate momentum relationship $\vec{k}_3 = \vec{k}_1 + \vec{k}_2 + \Delta\vec{k}$. Third harmonic generation and interaction between more waves is mentioned. Applications of the theory to the dc and microwave Kerr effect, light modulation, harmonic generation and parametric conversion are discussed.

- - - - -

TR359

A Self-Organizing Control System Based on Correlation Techniques and Selective Reinforcement

D. N. Streeter and K. S. Narendra

This report deals with control systems that exhibit a capacity to learn, in the sense of meaningful self-alteration based on experience. The relation between learning, adaptation, and self-organization in control systems and in animals is discussed. A system capable of synthesizing its controllers without explicit knowledge of the process or the spectra of the inputs is described. The synthesis is based on the cross-correlation between a signal representing the desired output state and the various components of the tentative input signal. The system, in a general way, exemplifies the principles of learning used by Mr. A. L. Samuel in programing a computer to play checkers. Results of computer simulation of the system are presented.

The purpose of the report is to present the motivation and the physical reasoning on which the system design was based. Results of computer simulation of a self-organizing system are presented to demonstrate the feasibility of the design.

- - - - -

TR367

Light Waves at the Boundary of Nonlinear Media

N. Bloembergen and P. S. Pershan

Solutions to Maxwell's equations in nonlinear dielectrics are presented which satisfy the boundary conditions at a plane interface between a linear and nonlinear medium. Harmonic waves emanate from the boundary. Generalizations of the well-known laws of reflection and refraction give the direction of the boundary harmonic waves. Their intensity and polarization conditions are described by generalizations of the Fresnel formulas. The equivalent Brewster angle for harmonic waves is derived. The various conditions for total reflection and transmission of boundary harmonics are discussed. The solution of the nonlinear plane parallel slab is presented which describes the harmonic generation in experimental situations. An integral equation formulation for wave propagation in nonlinear media is sketched. Implications of the nonlinear boundary theory for experimental systems and devices are pointed out.

- - - - -

TR368

Optimal Control Problems with Input and Output Constraints

Y. C. Ho

In this report, we consider the time optimal (or terminal error optimal) control of linear dynamic systems subject to amplitude constraints on both the control and state variables. Under certain general assumptions

on the nature of the system and the constraints, it is shown that the optimal solution is bang-bang either in the control variable or the state variable at all times. The proof of this property is constructive, and leads to a successive approximation technique for the numerical determination of the optimal solution.

Extension of the technique to general nonlinear problems shall also be mentioned.

- - - - -

TR371

Relaxation Time Measurements in Ruby by a DC Magnetization Technique

S. Y. Feng

In this research, a method of measuring the relaxation time of paramagnetic substances was developed. The change in the z-component of the magnetization was detected by a pick-up coil, and the signal was amplified, integrated, and displayed on an oscilloscope. The method was much simpler than any of the other methods, and the reliability of data was, therefore, better.

By this technique, the cross-relaxation and the spin-lattice relaxation times were measured for ruby crystals. High-order cross-relaxation processes involving three, four, and five spins were observed, and the relaxation signal could be described fairly well by the solution of a set of rate equations appropriate to the particular process. Spin-lattice relaxation times were measured at different temperatures and concentrations. A Bloembergen-Pershan model, involving an inverted Orbach-Wolf mechanism, could satisfactorily explain the observed data. The dependence on concentration, magnetic field strength was also discussed. A qualitative explanation, due to Orbach, was given, and the result was compared with the existing data. It seems that there is a mild field dependence, approximately linear with H , at high magnetic fields.

- - - - -

Contract Nonr-1866(17)/NR-371-011(Final Report)

TR326

Radio-Wave Propagation

H. R. Mimno

In this final report for Contract Nonr-1866(17), Professor Mimno gives a brief history of the work his group has done in the related enterprises of radio-wave propagation and electronics at Harvard University during the past thirty years.

Cruft Laboratory Technical Reports written in connection with this contract are listed below.

Technical Report No.	Title, Author, and Date of Report
3	"Ionization by Meteoric Bombardment in the E-Region on the Ionosphere, " J. A. Pierce, October 1946.
5	"The True Height of an Ionospheric Layer, " J. A. Pierce, November 1946. Phys. Rev. , May 1947.
7	"An Optical Directional Beacon, " J. A. Pierce, February 1947. J. Inst. Nav. , December 1946.
9	"The Basic Characteristics of Radio Aids to Navigation, " J. A. Pierce, February 1947. Electronics, 1948 ed.
13	"A Note on Temperature Control, " J. A. Pierce, May 1947.
14	"The Diurnal Variation of Absorr̄ion of a Radio Wave in the Ionosphere, " P. W. Lu, Jur 1947.
15	"The Phase Interference between Modulated Ground and Sky Waves, " J. A. Pierce, A. T. Waterman, Jr. , and E. H. Cooper, June 1947.
17	"Radux, " J. A. Pierce, July 1947.
19	"Final Report on Direction-Finder Type Tests, " P. M. Boolba, E. C. Dubbe, E. R. Myrbeck, H. D. Schwetman, and G. Worsley (compiled from data by P. M. Boolba, edited by H. L. Blackwell), April 1948.
26	"A Model of the Ionosphere, " R. H. Woodward, January 1948. J. Terr. Magn. Atmos. Elect., March 1948.
34	"Charts of Dielectric Constant of Refractive Index of the Troposphere," A. W. Friend, March 1948. Bull. Am. Meterol. Soc., December 1948.
82	"A Tentative Model of the Sun, " R. H. Woodward, June 1949. J. Geophys. Research, December 1949.
102	"Nomograms for the Computation of Tropospheric Refractive Index: Its Gradients and Discontinuities, " D. M. Swingle, February 1950.
112	"Reflections of Electromagnetic Waves from Media of Continuously Variable Refractive Index, " D. M. Swingle, July 1950.
113	"2800 Mc/s Vertical Incidence Reflections from the Troposphere, " D. M. Swingle, July 1950.
142	"Ray Theory Applied to a Spherical Ionosphere, " A. T. Waterman, Jr. , February 1952.
143	"Ionospheric Absorption of Obliquely Incident Radio Waves," A. T. Waterman, Jr. , March 1952.

158   "Sky-Wave Intensity I: Low and Very Low Radio Frequencies,"
        J. A. Pierce, September 1952.

190   "The Polarization of Radio Waves Reflected from the Ionosphere at
        Nonvertical Incidence. I. Theoretical Background," G. Inouye,
        September 1953.

191   "The Polarization of Radio Waves Reflected from the Ionosphere at
        Nonvertical Incidence. II. Measurement Techniques and Experi-
        mental Results," G. Inouye, September 1953.

207   "Movement of the F-Region," K. Toman, September 1954.

209   "The Diurnal Carrier-Phase Variation of a 16-Kilocycle Trans-
        atlantic Signal," J. A. Pierce. Proc. IRE, May 1955.

220   "Intercontinental Frequency Comparison by Very Low Frequency
        Radio Transmission," J. A. Pierce, February 1957.

230   "Characteristics of Sporadic E Ionization at Middle Latitude,"
        D. Davidson, June 1955.

233   "Diurnal Rotation of the Ionosphere," K. Toman, December 1955.

270   "Recent Long-Distance Frequency Comparisons," J. A. Pierce,
        September 1958.

326   "Radio-Wave Propagation," H. R. Mimno, September 1960.

        Research supported by this contract is also reported in Cruft
Laboratory Progress Reports Nos. 1 (April 30, 1946) through 50 (January 1,
1959) inclusive.

- - - - -

Contract Nonr-1866(26)/NR-371-015

TR317

Electromagnetic Reflection from Sound Waves

H. J. Schmitt and T. T. Wu

        The reflection of electromagnetic waves normally incident on the
wavefronts of a semi-infinite standing sound wave in a liquid is discussed
theoretically. Since the reflecting planes of maximum sound pressure
disappear periodically, the reflected electromagnetic signal is modulated
with the acoustic frequency. The modulated reflected electromagnetic wave
arises (1) from the microscopic movement of the liquid surface, and (2) from
the direct analog of Bragg reflection in optics. The second effect is most
pronounced when the wavelength of the electromagnetic radiation in the liquid
is twice the acoustic wavelength.
- - - - -

TR324

Diffraction of Electromagnetic Waves by Sound Waves

H. J. Schmitt

An experiment is described in which the diffraction of electromagnetic waves with a wavelength of 1.55 cm by a standing sound wave in oil is observed. The amplitudes of the first diffraction order are calculated by a perturbation method for the case of an idealized sound field. For acoustic disturbances of finite dimensions, the scattering is calculated from Born's approximation. The intensity of the diffracted waves depends upon the sound frequency and the polarization of the incident electromagnetic wave. The amplitude of the first diffraction order is experimentally determined using a superheterodyne system. The relative variation of the dielectric constant of oil with adiabatic compression is measured and the result is compared to data calculated from the Lorentz-Lorenz relation.

- - - - -

TR363

Electromagnetic Reflection from Sound Waves, II

H. J. Schmitt and T. T. Wu

The reflection of electromagnetic waves normally incident on the surface of a liquid supporting a spherical sound wave is discussed theoretically. The effect of Bragg reflection is neglected, and only the microscopic movement of the liquid surface is taken into account. Because of the periodic nature of the sound wave, the reflected electromagnetic signal contains frequency components that correspond to both the sum and the difference of the electromagnetic and acoustic frequencies. These two frequency components have quite different properties. The problem is treated by perturbation theory, and two special cases are examined in detail.

- - - - -

Contract Nonr-1866(32)/NR-371-016

TR318

Theory of the Dipole Antenna and the Two-Wire Transmission Line

T. T. Wu

The properties of the dipole antenna are studied by an approximate procedure that makes use of the Wiener-Hopf integral equation. In particular, the input admittance and the radiation pattern are found. Simple formulas

are obtained only when the dipole antenna is more than one wavelength long. The present results thus supplement the existing theories, which are concerned mostly with shorter dipoles.

The same procedure is then applied to several related problems. First, the back-scattering cross section of a dipole antenna is found approximately for normal incidence. Secondly, the two-wire transmission line is studied in detail by considering it to be two coupled dipole antennas. The capacitive end-correction for an open end is evaluated, and the radiated power and the radiation resistance are found for a resonant section of transmission line with both ends open. Finally, the dielectric-coated antenna is considered briefly.

- - - - -

TR319

Transient Response of a Dipole Antenna

T. T. Wu

The current distributed for a dipole antenna driven by a step-function voltage is found shortly after the switch-on of the voltage. Although many approximate methods have been devised to deal with the dipole antenna of finite length, no case has been solved exactly in a computable form so far as the author is aware. In this report, the initial behavior of the transient response of a model of the dipole antenna is considered.

- - - - -

TR320

Some Non-Equilibrium Properties of a Bose System of Hard Spheres at Extremely Low Temperatures

T. T. Wu

The pseudopotential method is used to study a special type of flow for a Bose system of hard spheres. In the first-order approximation, the wave function of the entire system is assumed to be the product of identical single-particle wave functions, which in general are time-dependent. Such a flow is necessarily irrotational, and the single-particle wave function satisfies a Schrodinger equation with a nonlinear self-coupling term. On the basis of this equation of motion, the following properties of the Bose system are discussed: the effect of the rigid wall, the moment of inertia, the compressional wave, and a type of "vortex filament. " In the second-order approximation, the wave function of the system is expressed in terms of two functions such that one of them describes the single-particle state suitable

for most of the particles, while the other one describes the pair excitations.
The much more complicated equations of motion are found, but in this
approximation the flow is no longer strictly irrotational.   The compressional
waves are also studied in the second-order approximation.

- -- - - -

TR321

Exchange Terms in Sawada Approximation (A Preliminary Discussion)

T. T. Wu

The Sawada approximation for a many-fermion system is modified
so that the exchange terms are treated on the same footing as the direct
terms.   The effects of this modification on the ground state energy per particle
and on the plasma oscillations are discussed.

- - - - -

TR344

Excitation of Surface Waves on a Unidirectionally Conducting Screen

S. R. Seshadri

The excitation of plane surface waves by a line source on a unidirection-
ally conducting i) infinite, and ii) semi-infinite screen is considered.   The
condition for the existence of the surface wave and the optimum location of the
line source for obtaining the highest efficiency of excitation are determined.

- - - - -

TR346

Perturbation Theory of Pion-Pion Interaction I: Renormalization

T. T. Wu

The problem of the pion-pion scattering is studied on the basis of the
model of four-particle direct interaction without derivative coupling.   Re-
normalization is carried out for this model with a detailed analysis of overlap
insertions.   To every finite order in the renormalized coupling constant, it
is shown that the unitarity relation holds, and that the Feynman integral rep-
resentation is still valid, and, hence, renormalization has no effect on
analytic properties.

- - - - -

TR348

Perturbation Theory of Pion-Pion Interaction. II. Two-Pion Approximation

T. T. Wu

        On the basis of the model of a four-particle direct interaction with-
out derivative coupling, relations are obtained between the various renor-
malized quantities related to pion-pion interaction. By considering only two-
pion intermediate states, but preserving crossing symmetry and unitarity up
to the production threshold, closed systems of nonlinear integral equations
are obtained from these relations to describe approximately the low-energy
pion-pion scattering.

- - - - -

TR349

Scattering by Discontinuities of Surface Waves on a Unidirectionally
Conducting Screen

S. R. Seshadri

        It is shown that a plane screen consisting of closely-spaced parallel
wires which are separated from one another and which are such that the radius
of the wires and the spacing between them are small in comparison to wave-
length can support a surface wave, the spread of whose field components de-
pends only on the angle which the direction of propagation makes with the
direction of the wires. The problem of radiation from a discontinuity in such
a semi-infinite waveguide is studied for the following three types of discontinu-
ities: i) when it terminates in empty space, ii) when it terminates at another
such semi-infinite waveguide having different propagation characteristics, and
iii) when it terminates at a perfectly conducting half-plane. In each case, the
power reflection coefficient, the power transmission coefficient where appli-
cable, and the loss of power due to radiation and its angular distribution are
evaluated. The motivation for this investigation is briefly indicated.

- - - - -

TR350

The Electrical Pumping of Dielectric Liquids

W. F. Pickard

        The problem of the pumping of dielectric fluids by the action of electric
fields is considered both theoretically and experimentally. The existing theory
of co-field effects is revised and extended; a qualitative theory is developed
for cross-field effects. A number of original experiments are described for

both the co- and cross-field cases; for example, the pressures generated in a cross-field pump are studied as a function of fluid temperature and rate of fluid flow. It is concluded that co-field pumping is due to the emission of ions from the electrodes, and that cross-field pumping is a result of Sumoto-type phenomena at fluid interfaces and of co-field effects in the fringing fields of the pump.

- - - - -

TR351

The Long Cylindrical Antenna: Current and Admittance

K. Iizuka, R. W. P. King, and S. Prasad

        The driving-point admittance, the relative amplitude, and the phase distributions of the current are given for long cylindrical dipole antennas ranging in electrical half-length from $\beta h = 0.3$ to $\beta h = 63.1$ when driven by a two-wire line. The measured values of the driving-point admittance are in good agreement with the King-Middleton second-order theory [1] for the shorter lengths of antennas and with Wu's theory [2] for the longer lengths.

        Particular care has been taken to determine the influence of an unbalanced feeding line on both the driving-point admittance and the current distribution on the antenna.

        The measured driving-point admittance of the long antenna was extrapolated to that of the infinite length. This extrapolated value is in good agreement with the theoretical values reported by Papas [4], and by King and Schmitt [5].

        The current distributions on the halves of the antenna when driven by symmetric currents (completely unbalanced line) and by anti-symmetric currents (balanced line) are compared.

References

1. R. W. P. King, Theory of Linear Antennas, Harvard University Press, Cambridge, Massachusetts, p. 179.

2. T. T. Wu, "Theory of the Dipole Antenna and the Two-Wire Transmission Line," J. Math. Phys., Vol. 2, No. 4, pp. 550-574, August 1961.

3. C. H. Papas, "On the Infinitely Long Cylindrical Antenna," Cruft Lab. Tech. Report No. 58, Harvard University, September 1948.

4. R. W. P. King and H. J. Schmitt, "The Transient Response of Linear
    Antennas and Loops, " Cruft Lab. Technical Report No. 338, Harvard
    University, March 1961.

- - - - -

TR352

Terminal-Zone Corrections for a Dipole Driven by a Two-Wire Line

K. Iizuka and R. W. P. King

The terminal-zone effects on the dipole antenna driven by a two-wire
transmission line have been re-examined. A series   inductive correction
$j\omega L_g$ together with other terminal-zone corrections is found necessary to
reduce the measured apparent admittance of the antenna terminating the two-
wire line with the ideal admittance of the dipole antenna when driven by a
delta-function generator. The series inductive correction takes account of
the absence of the antenna wire in the gap between the two wires of the trans-
mission line.

With this additional correction, the measured apparent admittance of
a dipole antenna may be brought into excellent agreement with theoretical
values and also reconciled with the quite different values measured with a
coaxial line for an antenna consisting of the vertical inner conductor of the
line extended over a horizontal ground plane. The results further justify the
use of a delta-function generator in the determination of the ideal theoretical
impedance of a dipole antenna.

- - - - -

TR353

Impedances and Admittances of Long Antennas in Air and in Dissipative
Media with Tables of the Functions $f(p) \pm i\,g\,(p) = \sqrt{1 \pm i\,p}$

D. W. Gooch, C. W. Harrison, Jr., R. W. P. King, and T. T. Wu

Tables and graphs are provided for the impedance and admittance of
cylindrical dipole antennas center driven by a delta-function generator when
immersed in air or in a dissipative medium. The electrical half-length ranges
from 1 to 100 for dipoles in air and from 1 to 19.7 for dipoles in a
dissipative medium. Three ratios of radius of the antenna to wavelength in
air have been used.

- - - - -

TR354

An Asymptotic Solution of Dipoles in a Conducting Medium

K. Sivaprasad

  The radiation fields of dipoles immersed in a semi-infinite dissipative medium are investigated. A method suggested by Lighthill [1] for asymptotic evaluation of Fourier integrals is suitably modified to obtain solutions valid for large distances both in air and the conducting medium. The advantage of this method is in its simplicity and ease of application. The results agree closely with those obtained earlier by Baños and Wesley [2].

<div align="center">References</div>

1. Lighthill, Generalized Functions and Fourier Transform Theory, Cambridge University Press, 1960.

2. Baños and Wesley, "Horizontal Dipole in Conducting Half-Space," University of California, Scripps Oceanographic Institute Reports, Nos. 53-54 and 54-61, 1953-1954.

<div align="center">- - - - -</div>

TR357

Input Admittance of Linear Antennas Driven from a Coaxial Line

T. T. Wu

  In two cases of a linear antenna driven from a coaxial line, it is shown that the apparent terminal admittance to the coaxial line can be additively separated into two parts when the transverse dimensions are small compared with the wavelength. One of these two parts depends only on the wavelength and the dimensions of the antenna, while the other part can be interpreted as a capacitance that depends only on the radii of the coaxial

line. The capacitance may be found exactly from the solution of an integral equation, in the sense that further corrections cannot be interpreted simply as a capacitance.

- - - - -

TR360

Diffraction by a Circular Aperture in a Unidirectionally Conducting Screen

S. R. Seshadri and T. T. Wu

The diffraction of a normally incident plane electromagnetic wave with a wave number k by a circular aperture of radius a in a unidirectionally conducting plane screen of zero thickness and infinite extent is considered. In the limit of large ka, the ratio of the transmission cross section to the geometrical optics value πa^2 is found up to the order $(ka)^{-3/2}$. A new feature of this problem is that a set of rays in the sense of Keller's geometrical theory of diffraction emanates from the regions of the aperture rim to which the current on the screen is nearly tangential and proceeds in all directions. However, for the case of normal incidence, these rays do not contribute to the transmission cross section up to the order $(ka)^{-3/2}$.

- - - - -

TR361

Theory of the Thin Circular Loop Antenna

T. T. Wu

The current distribution on a thin circular loop transmitting antenna driven by a delta-function generator is determined approximately by Fourier-series expansion. A difficulty encountered in previous analysis is shown to be due to an inadequate approximation.

- - - - -

TR362

Input Admittance of Infinitely Long Dipole Antennas Driven from Coaxial Lines

T. T. Wu

For an infinitely long dipole antenna driven from a coaxial line, the reflection coefficient and, hence, the apparent terminal admittance are determined approximately when the radii of the coaxial line are small compared

with the wavelength. This result is useful, because the differences of admittances for antennas with identical geometry near the driving point are less sensitive to the driving condition and, hence, can be found approximately by many existing theories.

- - - - -

TR364

A Method of Measuring the Time-Dependent Impedance of the Load

K. Iizuka

By processing a sequence of scope pictures of the output from the probe of a standing-wave detector placed successively at a sequence of positions along a slotted coaxial line, the instantaneous values of a non-stationary load impedance terminating a coaxial line may be measured. This method was applied to measure the instantaneous values of the impedance of a fast-response cadmium selenide photocell which has a rise and decay time of the order of milliseconds. The experiments were performed at 600 Mc/sec.

The experimental results were satisfactory and a change that took place in a few milliseconds could be measured easily. On the other hand, a change that occurs in a few tenths of a microsecond would be near the present limit of measurement. This technique could be extended to the measurement of the dynamic impedance of a plasma tube during the rise and decay period of the plasma intensity, or to the measurement of dynamic conductivities, or electric and magnetic susceptibilities in general.

- - - - -

TR365

A New Technique for Measuring an Electromagnetic Field by a Coil Spring

K. Iizuka

A thin coil spring whose length can be varied periodically by mechanical means has been used as a probe to measure the electric field intensity. The vibrating probe acts as a re-radiating antenna with periodically varying length that modulates and scatters the component of the $\overline{E}$ field which is parallel to the axis of the spring. The scattered signal is picked up by a receiving antenna (the sending antenna was used also as a receiving antenna) and amplified with an amplifier that is locked-in with the frequency of the mechanical vibration of the coil.

Measurements were made with coil springs of three different dimensions, and a gain constant K , which should be independent of the product of the axial length of the coil and the magnitude of the vibration, was experimentally checked.

Measurements of the field of a half-wave dipole antenna as measured with the spring probe are in general agreement with theory.

An expression for the gain of the system is obtained, based upon the field-pattern method, and the approximations involved in the reciprocity-theorem method are clarified. It is also demonstrated (in the appendix) that the effective length of a thin helical antenna equals the axial length of the helix.

- - - - -

TR366

Excitation of Surface Waves on a Perfectly Conducting Screen Covered with Anisotropic Plasma

S. R. Seshadri

The field due to a line source of magnetic current situated in a lossless plasma region above a perfectly conducting screen is considered when a uniform static magnetic field is impressed throughout the plasma region parallel to the direction of the line source. It is shown that under certain conditions surface waves are excited on the screen. The dependence of the efficiency of excitation of surface waves on the distance d of the line source from the ground screen is examined. Also, the asymptotic series for the radiation field is derived, and its leading term is shown to vanish for a particular value of d. Under these conditions a strong surface-wave field is maintained near the guiding surface.

- - - - -

TR369

The Small Loop Antenna Immersed in a Dissipative Medium

C. L. Chen

The input admittance of a small thin-wire circular loop antenna, driven by a slice generator, immersed in a dissipative medium is considered. It is found that the solution given by Storer, for the loop antenna in lossless medium, can be carried over readily by replacing ζ_0 by ζ , and k_0 by $\underline{k}$. The numerical values of the normalized input conductance and input susceptance of a small loop antenna, namely $\beta h = 0.3$, $\Omega = 10$, are calculated. It is to be noted that the input susceptance is practically independent of $\underline{k}$, while the input conductance changes as much as seventeen times in this special case.

- - - - -

TR370

Transient Response of Linear Antennas Driven from a Coaxial Line

T. T. Wu and R. W. P. King

The initial transient response of straight wires connected to coaxial lines is studied theoretically for the case where a pulse is applied to the coaxial line. The wave form of the return pulse is first found approximately for the case of a pulse of zero rise time. Since this does not correspond to any feasible experimental situation, the effect of a finite rise time is considered in detail. Numerical results are obtained for several special cases.

- - - - -

Contract AF19(604)-4118

SR10 (Series 2)

Linear Arrays: Currents, Impedances, and Fields, II

R. W. P. King and S. S. Sandler

A new solution is presented for the problem of determining the radiation pattern and driving-point impedances of an array of N parallel, in-line elements (curtain array). An approximate solution is found in terms of simple trigonometric functions. This solution is obtained from Hallèn's integral equation in terms of two separate distributions: a distribution of transmitting type as for an isolated antenna, and a distribution of receiving type to represent the induced currents. This analysis differs from the conventional theory, since it is not necessary to assume identical current distributions on each antenna. Two separate cases are considered: Case I, for specified base currents, and Case II, for specified base voltages.

As an example, the three- and four-element arrays with full wavelength elements and quarter-wave spacing between elements are investigated. For Case I with the main beam in the endfire position, a large discrepancy is found between the actual results and the conventional theory. However, it is

found that by specifying the base voltages as in Case II, the conventional results are almost completely recovered. The effect on the element currents and impedances due to element interaction is given for the complete range of beam position angles for a three-element array. The variation of the element currents and impedances is easily interpreted with the new theory.

- - - - -

SR11 (Series 2)

Plane Waves on a Periodic Structure of Circular Disks and their Application to Surface-Wave Antennas

J. Shefer

The structure supporting the surface-wave consists of a row of concentric circular disks embedded in a lossless dielectric medium. Exact solutions for the "dipole mode" (corresponding to the HE_{11} surface-wave mode on a dielectric rod antenna) are set up and an approximation is derived for calculating the propagation constants.

It is shown experimentally that a pure " dipole mode" can be excited by simple means, and that propagation constants may be controlled over a wide range by varying the geometrical parameters of the periodic structure.

The possible uses as a surface-wave antenna are discussed, and approximate radiation patterns are calculated from the field distribution in the terminal plane.

- - - - -

SR12 (Series 2)

Linear Arrays: Currents, Impedances, and Fields, III

R. W. P. King and S. S. Sandler

Further results are given for the curtain array with three-quarter and one-half wavelength elements. Since the general solution assumes an indeterminate form, a special solution is given for arrays with half-wavelength elements. This special solution is obtained from the original Hallén integral equation. Calculations are given for two three-element endfire arrays, for three-quarter and one-half wavelength elements and the base currents specified. The distortion in the distribution of current across the array decreases as the elements approach one-half wavelength. The new quasi zeroth-order theory shows that the conventional assumption of identical current distributions is justified only for the case of half-wavelength elements.

The new array solution is extended to arrays with elements of unequal length. This extension follows from the modification of representations for the coupling terms which appear in the integral equation. Two separate cases are considered: all elements driven by slice generators, and arrays with at least one parasitic element. Numerical calculations of the two-element parasitic couplet confirm the well-known phenomenon that the main radiation beam may be directed by adjusting the length of the parasitic element.

The solution for the array with elements of unequal length is extended to the Yagi array. This solution reduces to a simple form. Numerical results are presented for a representative three-element Yagi array.

- - - - -

SR13 (Series 2)

Fresnel Gain of Aperture Antenna

T. Soejima

When a transmitting aperture A_o and a receiving aperture B_o are coupled in the Fraunhofer region, the ratio of received to transmitted power is given by the Friis formula. It is well-known that the Fraunhofer gains G_{ao} and G_{bo} of A_o and B_o are constant and are determined independently.

In this report, the product of the gains $G_a G_b$ in the Fresnel region is determined as an integral over both apertures, assuming the gains G_a and G_b for A_o and B_o. It is pointed out that $G_a G_b$ cannot generally be separated into the individual factors, but a formula similar to that of Friis still holds in the Fresnel region. The author proposes to define the "gain-product reduction factor," $Y_a Y_b$, as the ratio of $G_a G_b$ to $G_{ao} G_{bo}$. The individual gain G_a or G_b may be determined only when A_o and B_o are identical and the illuminations of both apertures are the same. Then, the "gain-reduction factor," Y, is defined as the ratio of G_a to G_{ao}.

Assuming uniform amplitude and phase of illumination over A_o and B_o, $Y_a Y_b$ and Y are determined for circular and rectangular apertures. For circular apertures, the same factors are determined for a set of illuminations which approximate commonly used tapers, and the effect of defocusing the primary feed in lenses and dishes is also discussed.

- - - - -

SR14 (Series 2)

Periodic Cylinder Arrays as Transmission Lines

J. Shefer

Periodic structures of conducting cylinders have been used as radiators (Yagi antennas), and, more recently, as slow-wave lines in traveling-wave tubes and masers. In this report it is shown that a non-resonant structure may have interesting capabilities as an open surface-wave transmission line. By means of a relatively simple matching network, efficient excitation of a surface-wave on the periodic line is obtained. Response is flat over a 20% frequency range at X-band for several combinations of cylinder lengths and spacings. Total insertion losses are less than 3 dB and largely independent of length of transmission line. Conducting cylinders are imbedded in styrofoam.

The effects of bends and twists in the line have also been investigated. It is shown experimentally that a guided wave on this periodic structure can follow a circular path having 1.5λ radius of curvature with very little loss. The plane of polarization can easily be rotated 90° by inserting a short twisted section.

By terminating the transmission line with short circuits at both ends, a discrete series of transmission maxima is observed. Since these resonant peaks of transmission are of high Q-factor, the dispersion characteristic of the line is obtained with very good accuracy.

This type of open transmission line may offer advantages over heavy-weight and bulky conventional waveguides for some specialized applications.

- - - - -

Contract AF19(604)-7262

SR2

An Experimental Study of the Properties of Antennas Immersed in Conducting Media

K. Iizuka and R. W. P. King

Descriptions of the apparatus for measuring both the properties of the conducting solution in which the antennas are immersed and the properties of the dipole antennas themselves were given in Scientific Report No. 1, "Apparatus for the Study of the Properties of Antennas in a Conducting Medium," by the same authors. This report provides measured results of the driving-point admittance, the amplitude distribution of the current, and the phase distribution of the current relative to the phase at the driving-point for a dipole antenna when immersed in homogeneous and inhomogeneous conducting media.

Measurements have also been made of the amplitude distribution and phase distribution of the current for a half-wave dipole antenna immersed in a stratified medium for various gradients of the conductivity. The results

of these experiments indicate that either an antenna of short electrical length or a half-wave dipole antenna can be used as a probe to measure the dielectric constant and conductivity of the medium in which it is immersed. A half-wave dipole antenna could well be used to detect an inhomogeneity in an extended medium.

- - - - -

SR3

An Experimental Study of the Insulated Dipole Antenna Immersed in a Conducting Medium

K. Iizuka

The driving-point admittance and the amplitude and phase distributions of the current referred to the driving-point were measured for an insulated cylindrical antenna immersed in a conducting medium. The ratio $\frac{\sigma}{\omega \epsilon_r \epsilon_o}$ of the conducting medium was varied from $\frac{\sigma}{\omega \epsilon_r \epsilon_o} = 0.036$ to 8.8, a range which includes a variety of media such as poor insulators, the ionosphere, plasmas, dry earth, wet earth, lake water, and sea water. The antenna height βh in radians was varied from $\beta h = 0.1$ through $\beta h = 2\pi$ at intervals of 0.1. The thickness of the insulator was varied from $b/a = 1.25$ to $b/a = 12.0$ where a is the radius of the antenna and b the radius of the insulator.

Measurements have also been made of the admittance, current, and phase distributions along an insulated antenna with a conductive top load, that is, one whose tip is in direct contact with the conducting medium. It is found that when the tip of the antenna is in direct contact with the conducting medium, the current increases almost linearly as the end of the antenna is approached. This is quite unlike the decaying sinusoidal distribution on the completely insulated antenna.

The experimental results are in fair agreement in a general sense with an approximate theoretical expression for the admittance of an insulated antenna immersed in a highly conducting solution. The approximate theory is based on a mode-configuration method.

- - - - -

PR

Mr. J. Hewitt
Massachusetts Institute of Technology
Document Room
Research Laboratory of Electronics
Cambridge 39, Massachusetts

Library
General Electric Microwave Laboratory
Palo Alto, California

Electronics Research Laboratory
Stanford University
Stanford, California

Professor A. W. Straiton
Department of Electrical Engineering
University of Texas
Austin 12, Texas

Department of Electrical Engineering
Yale University
New Haven, Connecticut

Commanding General
Rome Air Development Center
Griffiss Air Force Base
Rome, New York
Attn: RCREC-4C

Commanding General
Rome Air Development Center
Griffiss Air Force Base
Rome, New York
Attn: RCR

Commanding General
Rome Air Development Center
Griffiss Air Force Base
Rome, New York   (2)
Attn: RCRW

Mr. A. Bedrosian
Signal Corps Liaison Office
Massachusetts Institute of Technology
Building 26, Room 131
Cambridge 39, Massachusetts

Director
Air University Library
Maxwell Air Force Base
Alabama   (2)

Commander
Patrick Air Force Base
Cocoa, Florida

Chief, European Office
Air Research and Development Command
Shell Building
60 Rue Ravenstein
Brussels, Belgium

Librarian
General Electric Research Laboratory
P. O. Box 1088
Schenectady, New York

Secretary
Working Group on Semiconductor Devices, AGET
346 Broadway, 8th Floor
New York 13, New York

M. A. Krivanich, Chief
Systems Component Branch
Electronic Warfare Division
Signal Corps Agency
White Sands Proving Ground
New Mixico

Librarian
National Bureau of Standards Library
Room 301 - Northwest Building
Washington 25, D. C.

Director
National Security Agency
Fort George Meade, Maryland
Attn: RADE-1

Activity Supply Officer
Building 2504, Charles Wood Area
Fort Monmouth, New Jersey   (50)
Attn: Director of Research

-2-